DOKUZ EYLÜL UNIVERSITY
GRADUATE SCHOOL OF NATURAL AND APPLIED SCIENCES

AN INVESTIGATION ON ATMOSPHERIC POLYCYCLIC AROMATIC HYDROCARBONS (PAHs) IN IZMIR

by
Eylem DEMİRCİOĞLU

March, 2008
İZMİR

AN INVESTIGATION ON ATMOSPHERIC POLYCYCLIC AROMATIC HYDROCARBONS (PAHs) IN IZMIR

A Thesis Submitted to the
Graduate School of Natural and Applied Sciences of Dokuz Eylül University
In Partial Fulfillment of the Requirements for the Degree of Doctor of Philosophy in Environmental Engineering, Environmental Technology Program

by
Eylem DEMİRCİOĞLU

March, 2008
İZMİR

Ph.D. THESIS EXAMINATION RESULT FORM

We have read the thesis entitled **"AN INVESTIGATION ON ATMOSPHERIC POLYCYCLIC AROMATIC HYDROCARBONS (PAHs) IN İZMİR"** completed by **EYLEM DEMİRCİOĞLU** under supervision of **ASSOC. PROF. MUSTAFA ODABAŞI** and we certify that in our opinion it is fully adequate, in scope and in quality, as a thesis for the degree of Doctor of Philosophy.

Assoc. Prof. Mustafa ODABAŞI

Supervisor

Prof. Dr. Abdurrahman BAYRAM	Assoc. Prof. Aysun SOFUOĞLU
Thesis Committee Member	Thesis Committee Member
Prof. Dr. Aysen MÜEZZİNOĞLU	Prof. Dr. Sermin ÖRNEKTEKİN
Examining Committee Member	Examining Committee Member

Prof.Dr. Cahit HELVACI
Director
Graduate School of Natural and Applied Sciences

ACKNOWLEDGMENTS

I would like to express my gratitude to my advisor Assoc. Prof. Dr. Mustafa ODABASI for his invaluable advice, guidance, encouragement, and support throughout this study. I would like to thank to my thesis committee members Prof. Dr. Abdurrahman BAYRAM, Assoc. Prof. Dr. Aysun SOFUOGLU, Prof. Dr. Aysen MUEZZINOGLU and Prof. Dr. Sermin ORNEKTEKIN for their reviews, comments and supports.

I would like to greatly thank to my husband Hulusi DEMIRCIOGLU, my mother Nazmiye CETIN, my father Hasan CETIN, and my brother Ali Emrah CETIN who encouraged and supported me to overcome the difficulties of preparing this thesis. Completion of this work would not have been possible without their supports. I would also like to greatly thank to my friends for their emotional supports.

I am grateful to Dr. Remzi SEYFIOGLU, Dr. Sinan YATKIN, Dr. James Gregory DAVIS, Sevde Seza BOZACIOGLU, Dr. Banu CETIN, Hasan ALTIOK and Yetkin DUMANOGLU for their help.

I would like to thank to Dokuz Eylül University (Project No. 03.KB.FEN.101) and The Scientific and Technical Research Council of Turkey (TUBITAK) (Project No. 104I144 and ICTAG-C033) for financially supporting of this study.

I would like to thank to Izmir Metropolitan Municipality, Kemal YATKIN and BESAŞ A.Ş. for supplying the location of the sampling station.

Eylem DEMIRCIOGLU

AN INVESTIGATION ON ATMOSPHERIC POLYCYCLIC AROMATIC HYDROCARBONS (PAHs) IN IZMIR

ABSTRACT

Fourteen PAH compounds including fluorene, phenanthrene, anthracene, carbazole, fluoranthene, pyrene, benz[*a*]anthracene, chrysene, benzo[*b*]fluoranthene, benzo[*k*]fluoranthene, benzo[*a*]pyrene, indeno[*1,2,3-cd*]pyrene, dibenzo[*a,h*]-anthracene, benzo[*g,h,i*]perylene were investigated in ambient air, soil and water samples in Izmir. Ambient air studies were carried out at three sampling sites a suburban and two urban sites and their spatial and seasonal variations were investigated. Phenanthrene was the most abundant compound at all sites, and all samples were dominated by low molecular weight PAHs. Gas-particle partitioning of PAHs were examined using octanol-based and soot-based partitioning models. Dry deposition samples were collected in suburban and urban sampling sites concurrently with ambient air samples. Particle dry deposition velocities were calculated using particle concentrations and fluxes. Soil samples were collected at suburban sampling site. Like the air samples the PAH profile in soil was dominated by lower molecular weight compounds. The net air-soil exchange of PAH fluxes were examined. Fluorene, phenanthrene, anthracene and carbazole were deposited to soil in winter while they were volatilized in summer seasons. Other compounds (flouranthene-benzo[*g,h,i*]perylene) were deposited to soil in both periods. Concurrent ambient air and water concentrations were measured at a coastal site of Izmir Bay. The net air-water exchange PAH fluxes were also examined. Net PAH fluxes were mainly deposition from air to water during the sampling periods.

Keywords: Polycyclic aromatic hydrocarbons (PAHs), ambient air, gas/particle partitioning, dry deposition, deposition velocity, air/water exchange, air/soil exchange.

İZMİR BÖLGESİNDE ATMOSFERİK POLİSİKLİK AROMATİK HİDROKARBONLARIN (PAHlar) BELİRLENMESİ

ÖZ

İzmir bölgesinde 14 adet polisiklik aromatik hidrokarbon bileşiği (PAHlar) (fluorene, phenanthrene, anthracene, carbazole, fluoranthene, pyrene, benz[*a*]anthracene, chrysene, benzo[*b*]fluoranthene, benzo[*k*]fluoranthene, benzo[*a*]-pyrene, indeno[*1,2,3-cd*]pyrene, dibenzo[*a,h*]anthracene, benzo[*g,h,i*]perylene) dış havada, toprakta ve su örneklerinde incelenmiştir. Dış hava çalışmaları üç örnekleme noktasında (yarıkentsel ve 2 kentsel) gerçekleştirilmiş ve PAH'ların mevsimsel ve yerel değişimleri incelenmiştir. Tüm ölçüm noktalarında ve örneklerde en çok bulunan bileşiğin phenanthrene olduğu ve düşük moleküler ağırlıklı PAH bileşiklerinin baskın olduğu gözlenmiştir. Absorpiyon ile absorpsiyon ve adsorpsiyon tabanlı modeller kullanılarak PAH'ların gaz-partikül dağılımları incelenmiştir. Kuru çökelme akıları yarıkentsel ve kentsel örnekleme bölgelerinde dış hava örnekleriyle eş zamanlı olarak ölçülmüş ve bu veriler kullanılarak partikül kuru çökelme hızları hesaplanmıştır. Toprak örnekleri yarı kentsel örnekleme noktasından alınmıştır. Dış hava örneklerinde olduğu gibi toprak örneklerinde de düşük moleküler ağırlıklı bileşiklerin baskın olduğu gözlenmiştir. Dış hava-toprak arakesitindeki net akı hesaplanmıştır. Fluorene, phenanthrene, anthracene ve carbazole kışın havadan toprağa çökelme eğilimi gösterirken, bu bileşiklerin yazın topraktan buharlaşma eğiliminde oldukları gözlenmiştir. Diğer bileşiklerin (flouranthene-benzo[*g,h,i*]perylene) ise her iki mevsimde de havadan toprağa çökelme eğilimi gösterdiği bulunmuştur. Dış hava ve su konsantrasyonları İzmir körfezi kıyısındaki bir noktada eş zamanlı olarak ölçülmüştür. Hava-su arakesitindeki net akı hesaplanmış ve örnekleme süresince havadan suya çökelme eğiliminde olduğu bulunmuştur.

Anahtar Sözcükler: Polisiklik aromatik hidrokarbonlar (PAHlar), dış hava, gaz-partikül dağılımı, kuru çökelme, çökelme hızı, hava/su arakesitinde taşınım, hava/toprak arakesitinde taşınım.

CONTENTS

Page

CHAPTER ONE
INTRODUCTION

1.1 Introduction

Polycyclic aromatic hydrocarbons are formed and released into the environment through natural and anthropogenic sources. Natural sources include volcanoes and forest fires while anthropogenic sources come from wood burning, automobile exhaust, industrial power generators, incinerators (Dabestani & Ivanov, 1999). PAHs are formed during incomplete combustion of organic matter (i.e., coal, oil, gasoline, diesel fuel, garbage, and tobacco) (Odabasi, 1998).

Polycyclic aromatic hydrocarbons consist of two or more benzene rings that may be joined in different configurations and comprise carbon and hydrogen only (European Commission DG Environment, 2001). The PAH family includes 660 substances indexed by the National Institute of Standards and Technology. Approximately 30 to 50 of them commonly occur in the environment (Slaski, Archambault, & Li, 2000). Only 16 PAH compounds have been classified by the Environmental Protection Agency (EPA) as priority pollutants (Dabestani & Ivanov, 1999).

In recent years, concern about persistent organic pollutants (POPs) has considerably increased. A global treaty, whose main purpose is the total elimination of 12 POPs on a global scale, was signed in May 2001 in the Stockholm Convention for regulation of POPs. In addition to the 12 POPs, polycyclic aromatic hydrocarbons (PAHs) were also included by the United Nations-European Committee (Nadal, Schuhmacher, & Domingo, 2004).

PAHs released into the atmosphere are subject to short- and long-range transport and are removed by wet and dry deposition onto soil, water, and vegetation (U.S. Department of Health and Human Services, Public Health Service, Agency for Toxic Substance and Diesease Registry, 1995). Despite their large emissions in

urban/industrial sites, PAHs occur at relatively high concentrations in rural and remote areas because of their ability to be transported over long distances as gases or aerosols, and their apparent resistance to atmospheric degradation (Manoli, Samara, Konstantinou, & Albanis, 2000).

Recently, PAHs have been investigated throughout the world in air, water, sediment, soil, vegetation, fish and mussels. Data from animal studies indicate that various PAHs may induce a number of adverse health effects. The International Agency for Research of Cancer (IARC) determined that benz[*a*]anthracene and benzo[*a*]pyrene are probably carcinogenic to humans, while benzo[*b*]fluoranthene, benzo[*k*]fluoranthene, and indeno[*1,2,3-c,d*]pyrene are possibly carcinogenic to humans (Nadal, Schuhmacher, & Domingo, 2004).

Atmospheric PAHs are distributed between gas and particle-phases. The partitioning of PAHs between the gas and particle-phases is an important factor affecting their removal processes. PAHs are removed from the atmosphere by transformation, wet and dry deposition, air-water exchange, and air-soil exchange. Atmospheric levels of PAHs were studied previously (Bozlaker, Muezzinoglu, & Odabasi, 2007; Dachs et al., 2002; Fang, Chang, Lu, & Bai, 2004a; Gigliotti et al., 2002; Halsall et al., 1994; Mandalakis, Tsapakis, Tsoga, & Stephanou, 2002; Odabasi, Vardar, Sofuoglu, Tasdemir, & Holsen, 1999a; Ohura, Amagai, Fusaya, & Matsushita, 2004; Park, Kim, & Kang, 2002; Possanzini, Di Palo, Gigliucci, Sciano, & Cecinato, 2004; Tasdemir & Esen, 2007a; Tsapakis & Stephanou, 2005). There are few studies on their concentration in soil (Bozlaker, Muezzinoglu, & Odabasi, 2007; Cousins & Jones, 1998; Motelay-Massei et al., 2004; Nadal, Schuhmacher, & Domingo, 2004; Zhang, Luo, Wong, Zhao, & Zhang, 2006) and water (Chen, Zhu, & Zhou, 2007; Gigliotti et al., 2002; Ko & Baker, 2004; Luo et al., 2004; Manoli et al., 2000; Pandit, Sahu, Puranik, & Raj, 2006; Telli-Karakoc et al., 2002; Zhang, Hong, Zhou, & Yu, 2004b; Zhang, Huang, Yu, & Hong, 2004a; Zhou & Maskaoui, 2003).

Despite their environmental relevance, only few studies have been conducted in Turkey on PAH levels in the atmosphere. Also, there are only few studies on partitioning of PAHs between gas and particle-phases, their soil and aqueous concentrations, and their air-water, and air-soil exchange. Thus, there is a lack of information in the study area on the presence of PAHs in environmental compartments (atmosphere, water, and soil) and transfer of PAHs between those compartments.

The specific objectives of this study are as follows:

1. To measure the ambient particle and gas phase concentrations of PAHs, to determine their temporal and seasonal variations and, to investigate their gas-particle partitioning.

2. To measure the PAH concentrations in soil, to evaluate the compound profile and their air-soil exchange.

3. To measure the particle-phase dry deposition fluxes and to estimate the relative importance of different mechanisms (i.e., dry deposition, gas absorption, and volatilization) to the local soil pollutant inventory.

4. To determine the magnitude and direction of air-water exchange fluxes of PAHs at a coastal site in Izmir Bay.

5. To investigate the sources of PAHs in the study area.

The PAH compounds that have been extensively detected in the environment and reported in the literature were investigated in this study: naphthalene (NAP), acenaphthene (ACN), acenaphthylene (ACT), fluorene (FLN), phenanthrene (PHE), anthracene (ANT), carbazole (CRB), fluoranthene (FL), pyrene (PY), benz[*a*]anthracene (BaA), chrysene (CHR), benzo[*b*]fluoranthene (BbF),

benzo[*k*]fluoranthene (BkF), benzo[*a*]pyrene (BaP), indeno[*1,2,3-cd*]pyrene (IcdP), dibenzo[*a,h*]anthracene (DahA), benzo[*g,h,i*]perylene (BghiP).

This study consists of five chapters. An overview and objectives of the study were presented in Chapter 1. Chapter 2 reviews the concepts and previous studies related to this work. Experimental work is summarized in Chapter 3. Results and discussions are presented in Chapter 4. Chapter 5 includes the conclusions and suggestions drawn from this study.

CHAPTER TWO
LITERATURE REVIEW

This chapter presents information on structures and general properties of PAHs, sources, their health effects, and previous studies on PAHs in different environmental compartments including air, water and soil.

2.1 Chemical Structure and Properties of PAHs

Polycyclic aromatic hydrocarbons (PAHs) are a complex class of organic compounds containing two or more fused aromatic rings, and containing only carbon and hydrogen. The PAH family includes 660 substances indexed by the National Institute of Standards and Technology. Approximately 30 to 50 of them commonly occur in the environment (Slaski, Archambault, & Li, 2000). Only 16 PAH compounds have been classified by the Environmental Protection Agency (EPA) as priority pollutants (Dabestani & Ivanov, 1999). Table 2.1 shows the structure and the important properties of PAHs analyzed in this study. At ambient temperatures, PAH are solids. The general characteristics common to the class are high melting- and boiling-points, low vapor pressure, and very low water solubility (Odabasi, 1998; World Health Organization [WHO], 1998). As pure chemicals, PAHs are generally colorless, white, or pale yellow-green solids. They can have a faint, pleasant odor (U.S. Department of Health and Human Services, Public Health Service Agency for Toxic Substance and Diesease Registry, 1995).

PAHs can be divided into two groups based on their physical, chemical, and biological characteristics. The lower molecular weights PAHs have significant acute toxicity to aquatic organisms, whereas the high molecular weight PAHs, 4 to 7 ring do not. However, several members of the high molecular weight PAHs have been known to be carcinogenic (Environmental Protection Division, 1993). Most PAHs are known to be toxic to living organisms. Toxicity of PAHs can also be associated with their photochemical conversion to more toxic photoproducts (Dabestani & Ivanov, 1999).

Table 2.1 Structures and important properties of selected PAHs (Page 1 of 3)

PAHs	Naphthalene	Acenaphthylene	Acenaphthene	Fluorene	Phenanthrene	Anthracene
CAS Number	91-20-3	208-96-8	83-32-9	86-73-7	85-01-8	120-12-7
Molecular formula	$C_{10}H_8$	$C_{12}H_8$	$C_{12}H_{10}$	$C_{13}H_{10}$	$C_{14}H_{10}$	$C_{14}H_{10}$
Structure	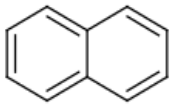	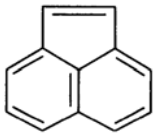	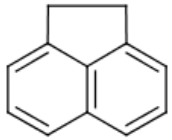	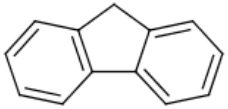	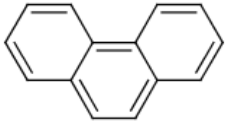	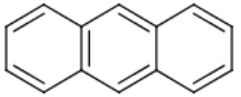
Molecular weight (g mol^{-1})	128.17	152.19	154.21	166.22	178.23	178.23
Melting point (°C)[a, c]	80.2	92.5	93.4	114.8	99.2	215
Boiling point (°C)[a, c]	217.9	280	279	295	340	339.9
Log K_{OA}[b]	-	6.34	6.52	6.90	7.68	7.71
Log K_{OW}	3.3[a, c]	3.94[d]	4.15[d]	4.18[d]	4.57[a]	4.45[a]
Henry's law constant (L atm mol^{-1})	0.44[a, c]	0.12[i]	0.18[i]	0.10[i]	0.04[i]	0.06[i]
Water solubility (mg L^{-1})[a, c]	31	16.1	3.9	1.69	1.15	0.0434
Vapor pressure (Pa)	11.332 [a, c]	0.891 [a, c]	0.287 [a, c]	0.080 [a, c]	0.016 [a, c]	0.0009[c]

[a] National Library of Medicine (NLM), 2004; [b] Odabasi, Cetin, & Sofuoglu, 2006; [c] EPI Suite Estimation Software, 2007; [d] Virtual Computational Chemistry Laboratory (VCCL), 2004 ; [e] Enviromental Protection Agency (EPA), 1996; [f] Finizio, Mackay, Bidleman, & Harner, 1997; [g] Jonker & Koelmans, 2002; [h] Odabasi, M., Cetin, B., & Sofuoglu, A., (2006), [i] Bamford, Poster, & Baker, 1999; [j] Ten Hulscher, Van Der Velde, & Bruggeman, 1992

Table 2.1 Structures and important properties of selected PAHs (Page 2 of 3)

PAHs	Carbazole	Fluoranthene	Pyrene	Benz[*a*]anthracene	Chrysene	Benzo[*b*]fluoranthene
CAS Number	86-74-8	206-44-0	129-00-0	56-55-3	218-01-9	205-99-2
Molecular formula	$C_{12}H_9N$	$C_{16}H_{10}$	$C_{16}H_{10}$	$C_{18}H_{12}$	$C_{18}H_{12}$	$C_{20}H_{12}$
Structure	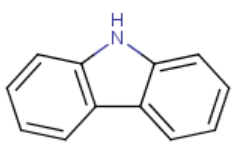	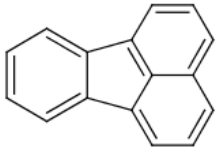	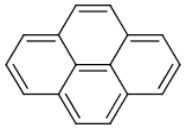	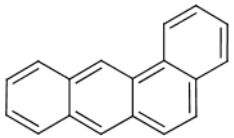	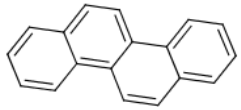	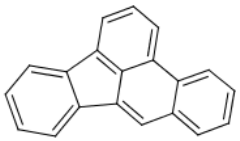
Molecular weight ($g\ mol^{-1}$)	167.21	202.25	202.25	228.29	228.29	252.31
Melting point (°C)[a, c]	246.2	107.8	151.2	84	258.2	168
Boiling point (°C)[a, c]	354.7	384	404	437.6	448	-
Log K_{OA}[b]	8.03[h]	8.76	8.81[h]	10.28	10.30	11.34
Log K_{OW}	3.72[d]	5.22[f]	4.88[c]	5.79[a]	5.73[a]	6.11[d]
Henry's law constant ($L\ atm\ mol^{-1}$)	0.0001[h]	0.019[i]	0.007[i]	0.012[i]	0.005[i]	0.0007[j]
Water solubility ($mg\ L^{-1}$)[a, c]	1.8	0.26	0.135	0.0094	0.002	0.0015
Vapor pressure (Pa)	1.00E-04[c]	1.23E-03 [a, c]	6.00E-04 [a, c]	2.80E-05 [a, c]	8.31E-07 [a, c]	6.67E-05 [a, c]

[a] National Library of Medicine (NLM), 2004; [b] Odabasi, Cetin, & Sofuoglu, 2006; [c] EPI Suite Estimation Software, 2007; [d] Virtual Computational Chemistry Laboratory (VCCL), 2004 ; [e] Enviromental Protection Agency (EPA), 1996; [f] Finizio, Mackay, Bidleman, & Harner, 1997; [g] Jonker & Koelmans, 2002; [h] Odabasi, M., Cetin, B., & Sofuoglu, A., (2006), [i] Bamford, Poster, & Baker, 1999; [j] Ten Hulscher, Van Der Velde, & Bruggeman, 1992

Table 2.1 Structures and important properties of selected PAHs (Page 3 of 3)

PAHs	Benzo[*k*]fluoranthene	Benzo[*a*]pyrene	Indeno[*1,2,3-cd*]pyrene	Dibenz[*a,h*]anthracene	Benzo[*g,h,i*]perylene
CAS Number	207-08-9	50-32-8	193-39-5	53-70-3	191-24-2
Molecular formula	$C_{20}H_{12}$	$C_{20}H_{12}$	$C_{22}H_{12}$	$C_{22}H_{14}$	$C_{22}H_{12}$
Structure	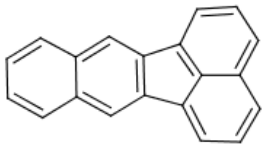	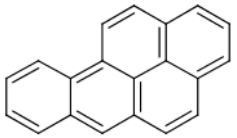	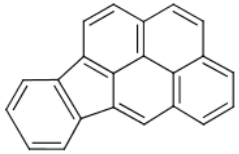	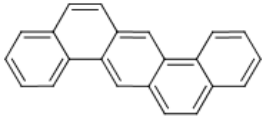	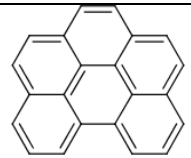
Molecular weight (g mol^{-1})	252.31	252.31	276.33	278.35	276.33
Melting point (°C)[a, c]	217	176.5	163.6	269.5	278
Boiling point (°C)[a, c]	480	495[c]	536	524	>500
Log K_{OA}[b]	11.37	11.56	12.43	12.59	12.55
Log K_{OW}	6.11[d]	6.13[d]	6.72[a]	6.50[a]	6.90[g]
Henry's law constant (L atm mol^{-1})	0.0006[j]	0.0005[j]	0.0003[j]	0.00001[e]	0.0003[j]
Water solubility (mg L^{-1})[a, c]	8.00E-04	0.00162	1.90E-04	0.00249	2.60E-04
Vapor pressure (Pa)	1.29E-07[c]	7.32E-07[c]	1.67E-08[a]	1.27E-07[c]	1.33E-08 [a, c]

[a] National Library of Medicine (NLM), 2004; [b] Odabasi, Cetin, & Sofuoglu, 2006; [c] EPI Suite Estimation Software, 2007; [d] Virtual Computational Chemistry Laboratory (VCCL), 2004 ; [e] Enviromental Protection Agency (EPA), 1996; [f] Finizio, Mackay, Bidleman, & Harner, 1997; [g] Jonker & Koelmans, 2002; [h] Odabasi, M., Cetin, B., & Sofuoglu, A., (2006), [i] Bamford, Poster, & Baker, 1999; [j] Ten Hulscher, Van Der Velde, & Bruggeman, 1992

2.2 Sources of PAHs

Polycyclic aromatic hydrocarbons (PAH) are formed and released into the environment through natural and anthropogenic sources. Natural sources include volcanoes and forest fires, while the anthropogenic sources are wood burning, automobile exhaust, industrial power generators, incinerators, aluminum smelting, carbon black production, iron smelting, production of coal tar, coke, asphalt and petroleum, incomplete combustion of coal, oil, gas, garbage, tobacco and charbroiled meat (Dabestani & Ivanov, 1999; Environment Canada, 2002).

PAHs generally occur as complex mixtures. A few PAHs are used in medicines and to make dyes, plastics, and pesticides. Others are contained in asphalt used in road construction. They can also be found in substances such as crude oil, coal, coal tar pitch, creosote, and roofing tar (U.S. Department of Health and Human Services, Public Health Service Agency for Toxic Substance and Diesease Registry, 1995).

Anthracene is used as intermediate in dye production, in the manufacture of synthetic fibers, and as a diluent for wood preservatives. Acenaphthene is used as a dye intermediate, in the manufacture of pharmaceuticals and plastics, and as an insecticide and fungicide (U.S. Department of Health and Human Services, Public Health Service Agency for Toxic Substance and Diesease Registry, 1995).

Fluorene is used as a chemical intermediate in many chemical processes, in the formation of polyradicals for resins, and in the manufacture of dyestuffs. Phenanthrene is used in the manufacture of dyestuffs and explosives and in biological research (U.S. Department of Health and Human Services, Public Health Service Agency for Toxic Substance and Diesease Registry, 1995).

Fluoranthene is used as a lining material to protect the interior of steel and ductile-iron drinking water pipes and storage tanks (U.S. Department of Health and Human Services, Public Health Service Agency for Toxic Substance and Diesease Registry, 1995).

Atmospheric PAHs are primarily generated from the combustion of fossil fuels, wood burning, refuse burning and coal tar. PAHs enter to surface and ground waters via various mechanisms such as dry and wet deposition from atmosphere (Dabestani & Ivanov, 1999). They can also enter surface waters through discharges from industrial plants and waste water treatment plants, and they can be released to soils at hazardous waste sites if they migrate from storage containers (U.S. Department of Health and Human Services, Public Health Service Agency for Toxic Substance and Diesease Registry, 1995). Accumulation of PAHs in soils can also be due to long-range transport and atmospheric deposition (Dabestani & Ivanov, 1999).

2.3 Health Effects of PAHs

Human exposure to PAHs occurs principally by direct inhalation, ingestion or dermal contact, as a result of the widespread presence and persistence of PAHs in the environment (Berko, 1999). The effect of most concern is elevated incidence of lung cancer. Other health effects include increased incidence of skin and bladder cancers, though there is less evidence for these than for lung cancers. A variety of other cancers (skin, pancreatic, kidney) have been linked to PAH exposure, though evidence for them is relatively weak (European Commission DG Environment, 2001). Several PAHs have been accepted as probable or possible human carcinogens, most of them are known to be associated with airborne particles. Benzo[a]pyrene, a probable human carcinogen found in appreciable concentrations in the atmosphere, can be used as a marker of the carcinogenic risk of airborne PAHs (European Communities, 2001).

2.4 Ecological Impacts of PAHs

There has been little investigation on the ecological impact of PAHs. There is limited evidence of ecotoxic effects in terrestrial and aquatic organisms. No data is available on the effects of PAH on plants, wild mammals, or birds. PAH levels in soil are generally below the no observed adverse effect level for the survival and reproduction of earthworm species (Berko, 1999).

2.5 Environmental Transport, Distribution, and Transformation

By chemical and photochemical transformations in the environment, PAHs can be converted to other products that may or may not be biologically more inert than the parent compound (Dabestani & Ivanov, 1999). Several distribution and transformation processes determine the fate of both individual PAHs and mixtures (WHO, 1998). The fate of PAHs in the environment depends largely on the media they are exposed to (Dabestani & Ivanov, 1999).

The global movement of PAHs can be summarized as follows (U.S. Department of Health and Human Services, Public Health Service Agency for Toxic Substance and Diesease Registry, 1995):

- PAHs released to the atmosphere are subject to short- and long-range transport and are removed by wet and dry deposition onto soil, water, and vegetation.
- In surface waters, PAHs may be volatilized, photolyzed, oxidized, biodegraded, sorbed onto suspended particles or sediments, or accumulate in aquatic organisms.
- In sediments, PAHs can be biodegraded or accumulated in aquatic organisms.
- PAHs in soil can be volatilized, undergo abiotic degradation (photolysis and oxidation), biodegraded, or accumulated in plants. PAHs in soil can also enter to groundwater and be transported within an aquifer.

PAHs are present in the atmosphere in the gas-phase or sorbed to particles. In general, PAHs having two to three rings are present in air predominantly in the gas-phase. Four-ring PAHs exist both in the gas and particle-phases, and PAHs having five or more rings are found predominantly in particle-phase (U.S. Department of Health and Human Services, Public Health Service Agency for Toxic Substance and Diesease Registry, 1995). The processes that transform and degrade PAHs in the atmosphere include photolysis and reaction with NO_x, N_2O_5, OH, O_3, SO_2, and peroxyacetyl nitrate. Possible atmospheric reaction products are oxy-, hydroxy-,

nitro- and hydroxynitro-PAH derivatives (U.S. Department of Health and Human Services, Public Health Service Agency for Toxic Substance and Diesease Registry, 1995). The most important processes contributing to the degradation of PAHs in water are photo oxidation, chemical oxidation, and biodegradation by aquatic microorganisms. Hydrolysis is not considered to be an important degradation process for PAHs (Debastini & Ivanov, 1999; U.S. Department of Health and Human Services, Public Health Service Agency for Toxic Substance and Diesease Registry, 1995). PAHs in water can be chemically oxidized by chlorination and ozonation (U.S. Department of Health and Human Services, Public Health Service Agency for Toxic Substance and Diesease Registry, 1995). Chlorine and ozone react with PAHs to produce quinones and polychlorinated aromatics (Environmental Protection Division, 1993). Microbial metabolism is the major process for degradation of PAHs in soil. Photolysis, hydrolysis, and oxidation generally are not considered to be important processes for the degradation of PAHs in soils (U.S. Department of Health and Human Services, Public Health Service Agency for Toxic Substance and Diesease Registry, 1995).

2.6 PAHs in Air

Ambient air concentrations of PAHs have been measured in industrial, urban, rural, and coastal areas throughout the world. Although there are numerous studies on ambient air PAH concentrations, they differ greatly from each other in terms of effect of local PAH sources, sampling method, sampling duration, sample preparation, and analysis. The total (p+g) concentrations of PAH measured in different locations (industrial, urban, rural, and coastal) are presented Table 2.2.

Table 2.2 Reported concentrations of total (particle+gas) PAHs in ambient air (in ng m^{-3}).

Location	Area	Period	Comp. number	ΣPAH	References
Taichung, Taiwan	Industrial	Aug-Dec, 2002	13	678.7	Fang et al., 2004a
Taichung, Taiwan	Urban	Aug-Dec, 2002	13	476.7	Fang et al., 2004a
Taichung, Taiwan	Rural	Aug-Dec, 2002	13	319.4	Fang et al., 2004a
Chicago, USA	Urban	June-Oct, 1995	13	351.8	Odabasi et al., 1999a
Bursa, Turkey	Urban/ Industrial	Aug, 2004- May, 2005	13	224.6	Tasdemir & Esen, 2007a
Rome, Italy	Urban	Nov, 2002- Apr, 2003	12	162.4	Possanzini et al., 2004
London, UK	Urban	1991 1992	11	160.6 118.1	Halsall et al., 1994
Manchester, UK	Urban	1991 1992	11	110.3 65.3	Halsall et al., 1994
Stevenage, UK	Industrial	1991 1992	11	90.3 78.0	Halsall et al., 1994
Cardiff, UK	Urban	1991 1992	11	79 46.5	Halsall et al., 1994
Seoul, Korea	Urban	1998- 1999	13	67.3	Park, Kim, & Kang, 2002
Heraklion, Greece	Urban	Nov, 2000- Feb, 2002	12	51.5	Tsapakis & Stephanou, 2005
Fuji, Japan	Industrial	August, 1999 December, 1999	13	46.0 33.8	Ohura et al., 2004
Shimizu, Japan	Industrial	August, 2000 December, 2000	13	27.1 22.6	Ohura et al., 2004
Izmir, Turkey	Industrial	August, 2004 March, 2005	14	24.9 43.5	Bozlaker, Muezzinoglu, & Odabasi, 2007
Baltimore, USA	Urban/ Industrial	July, 1997	13	24.0	Dachs et al., 2002
Chesapeake Bay, USA	Rural	February, 1997 July, 1997	13	8.0 10.2	Dachs et al., 2002
Athens, Greece	Urban	July, 2000	10	15.4	Mandalakis et al., 2002
Athens, Greece	Coastal	July, 2000	10	12.8	Mandalakis et al., 2002
New Jersey, USA	Urban	July, 1998	10	27.5	Gigliotti et al., 2002
New Jersey, USA	Coastal	July, 1998	10	9.2	Gigliotti et al., 2002

In Taiwan, PAHs were investigated in industrial, urban and rural sites. The results indicated that PAH concentrations were higher at industry and urban sites than the rural sites because of the more industrial processes, traffic exhausts and human activities. Due to fewer human activities in the rural areas, the measured total PAH concentrations were lower than other sites Fang et al. (2004a). In a study conducted by Odabasi et al. (1999a) in the atmosphere of Chicago, it was found that the PAH concentrations was higher than that at other urban sites (Table 2.2). According to

their results, more volatile compounds such as phenanthrene and fluorene were dominated and the highest ambient concentrations were predominantly in the gas-phase.

In U.K., 11 PAH compounds were investigated at four different sites. London and Manchester had the highest concentrations throughout the 2 years, followed by Stevenage and Cardiff. Stevenage, the smallest urban site, had ΣPAH concentration greater than that in Cardiff, a coastal site (Halsall et al., 1994). At all the sites, the lighter compounds were dominated, notably phenanthrene and fluorene. This is also consistent with other studies in urban air. Bozlaker, Muezzinoglu, & Odabasi (2007) and Tasdemir & Esen (2007a) performed studies on ambient concentrations of PAHs in Turkey. In Bursa, measured PAH concentrations were consistent with the other studies for urban areas. Higher concentrations were observed for lighter PAHs and ~90% of total PAHs were in the gas-phase (Tasdemir & Esen, 2007a). In Aliaga, higher PAH concentrations were observed during winter that was attributed to the increasing emissions from residential heating (Bozlaker, Muezzinoglu, & Odabasi, 2007). Similar increases in winter PAH concentrations were recently reported. PAH levels were similar those reported by Dachs et al. (2002) for urban/industrial Baltimore, Gigliotti et al. (2002) for urban site in New Jersey, Ohura et al. (2004) for industrial sites in Fuji and Shimizu, Park, Kim, & Kang (2002) for urban site in Seoul and Tsapakis & Stephanou (2005) for urban Heraklion.

2.7 Gas-Particle Partitioning

Atmospheric PAHs are partitioned between gas and particle-phases (Caricchia, Chiavarini, & Pezza, 1999). The distribution of PAHs between the gas and the particle-phases is the most important parameter in describing their atmospheric fate, transport, transformation and removal (dry and wet deposition) (Lohmann & Lammel, 2004; Odabasi, 1998). Phase partitioning is influenced by particle properties (size distribution, organic carbon content), total suspended particle (TSP) concentration, ambient air temperature and concentrations (Tasdemir & Esen, 2007a). Atmospheric degradation and deposition strongly depend on the presence of

PAHs in the gas or particle-phase, which together limit the long-range transport (Lohmann & Lammel, 2004).

Partitioning of atmospheric organic compounds between the gas and particle-phases is parameterized using the gas/particle partition coefficient, K_P (m^3 μg^{-1}) (Harner & Bidleman, 1998; Odabasi, M., Cetin, E., & Sofuoglu, A., 2006):

$$K_P = (C_p / C_{TSP}) / C_g \qquad (2.1)$$

where C_p and C_g are the organic compound concentrations in the particle and gas phases, respectively (ng m^{-3}), and C_{TSP} is the concentration of total suspended particles in the air (μg m^{-3}).

The octanol-air partitioning coefficient (K_{OA}) can be used to predict K_P with the assumption of predominant distribution process is absorption (Harner & Bidleman, 1998; Odabasi, M., Cetin, E., & Sofuoglu, A., 2006). K_{OA} is the ratio of the concentration in octanol, to the concentration in air, when the octanol-air system is at equilibrium. This ratio can be employed as an interpretive value of the partitioning of semivolatile compounds between gas and particle-phases in the atmosphere (Harner & Bidleman, 1998; Odabasi, M., Cetin, E., & Sofuoglu, A., 2006). The relationship between K_P and K_{OA} is:

$$K_P = (f_{OM}\, MW_{OCT}\, \zeta_{OCT})\, K_{OA} / (\rho_{OCT}\, MW_{OM}\, \zeta_{OM}\, 10^{12}) \qquad (2.2)$$

where f_{OM} is the fraction of organic matter phase on TSP, MW_{OCT} and MW_{OM} are the mean molecular weights of octanol and the organic matter phase (g mol^{-1}), ρ_{OCT} is the density of octanol (0.820 kg L^{-1}), ζ_{OCT} is the activity coefficient of the absorbing compound in octanol, ζ_{OM} is the activity coefficient of the compound in the organic matter phase. With the assumptions that ζ_{OCT}/ζ_{OM} and MW_{OCT}/MW_{OM}=1, Equation (2.2) can be written as:

$$\log K_P = \log K_{OA} + \log f_{OM} - 11.91 \qquad (2.3)$$

Strong association of PAHs with soot particles in soot-water systems suggests that besides absorption, adsorption partitioning could also be an important sorption mechanism in the atmosphere. Therefore, the following equation for the overall gas-particle partition coefficient that accounts for both organic matter absorption and soot carbon adsorption was derived by Dachs & Eisenreich (2000):

$$K_P=[(f_{OM}MW_{OCT}\,\zeta_{OCT})K_{OA}/(\rho_{OCT}\,MW_{OM}\,\zeta_{OM}\,10^{12})]+[(f_{EC}\,a_{EC})K_{SootAir}/a_{AC}\,10^{12}] \quad (2.4)$$

where f_{EC} is the fraction of elemental carbon in the aerosol, a_{EC} and a_{AC} are the specific surface areas of elemental carbon and activated carbon, respectively; $K_{SootAir}$ is the soot-air partition coefficient. Elemental carbon and octanol are the surrogates for the soot carbon in adsorptive partitioning, and organic matter in absorptive partitioning, respectively.

K_{OA} values can be calculated as a function temperature using:

$$\log K_{OA} = A + B/(T, K) \quad (2.5)$$

where A is the intercepts and B is slopes of the temperature regressions.

Dachs, Ribes, Drooge, & Grimalt (2004) have suggested that the thermodynamics-based model recently reported by van Noort (2003) can be used to estimate $K_{SootAir}$ values for PAHs as a function of supercooled liquid vapor pressure (P_L, Pa) and elemental carbon specific surface area (a_{EC}, $m^2\ g^{-1}$):

$$\log K_{SootAir}= -0.85 \log P_L + 8.94 -\log (998/a_{EC}) \quad (2.6)$$

P_L values as function of temperature can be calculated using:

$$\log P_L\ (Pa) = m_L\ (T, K)^{-1} + b_L \quad (2.7)$$

where b_L is the intercepts and m_L is slopes of the temperature regressions.

The partition between the particle and gas-phases plays a critical role in environmental fate of PAHs and it has been studied extensively over recent decades as recently reviewed by Galarneau, Bidleman, & Blanchard, (2006). Vardar, Tasdemir, Odabasi, & Noll (2004) have found that gas-particle partitioning of PAHs showed a consistent difference between the land and lake samples. It was suggested that the lake samples were closer to equilibrium than the land samples because they travel further from their sources and had higher residence times in the atmosphere (aged particles). Octanol based adsorptive partitioning model generally predicts lower partition coefficients for all PAHs. Despite the uncertainties on some parameters, the study performed by Vardar et al. (2004) demonstrated that the soot and octanol-based model is the most powerful approach for predicting the gas-particle partitioning coefficients for PAHs in Chicago atmosphere.

Experimentally-determined K_P values have been compared to the predictions of an octanol based absorptive partitioning model (K_{Poct}) and a soot and octanol-based model ($K_{Psoot+oct}$) in Bursa (Esen, Tasdemir, & Vardar, 2007). Both models predicted similar K_P values. However, models did not explain the observed variability in the experimental K_P values. In another study conducted by Tasdemir & Esen (2007a), the measured log K_P/modeled K_{Poct} ratios were between 0.8 for pyrene and 0.5 for chrysene while measured log K_P/modeled $K_{Poct+soot}$ ranged from 2.0 for chrysene to 0.8 for fluorene. The overall average values for 5 PAH compounds were 0.7±0.1 and 1.3±0.5 for measured log K_P/modeled K_{Poct} and measured log K_P/modeled $K_{Poct+ soot}$, respectively.

The study by Possanzini et al. (2004) indicated that 2- and 3-ring PAHs are found for more than 90% in the gas-phase. The particle-phase was predominant for 4-ring PAHs with the exception of fluoranthene. More than 90% of the 5-ring PAHs were present in the particle-phase. The gas phase percentage generally decreased with increasing molecular weight and ranged from 1.1 to 99.4%. These results were generally consistent with the particle/gas phase distributions reported in other studies (Odabasi et al., 1999a). A greater fraction of the lower molecular weight PAHs are associated with coarse particles relative to the higher molecular weight compounds.

Therefore, PAHs with lower molecular weights have higher dry deposition velocities and consequently are removed by dry deposition more effectively than higher molecular weight compounds (Odabasi et al., 1999a).

2.8 Particle Dry Deposition of PAHs

In addition to photolysis and chemical reactions, wet and dry deposition can also remove gas and particle-phase compounds from the troposphere. Dry deposition refers to the removal of the chemical or particle-associated chemical from the atmosphere to the Earth's surface, including soil, water and vegetation by diffusion and/or sedimentation (Odabasi, 1998; Roger, 2000; Tasdemir & Esen, 2007b). The removal rate by dry deposition is a function of physical and chemical properties of the pollutant, meteorological conditions (temperature, wind speed, atmospheric stability) and surface characteristics (Odabasi, 1998; Seyfioglu, 2004).

Direct and indirect methods are used to measure particle-phase dry deposition flux. In the direct method, a surrogate surfaces are generally used (Bozlaker, Muezzinoglu, & Odabasi, 2007; Cetin, 2007). Different kinds of surrogate surfaces including teflon plates, petri dishes, dry or diol-coated filters, buckets, pans filled with water, oil-coated glass plates, and greased strips have been used to measure particle dry deposition (Odabasi, 1998; Tasdemir & Esen, 2007b, Tasdemir et al., 2004). Smooth plates with a sharp leading edge that is pointed into the wind by a wind vane have been commonly used to measure dry deposition fluxes. This collection surface provides minimum air flow disruption and thus provides an estimation of the lower limit for dry deposition flux (Fang et al., 2004a; Tasdemir et al., 2004). In the indirect method measured ambient concentrations (C_p) are multiplied by an assumed or modeled deposition velocity (V_p) to determine the dry deposition flux (F_p) (Bozlaker, Muezzinoglu, & Odabasi, 2007; Cetin, 2007; Odabasi, Sofuoglu, Vardar, Tasdemir, & Holsen, 1999b):

$$F_p = V_p C_p \qquad (2.8)$$

Deposition velocity is affected by the meteorological parameters, physical properties of the particle (i.e., size, shape and density), and the type and roughness characteristics of the receptor surface. The selection of an appropriate deposition velocity is crucial since it may introduce large uncertainties in the calculation of dry deposition fluxes (Bozlaker, Muezzinoglu, & Odabasi, 2007; Cetin, 2007).

Interest in atmospheric deposition has increased over the past decades due to concerns about the effects of the deposited materials on the environment (Fang et al., 2004a). The particulate dry deposition fluxes of PAHs reported by different researchers are presented in Table 2.3.

Table 2.3 Reported particle-phase dry deposition fluxes (ng m^{-2} day^{-1}) of PAHs.

Location	Area	Period	Comp. number	ΣPAH Flux	References
Chicago, USA	Urban	June-Oct, 1995	14	156900	Odabasi et al., 1999b
Taichung, Taiwan	Industrial	Aug-Dec, 2002	13	21860	Fang et al., 2004a
Taichung, Taiwan	Urban	Aug-Dec, 2002	13	15440	Fang et al., 2004a
Taichung, Taiwan	Rural	Aug-Dec, 2002	13	14510	Fang et al., 2004a
Chicago, USA	Urban	Nov, 1993- Oct, 1995	13	15880	Franz, Eisenreich, & Holsen, 1998
Lake Michigan	Rural	Nov, 1993- Oct, 1995	13	634	Franz, Eisenreich, & Holsen, 1998
Bursa, Turkey	Urban/ Industrial	Aug, 2004- May, 2005	13	2720	Tasdemir, & Esen, 2007b
Izmir, Turkey	Industrial	August, 2004 March, 2005	14	5089 2410	Bozlaker, Muezzinoglu, & Odabasi, 2007

The particle-phase PAH dry deposition fluxes measured by Franz, Eisenreich, & Holsen (1998) for rural Lake Michigan and for urban Chicago. Particle dry deposition fluxes were higher in Chicago than those measured over Lake Michigan. The higher fluxes in Chicago reflect not only the greater degree of anthropogenic activity within the metropolitan area but also greater atmospheric burden, and subsequent deposition, of coarse particles generated within the area. Coarse particles tend to be deposited within a few kilometers of their sources, while fine particles

may remain suspended in the air becoming dispersed throughout the mixing layer with minimal deposition. Thus, complex atmospheric concentration and deposition patterns exist near coastal zones. The fluxes during the winter were higher than the measured during the summer. The increasing flux during the winter may be due to the higher wind speeds that resuspended more soil and road dust than the summer in Chicago. Similar results were reported by Bae, Yi, & Kim (2002). The dry deposition fluxes in winter were higher than those measured in spring in Korea.

In a recent study performed by Tasdemir & Esen (2007b), the particulate PAH fluxes were dominated by phenanthrene, fluoranthene, and pyrene. Similar results were also reported by Odabasi et al. (1999b). In Aliaga, Izmir low molecular weight PAHs had a larger fraction in the dry deposition flux similar to atmospheric concentrations. Dry deposition fluxes measured in summer were higher than measured in winter. Since large particles dominate the atmospheric dry deposition, higher summer fluxes were attributed to larger particles from enhanced re-suspension of polluted soil particles and road dust (Bozlaker, Muezzinoglu, & Odabasi, 2007).

In Taiwan, the dry deposition fluxes measured at urban and rural sites were lower than the industrial site suggesting that the industrial processes were significant PAH sources (Fang et al., 2004a).

Using greased dry deposition plates, Franz, Eisenreich, & Holsen (1998) have reported that deposition velocities for the individual PAHs were between 0.4-2.1 and 1.0-3.7 cm s^{-1} in summer and winter in Chicago, respectively. Odabasi et al. (1999b) calculated V_d values between 4.3-9.8 cm s^{-1} with an average of 6.7 cm s^{-1} in urban Chicago for summer/fall period. Similarly, Vardar, Odabasi, & Holsen (2002) have reported the mean overall dry deposition velocity of PAHs as 4.5 cm s^{-1} for winter period in Chicago. The overall average deposition velocity for PAHs was 2.9 cm s^{-1} in Aliaga (Bozlaker, Muezzinoglu, & Odabasi, 2007).

2.9 PAHs in Soil

The soil is the major environmental reservoir of semivolatile organic compounds (SOCs) in the terrestrial environment (Cousins & Jones, 1998; Hippelein & Mclachlan, 1998; Ribes, Van Drooge, Dachs, Gustafsson, & Grimalt, 2003). Dry and wet atmospheric deposition constitutes the main input of semi-volatile organic compounds to soil. Persistent organic pollutants (POPs) are transported in the atmosphere at over short and long distances in both gas and particle-phases (Motelay-Massei et al, 2004). Therefore, in the atmospheric studies of PAHs, soil samples have a great importance to evaluate their air-surface exchange rates, transport and sources.

The reported PAH concentrations in soil are presented in Table 2.4. Motelay-Massei et al. (2004) performed a study on PAHs in soils at seven different sites in France. They have found that ΣPAH concentrations ranged between 492.6 and 5622 μg kg^{-1} dry wt. PAH concentrations were strongly linked to the land use of the sites. The industrial sites had highest total PAH concentrations followed by the urban and suburban sites. The remote sites had the lowest concentrations. The major PAHs were fluoranthene and pyrene and the PAH profiles varied according to the nature of the sites and its proximity to the sources.

Table 2.4 Reported concentrations of total PAHs in soil (in μg kg^{-1} dry wt).

Location	Area	Period	Comp. number	ΣPAH	References
Seine River, France	Industrial-1	November, 2000	13	5622	Motelay-Massei et al., 2004
Seine River, France	Industrial-2	November, 2000	13	3357.3	Motelay-Massei et al., 2004
Seine River, France	Suburban-1	November, 2000	13	2977.6	Motelay-Massei et al., 2004
Seine River, France	Suburban-2	November, 2000	13	1642.8	Motelay-Massei et al., 2004
Seine River, France	Urban	November, 2000	13	1645.7	Motelay-Massei et al., 2004
Seine River, France	Remote-1	November, 2000	13	943	Motelay-Massei et al., 2004
Seine River, France	Remote-2	November, 2000	13	492.6	Motelay-Massei et al., 2004
Tarragana, Spain	Industrial-1	January, 2002	13	982	Nadal, Schuhmacher, & Domingo, 2004
Tarragana, Spain	Residential	January, 2002	13	699.4	Nadal, Schuhmacher, & Domingo, 2004
Tarragana, Spain	Industrial-2	January, 2002	13	149.4	Nadal, Schuhmacher, & Domingo, 2004
Tarragana, Spain	Unpolluted	January, 2002	13	103.5	Nadal, Schuhmacher, & Domingo, 2004
Lancester, UK	Rural	1993	6	413	Cousins & Jones, 1998
Izmir, Turkey	Industrial	March, 2006	14	338.8	Bozlaker, Muezzinoglu, & Odabasi, 2007
Hong Kong, China	Urban	December, 2000	12	159.8	Zhang et al., 2006
Hong Kong, China	Rural	December, 2000	12	26.6	Zhang et al., 2006

In Spain, the area close to an industrial complex (petrochemical) was not notably affected by PAH contamination and the levels in soil samples were similar to those found in unpolluted sites (Nadal, Schuhmacher & Domingo, 2004). However, residential/urban and industrial (chemical) sites had the highest PAH concentrations. In a study by Zhang et al. (2006), higher weight molecular PAHs were observed in urban soils. Fluoranthene and pyrene were dominated in rural soils, while fluoranthene, benzo[*b*+*k*]fluoranthene in urban soils. The profile of PAHs varied slightly among different types of land use for rural soils. It was suggested that the biomass burning might be the major source of PAHs in rural soils whereas vehicular emissions may be important for urban soils. Σ_{14}PAH concentrations in soils taken from 50 points in Aliaga ranged between 11 and 4600 μg kg^{-1} in dry weight. The spatial distribution of these concentrations indicated that the urban Aliaga, steel plants, the petroleum refinery, and the petrochemical plant are the major Σ_{14}PAH sources in the area (Bozlaker, Muezzinoglu, & Odabasi, 2007). However, at the air sampling site the average ΣPAH concentration in soil was relatively low suggesting that the sampling site was not affected significantly by the major sources in the area although the sampling site was relatively close to the local sources. PAH profile in soil at that site was dominated by high molecular weight compounds. This observation was explained by the 4-6-ring PAHs being deposited more easily close to the point sources than the lower molecular weight ones which are mainly in the gas-phase that are capable of long-range transport.

2.10 Air-Soil Exchange

Once deposited, PAHs tend to accumulate in soil for a long period of time and subject to various partitioning, degradation and transport processes depending on their physical-chemical properties and microbiological stability (Bozlaker, Muezzinoglu, & Odabasi, 2007).

Air/soil exchange of gas-phase PAHs is also an important process due to significant partition of PAHs to gas-phase. Fugacity is a measure of chemical potential or partial pressure of a chemical in a particular medium that controls the

transfer of chemicals between media. Chemicals try to establish an equal fugacity (equilibrium) in the soil-air system (Meijer et al., 2001). The equilibrium partitioning of a chemical between air and soil is described by the dimensionless soil-air partition coefficient, K_{SA} as fallows:

$$K_{SA}=C_S\,\rho_s/C_A \qquad (2.9)$$

where C_S is the soil concentration (ng g^{-1}, dry weight), ρ_s is the density of soil solids (g m^{-3}), and C_A is the gas-phase air concentration (ng m^{-3}). If the system is not at equilibrium the use of the term K_{SA} is incorrect and the values obtained from Equation (2.9) are defined as soil-air quotients (Q_{SA}) (Meijer, Shoeib, Jantunen, Jones, & Harner, 2003).

K_{SA} is dependent on temperature, humidity and the chemical and soil properties (Meijer et al., 2003). Partitioning of persistent organic pollutants to soil occurs via absorption to the organic carbon fraction. The octanol-air partition coefficient (K_{OA}) is a key descriptor of chemical partitioning between the atmosphere and organic phases (Harner, Green, & Jones, 2000). Hippelein & Mclachlan (1998) formulated a linear relationship that relates K_{SA} to K_{OA} and the organic carbon fraction of the soil as fallows:

$$K_{SA}=0.411\,\rho_s\,\phi_{OC}\,K_{OA} \qquad (2.10)$$

where ρ_s is the density of the soil solids (kg L^{-1}) and ϕ_{OC} is the fraction of organic carbon on a dry soil basis. The factor 0.411 improves the correlation between the K_{SA} and K_{OA} (Bidleman & Leone, 2004; Hippelein & Mclachlan, 1998). In calculation of K_{SA}, it is assumed that the fugacity capacity of soil is due to entirely the organic carbon fraction (Bidleman & Leone, 2004; Meijer et al., 2001).

The net air/soil gas exchange flux is driven by the fugacity difference between air and surface soil (Van Jaarsveld, Van Pul, & De Leeuw, 1997). The gas flux is a function of dimensionless soil-air partition coefficient, the concentration gradient and the overall mass transfer coefficient. The instantaneous net flux (F_g, ng m^{-2} day^{-1}) is:

$$F_g = MTC\ (C_A - C_S\rho_S/K_{SA}) \qquad (2.11)$$

where C_S is soil concentrations (ng g^{-1}, dry weight) and C_A is air concentrations (ng m^{-3}), MTC is overall mass transfer coefficient (cm s^{-1}), ρ_S is the density of the soil solids (kg L^{-1}) and K_{SA} is soil-air partition coefficient.

The overall mass transfer coefficients (MTC) of gaseous pollutants can be predicted by resistance model developed by analogy to electrical resistance. In this model, the atmosphere is considered to have three major resistances: aerodynamic (R_a), quasi-laminar boundary layer (R_b), and canopy (R_c). The overall MTC is the reciprocal of the overall resistance and can be expressed as:

$$MTC = 1/(R_a + R_b + R_c) \qquad (2.12)$$

Aerodynamic resistance accounts for turbulent diffusion transfer from the bulk atmosphere to the canopy. It depends on the wind speed, atmospheric stability and surface roughness. The aerodynamic resistance can be represented by Hicks, Baldocchi, Meyers, Hosker, & Matt (1987). For unstable atmospheres:

$$R_a = 9/(u_{10}\sigma_\theta^2) \qquad (2.13)$$

where u_{10} is the wind speed 10 m above the surface, and σ_θ is the standard deviation of the wind direction in radians.

Boundary layer resistance is the resistance in the laminar sublayer and depends on the molecular diffusion. It can be calculated from the equation developed by Wesely & Hicks (1977) and is given as

$$R_b = (2/\kappa u^*)\,(Sc/Pr)^{2/3} \qquad (2.14)$$

where Pr is Prandtl number of air (~0.72), Sc is the Schmidt number (ν/D_A); ν ($cm^2\ s^{-1}$) is the kinematic viscosity, D_A ($cm^2\ s^{-1}$) is the molecular diffusion coefficient of the contaminant in air, κ (~0.4) is the Karman's constant, u^* (cm s^{-1}) is the friction velocity. Canopy resistance is not applicable to surface soils since it is associated with deposition to vegetated land.

Concurrent air and soil concentrations are ideally used to assess the fugacity gradients of individual PAHs between the soil-air interfaces. The soil-air fugacity ratio $(f_S/f_A)=(C_S\rho_S/K_{SA})/C_A$ greater than 1 indicates that the soil is a source with net volatilization of compounds from soil, values less than 1 indicate that the soil is a sink and net gas-phase deposition occurs from air to soil.

The soil-air partition coefficient (K_{SA}) values and soil-air equilibrium status for various semivolatile compounds (SOCs) have been calculated previously (Bidlemean & Leone, 2004; Cousins, McLachlan, & Jones, 1998; Harner, Green, & Jones, 2000; Hippelein & McLachlan, 1998; Meijer et al., 2003; Meijer et al., 2001). However, there has been limited investigation on soil-air partition coefficients and fugacities of PAHs (Bozlaker, Muezzinoglu, & Odabasi, 2007; Cousins & Jones, 1998; Hippelein & McLachlan, 1998).

A study by Cousins, & Jones (1998) indicated that the soil is a source for some low molecular weight PAHs to the atmosphere whereas it is a sink for the heavier molecular weight PAHs. Similar results were also reported by Bozlaker, Muezzinoglu, & Odabasi (2007) for an industrial site in Aliaga, Izmir.

2.11 PAHs in Water

Aqueous PAH concentrations reported in the literature are presented in Table 2.5. Zhang et al. (2004a) have measured water PAH concentrations in Tonghui River in China. The levels of PAHs in surface waters were relatively high. Two-three-ring PAHs were the most abundant components, four-ring PAH concentrations were also high (Zhang et al., 2004a). Analysis of the possible PAH sources suggested that heavy fuel combustion dominated their origin. In Minjiang River, China, 5- and 6-ring PAHs were the most abundant ones followed by 3- and 4-ring PAHs (Zhang et al., 2004b). The total aqueous PAH concentrations measured by Zhang et al. (2004b) were an order of magnitude higher than those found in waters in Daya Bay, China (Zhou & Maskaoui, 2003). The observed wide range of PAH concentrations have been attributed to different sources in the area, including combustion followed by atmospheric fallout, oil residues, sewage outfalls and industrial wastewater.

Table 2.5 Reported concentrations of total (particle+dissolved) PAHs in water (in ng L^{-1}).

Location	Period	Comp. number	ΣPAH	References
Minjiang River, China	November, 1998	13	70730	Zhang et al., 2004b
Daya Bay, China	August, 1999	13	7596	Zhou & Maskaoui, 2003
Tonghui River, China	April, 2002	13	332.7	Zhang et al., 2004a
Pearl River, China	October, 2001	12	247	Luo et al., 2004
Macao Harbor, China	April, 2001	12	196.3	Luo et al., 2004
Qiantang River, China	Jan- Oct, 2005	12	119.2	Chen, Zhu, & Zhou, 2007
Macedonia, Greece	July- Aug, 1996	12	61.3-133	Manoli et al., 2000
New York Harbor, USA	July, 1998	11	44.4- 97.2	Gigliotti et al., 2002
Raritan Bay, USA	July, 1998	11	7.5- 11.5	Gigliotti et al., 2002
Susquehanna River, USA	1997-1998	11	39.9	Ko & Baker, 2004
Izmit Bay, Turkey	1999	13	0.2- 7.2	Telli-Karakoc et al., 2002

In China, Luo et al. (2004) found similar aqueous ΣPAH concentrations in Pearl River and Macao Harbor. Two and three-ring PAHs were dominant at both sites. The results of the study by Chen, Zhu, & Zhou (2007) showed that concentrations of total and individual PAHs in surface waters varied significantly among sampling locations. Two- and three-ring PAHs were abundant in water. The ΣPAH concentrations in water ranged between 61.3 to 133 ng L^{-1} in Greece (Manoli et al., 2000). The ΣPAH concentrations were higher in New York Harbor than those measured in Raritan Bay (Gigliotti et al., 2002). It was suggested that although both water bodies are impacted by PAH emissions from urban/industrial activities in New York-New Jersey metropolitan area, the higher atmospheric concentrations measured in Jersey City provide larger atmospheric loadings to the adjacent New York Harbor than to Raritan Bay, located farther southeast. Ko & Baker (2004) found that ΣPAH concentration in Susquehanna River was ~40 ng L^{-1}. This contaminant level was generally higher than those in the northern and mid-Chesapeake Bay, suggesting that the Susquehanna River was an important source of PAHs to the Chesapeake Bay (Ko & Baker, 2004). The only previous study on aqueous PAH concentrations in Turkey was conducted in Izmit Bay (Telli-Karakoc et al., 2002). Benzo[*a*]pyrene and benz[*a*]anthracene were the most frequently detected compounds in this study.

2.12 Air-Water Exchange

Loading of PAHs into lakes and oceans takes places by precipitation scavenging and dry deposition and by gas exchange across the air-water interface. The gas exchange across the air-water interface is one of the major processes that controls the concentrations and residence times of PAHs in natural waters (Pandit et al., 2006).

The dynamics of air-ocean exchange and processes within the ocean are critical to the global fate and behavior of POPs. The capacity of surface waters to store POPs is spatially and temporarily variable, and influenced by the temperature, mixing depth, and biogeochemical processes (Cetin, 2007; Cetin & Odabasi, 2007). POPs deposited to surface waters may be further subject to incorporation into the marine food chain, degradation, and eventually deposition into the deep sea. Surface waters may

therefore act as “buffers” between the atmosphere and deep-sea. (Cetin, 2007; Cetin & Odabasi, 2007).

According to the Whitman two-film model, mass transfer is limited by the rate of molecular diffusion through thin films of air and water on either side of the surface (Schwarzenbach, Gschwend, & Imboden, 2003). The gas flux across a water surface is a function of Henry's law constant, the concentration gradient and the overall mass transfer coefficient (Hoff et al., 1996; Schwarzenbach, Gschwend, & Imboden, 2003). The net diffusion gas-exchange flux (F_g, ng m^{-2} day^{-1}) is driven by the fugacity difference between air and surface water:

$$F_g = K_a (C_a - C_w H / R T) \quad (2.15)$$

where C_w and C_a are the water and air concentrations (ng m^{-3}), H is the Henry’s law constant (Pa m^{-3} mol^{-1}), R is the universal gas constant (8.314 Pa m^3 mol^{-1} K^{-1}), K_a is the gas-phase overall mass transfer coefficient, and T is temperature at the air-water interface (K).

The gaseous absorption flux (F_{abs}, ng m^{-2} day^{-1}) quantifies movement of compounds from air into the water column:

$$F_{abs} = K_a C_a \quad (2.16)$$

The gaseous volatilization flux (F_{vol}, ng m^{-2} day^{-1}) quantifies transfer of compounds from the water column into the air:

$$F_{vol} = K_a C_w (H / RT) \quad (2.17)$$

K_a is related to individual mass transfer coefficients for the liquid and gas films, k_w and k_a, as follows:

$$1 / K_a = (1 / k_a) + (H / R T k_w) \quad (2.18)$$

Mass transfer coefficients of water vapor, oxygen (O_2) and carbon dioxide (CO_2) have been related to wind speed by many researchers. The following equations can be used to estimate k_a and k_w for organic compounds (cm s^{-1}) (Nightingale, Liss, & Schlosser, 2000; Schwarzenbach, Gschwend, & Imboden, 2003):

$$k_{a(compound)}\ (cm\ s^{-1}) = (0.2\ U_{10} + 0.3)\ [D_{a(compound)}/D_{a(H2O)}]^{0.67} \qquad (2.19)$$

$$k_{w(compound}\ (cm\ s^{-1}) = [(0.24\ U_{10}^{2} + 0.061\ U_{10})/3600]\ [D_{w(compound)}/D_{w(CO2)}]^{0.5} \qquad (2.20)$$

where D_a and D_w ($cm^2\ s^{-1}$) are the diffusivities in air and water, respectively, and U_{10} is the wind speed 10 m above the water surface (m s^{-1}).

Concurrent air and water concentrations are ideally used to assess the state of equilibrium for individual POPs between the air-water interfaces. The water-air fugacity ratio ($f_W/f_A = H'C_w/C_g$) >1.0 indicates net volatilization of compounds from water, values <1.0 indicate net gas-phase deposition from air. For a system in equilibrium, f_W/f_A value is ~1.0.

In study by performed by Pandit et al. (2006), air-water exchange fluxes were calculated for 45 air and surface water samples collected from five different locations in Mumbai Harbor. The lower molecular weight PAHs mainly volatilized from water indicating that the marine water principally act as a source for low molecular weight atmospheric PAHs. However, the results indicated that high molecular weight gas-phase PAHs were deposited into the surface water (Pandit et al., 2006). Simultaneous air and water sampling over an annual cycle was used to calculate fugacity quotients for individual PAHs in Cumbria (Gevao, Hamilton-Taylor, & Jones, 1998). These calculations showed that PAH transfer varied seasonally with net deposition in winter months when there is no ice cover, and net volatilization at all other times. In the study performed by Gigliotti et al. (2002), the majority of PAHs have a net volatilization flux, showing that the Harbor Estuary acts as a source of PAHs to the air in the summer.

CHAPTER THREE
MATERIALS AND METHODS

Sampling techniques and the experimental methods used for the measurement of PAHs during this study are explained in this chapter.

3.1 Sampling Program

Ambient air samples were collected at two sampling sites located at Suburban and urban sites (Urban 1) in Izmir. The Suburban samples were collected on a 4 m-high platform located on the Kaynaklar Campus of the Dokuz Eylul University, 10 km southeast of Izmir's center. The Campus is relatively far from any settlement zones or Industrial facilities. There are residential areas located approximately 2 km southwest and a highway 0.5 km south of the sampling site. Land cover in the immediate area is a young coniferous forest. There are steel plants, a petroleum refinery and petrochemical industry located 45 km to the northwest. The nearest industrial facility is a cement work about 10 km at the north and an open road gravel storage site nearly 3 km at the east. Samples were also collected from Urban 1 site (Yesildere) located near a main street with heavy traffic and residential areas (Figure 3.1).

Twenty short-term (subsequent daytime and nighttime samples during 10 days), and 43 long-term (daytime) ambient air samples were collected for PAHs between May 2003 and May 2004 at the Suburban sampling site. All samples were collected when there was no rain. Long-term samples were collected once in every six days in order to see if any fluctuation occurs throughout a week. Another two additional sampling programs were conducted between March 17-24, 2004 (winter) and July 15-22, 2004 (summer) at the Urban 1 sampling site. Successive 7 ambient air samples were collected for each sampling period. Concurrent ambient air and particle dry deposition samples were also collected at the two sampling sites (Suburban and Urban 1). Samples were also collected to determine the total suspended particles (TSP) and their organic matter content (OM). Meteorological data was obtained from

a 10 m high tower in the Kaynaklar Campus of the Dokuz Eylul University, Izmir, Turkey that is located a few kilometers away from the Urban 1 sampling site. However, when the instruments on the tower malfunctioned, meteorological data was obtained from Izmir Adnan Menderes Airport's meteorological station. Detailed information on sampling is presented in Tables 3.1 and 3.2.

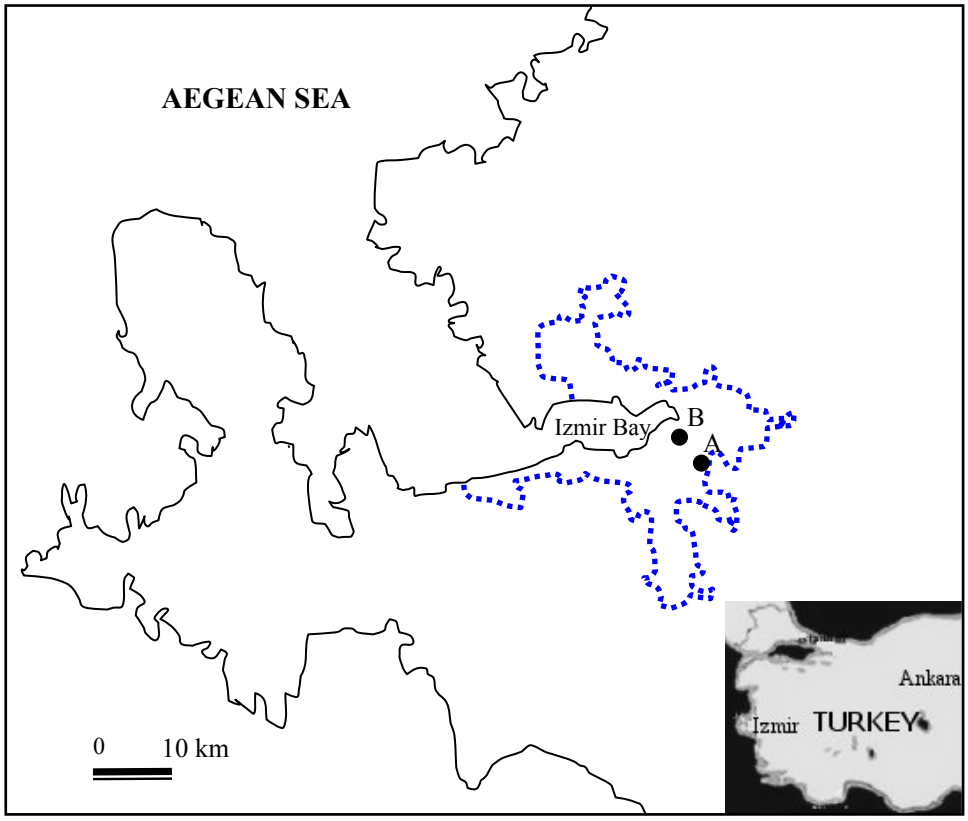

Figure 3.1 Map of the Izmir showing the sampling sites. A- Suburban sampling site, B- Urban 1 sampling site. Dashed line is border of densely populated areas

Table 3.1 Summary of sampling information, TSP and OM data collected from Suburban site (Page 1 of 2)

SN	Date	T (°C)	RH (%)	WS ($m\ s^{-1}$)	WD	C (TSP) ($\mu g\ m^{-3}$)	C (OM) ($\mu g\ m^{-3}$)	OM (%)
1	12.05.03	25.5	37.3	3.0	NW	105.5	56.8	53.8
2	14.05.03[a]	23.5	53.2	2.8	WNW	72.4	59.0	81.5
3	14.05.03[b]	18.2	68.9	1.4	ESE	72.8	44.8	61.5
4	15.05.03[a]	25.0	46.7	2.2	WNW	84.5	43.6	51.6
5	15.05.03[b]	20.1	64.1	0.8	N	101.4	52.1	51.4
6	16.05.03[a]	26.4	43.1	3.4	WNW	127.4	54.2	42.6
7	16.05.03[b]	20.8	62.7	0.9	N	95.3	38.6	40.5
8	17.05.03[a]	25.7	45.1	3.5	WNW	94.6	58.8	62.2
9	17.05.03[b]	20.0	68.0	1.2	N	88.7	17.7	20.0
10	18.05.03[a]	23.2	58.2	5.0	WNW	109.0	57.1	52.4
11	18.05.03[b]	18.0	78.6	1.7	NW	89.5	34.8	38.9
12	19.05.03[a]	21.9	63.9	5.1	WNW	108.2	59.3	54.8
13	19.05.03[b]	17.2	74.1	4.3	N	77.4	37.4	48.4
14	20.05.03[a]	22.5	55.9	5.5	NW	107.5	47.3	44.0
15	20.05.03[b]	18.5	72.4	1.0	ESE	125.4	86.7	69.1
16	21.05.03[a]	24.2	53.3	3.1	WNW	93.4	55.1	59.0
17	21.05.03[b]	16.9	71.7	2.4	ESE	48.2	27.2	56.5
18	22.05.03[a]	22.6	50.8	6.0	SSE	72.6	34.2	47.1
19	22.05.03[b]	17.3	71.6	3.8	SE	25.0	13.6	54.5
20	23.05.03[a]	21.5	50.5	3.8	SE	42.9	24.9	57.9
21	23.05.03[b]	15.7	82.6	2.2	N	33.2	24.4	73.3
22	30.05.03	21.0	60.1	6.1	N	50.9	7.3	14.3
23	25.06.03	31.7	28.6	5.2	WNW	163.2	64.9	39.7
24	27.06.03	29.5	34.3	5.8	WNW	103.1	59.8	58.0
25	29.06.03	30.2	25.6	5.0	WNW	73.3	50.3	68.6
26	05.07.03	34.6	25.4	4.3	S	71.0	22.3	31.4
27	17.07.03	30.0	32.1	6.9	N	52.2	25.1	48.0
28	23.07.03	30.0	29.2	7.2	N	24.6	12.3	50.0
29	29.07.03	29.6	30.5	7.0	N	39.1	30.9	78.9
30	04.08.03	30.4	41.6	8.3	N	73.3	12.2	16.7
31	10.08.03	27.4	47.9	6.7	WNW	44.3	23.2	52.4
32	16.08.03	30.8	29.1	3.9	WNW	n.a.	n.a	n.a

SN: Sample no, T: Temperature, RH: Relative humidity, WS: Wind speed, WD: Wind direction, TSP: Concentration of total suspended particulate matter, OM: Organic matter content of TSP
[a] Daytime sample, [b] Nighttime sample

Table 3.1 Summary of sampling information, TSP and OM data collected from Suburban site (Page 2 of 2)

SN	Date	T (°C)	RH (%)	WS ($m\ s^{-1}$)	WD	C (TSP) ($\mu g\ m^{-3}$)	C (OM) ($\mu g\ m^{-3}$)	OM (%)
33	28.08.03	28.4	45.5	3.4	WNW	40.6	28.5	70.0
34	03.09.03	27.9	51.7	4.9	WNW	87.5	27.2	31.1
35	08.09.03	22.8	36.7	4.1	WNW	48.9	15.5	31.8
36	15.09.03	21.3	58.0	5.7	WNW	104.4	54.0	51.7
37	21.09.03	24.5	30.6	7.8	N	57.2	44.0	76.9
38	27.09.03	22.7	55.7	5.2	N	76.2	30.0	39.4
39	03.10.03	21.5	53.7	4.2	WNW	70.8	30.7	43.3
40	10.10.03	16.5	55.0	4.6	NNW	28.4	26.0	91.7
41	15.10.03	19.4	47.4	4.7	N	84.7	44.7	52.8
42	22.10.03	25.3	42.0	4.9	SSE	38.7	13.7	35.3
43	05.11.03	18.2	67.1	9.2	N	n.a.	n.a	n.a
44	10.11.03	9.1	62.9	8.4	N	23.3	20.4	87.5
45	16.11.03	13.7	57.6	1.6	WNW	86.1	80.8	93.8
46	22.11.03	17.1	56.0	2.4	SSE	36.8	30.7	83.3
47	05.12.03	9.0	61.6	5.9	N	35.7	6.5	18.2
48	18.12.03	1.9	60.0	8.0	N	n.a.	n.a	n.a
49	27.12.03	6.8	72.9	7.3	N	78.5	75.5	96.2
50	07.01.04	-1.5	54.4	8.1	N	44.8	11.9	26.7
51	14.01.04	9.5	81.5	0.2	N	23.2	8.7	37.5
52	30.01.04	11.2	72.1	4.1	SSE	477.8	235.8	49.4
53	05.02.04	7.9	54.3	5.6	NW	91.4	22.9	25.0
54	11.02.04	5.8	35.2	4.7	N	27.7	22.1	80.0
55	19.02.04	7.7	54.6	1.5	WNW	80.7	53.8	66.7
56	26.02.04	15.6	60.5	8.7	SE	44.0	12.6	28.6
57	05.03.04	5.1	58.7	10.4	N	48.5	10.8	22.2
58	11.03.04	10.0	52.2	5.3	N	45.6	22.8	50.0
59	31.03.04	13.9	46.5	7.4	N	486.8	347.7	71.4
60	06.04.04	15.2	46.8	5.2	SSE	16.7	11.9	71.4
61	16.04.04	13.9	33.5	6.2	N	54.1	20.3	37.5
62	22.04.04	14.3	62.4	7.3	N	55.9	34.9	62.5
63	30.04.04	18.9	47.6	2.2	WNW	77.2	49.5	64.1

SN: Sample no, T: Temperature, RH: Relative humidity, WS: Wind speed, WD: Wind direction, TSP: Concentration of total suspended particulate matter, OM: Organic matter content of TSP

Table 3.2 Summary of sampling information, TSP and OM data collected from Urban 1 site

SN	Date	T (°C)	RH (%)	WS (m s^{-1})	WD	C (TSP) (μg m^{-3})	C (OM) (μg m^{-3})	OM (%)
1	17.03.04	11.8	47.7	4.4	N	114.4	55.5	48.5
2	18.03.04	11.3	59.0	6.4	N	81.7	46.4	56.8
3	19.03.04	12.0	52.3	3.2	N	115.3	71.4	61.9
4	20.03.04	14.1	48.4	2.4	ESE	77.6	53.9	69.4
5	21.03.04	14.2	65.4	5.1	SE	67.2	29.9	44.4
6	22.03.04	13.6	67.5	5.7	SE	110.3	42.1	38.2
7	23.03.04	12.6	53.5	3.3	SSE	98.1	60.6	61.8
8	15.07.04	23.8	36.1	6.4	N	74.6	30.5	40.8
9	16.07.04	22.8	43.7	7.0	N	78.1	39.1	50.0
10	17.07.04	24.1	44.7	7.3	N	64.4	31.7	49.2
11	18.07.04	25.7	39.0	6.2	N	71.7	28.7	40.0
12	19.07.04	27.0	39.5	7.4	N	94.3	44.4	47.1
13	20.07.04	27.2	39.9	7.3	N	109.1	35.7	32.8
14	21.07.04	26.6	38.8	7.0	N	102.3	42.8	41.8

SN: Sample no, T: Temperature, RH: Relative humidity, WS: Wind speed, WD: Wind direction, TSP: Concentration of total suspended particulate matter, OM: Organic matter content of TSP

Soil samples were also collected from Suburban site near the sampling platform (Figure 3.1). In a total, 10 soil samples were collected from May 2003 to May 2004. A summary of sampling information is shown in Table 3.3.

Table 3.3 Summary of sampling information, water and OM content of soil samples

SN	Date	WC (%)	OM (Dry Sample) (%)
1	23.05.2003	4.8	10.0
2	26.05.2003	5.1	9.7
3	25.06.2003	1.6	11.3
4	29.07.2003	3.5	11.1
5	28.08.2003	4.2	10.5
6	04.11.2003	4.2	11.3
7	05.12.2003	5.7	11.2
8	14.01.2004	7.3	10.6
9	11.02.2004	5.7	9.6
10	01.04.2004	5.7	10.1

SN: Sample no, WC: Water content of soil, OM: Organic matter content of soil

Surface water and concurrent air samples (n=16) from Guzelyali Port (Urban 2) were collected during two sampling programs in February and July, 2005. All samples were collected when there was no rain. Guzelyali Port is an urban site located at the south of Izmir Bay (Figure 3.2). Sampling data and meteorological conditions are given in Table 3.4. Meteorological data (air temperature, wind speed and direction, and relative humidity) was taken from Guzelyali station located ~ 500 meters from the sampling site while surface water temperatures were measured on-site. Long-term observation indicate that the prevailing wind direction in the area is NW. During the sampling programs generally northerly winds were prevailed (except the two days of winter sampling). These wind directions indicate that sampled air was off the bay water but also affected by the urban plume since there are densely populated areas around the Izmir Bay (Figure 3.2).

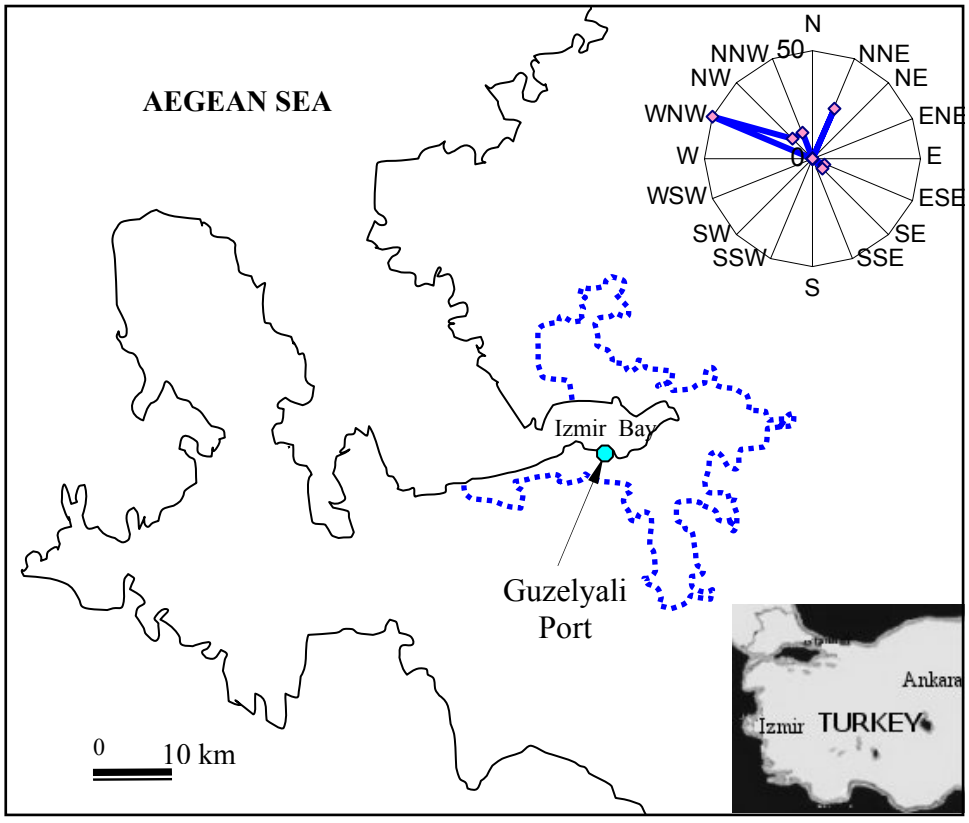

Figure 3.2 Map of the Izmir Bay showing Guzelyali Port (Urban 2) sampling site. Dashed line is the border of densely populated areas. Wind rose shows the frequency (%) of prevailing wind directions during the sampling programs

Table 3.4 Summary of sampling information collected from Guzelyali (Urban 2)

SN	DATE	T_a (°C)	T_w (°C)	RH (%)	WS (m s^{-1})	WD	V_a (m^3)	V_w (L)
1	09.02.05	6.1	9.5	48	5.2	NNE	88.8	76
2	10.02.05	6.9	9.5	49	4.3	NNE	65.8	38
3	11.02.05	6.6	9.5	49	3.9	NNW	89.3	38
4	12.02.05	6.4	9.5	64	2.4	WNW	90.5	38
5	24.02.05	15.8	10	62	4.4	ESE	87.9	38
6	25.02.05	15.4	10	68	4.5	SE	86.7	38
7	03.03.05	10.1	11	79	4.2	WNW	85.9	38
8	04.03.05	10.1	11.5	68	2.5	WNW	89.3	38
9	06.07.05	29.3	26	38	5.2	WNW	82.7	55
10	07.07.05	31.8	26	39	2.7	NNE	61.0	55
11	08.07.05	32.9	27	42	3.3	WNW	97.3	55
12	09.07.05	31.7	27	48	5.1	WNW	133.2	55
13	10.07.05	31.6	28	47	5	WNW	109.8	55
14	11.07.05	32.7	28	39	3.3	NNW, NW	81.1	55
15	12.07.05	32.7	27	48	2.7	NNE	79.8	55
16	13.07.05	30.1	27	54	4	WNW, NW	89.3	55

T_a: Ambient air temperature, T_w: Water temperature, RH: Relative humidity, WS: Wind speed, WD: Wind direction, V_a: Sampling volume for air samples, V_w: Volume of water sample.

3.2 Sampling Method

3.2.1 Ambient Air Samples

Air samples were collected using a modified high-volume sampler (PS-1), Model GPS-11 (Thermo-Andersen Inc.). The PS-1 sampling train is designed to collect suspended airborne particulate matter on a filter and gas-phase compounds on a backup sorbent. Particles were collected on 10.5-cm diameter quartz filters. The gas-phase compounds were collected in a modified cartridge containing XAD-2 resin placed between layers of polyurethane foam (PUF). The PUF is 2-inch thick sheet stock polyurethane type (density 0.022 g cm^{-3}). The PUF cylinders (plugs) were slightly larger in diameter than the internal diameter of the cartridge.

Concurrently, particulate samples were collected on 11-cm diameter glass fiber filters using another high volume sampler to determine total suspended particulate matter (TSP) and its organic matter (OM) content. The high volume sampler is a compact unit consisting of a protective housing, an electric motor driven, a high-speed, high-volume blower, a filter holder capable of supporting a filter. The average sampling volumes for PAH were 173±44 m^3 and 277±62 m^3 and the average sampling volume for TSP were 40.5±8.5 m^3 and 93.9±13.0 m^3 at Suburban and Urban 1 sampling sites, respectively. Sampling time ranged between 11 hours (Suburban site) and 22 hours (Urban 1 site).

3.2.2 Dry Deposition Samples

The particle-phase dry deposition fluxes of PAHs was measured using a smooth deposition plate (22x7.5 cm) with a sharp leading edge (<10°), mounted on a wind vane. Glass fiber filter (GFF) sheets mounted with cellulose acetate strips on the plates were used to collect the deposited particles. The dimensions of the GFF sheet's deposition surface were 5.5x12 cm. Five plates and sheets with a total collection area of 330 cm^2 were used for sampling.

3.2.3 Soil Samples

The soil samples were collected manually from surface of three different sampling points at 0-5 cm depth and sieved through a 0.5 mm mesh sieve to remove large particles and organic debris. About 500 gr of the soil for each point transferred into storage bags. About 30 g soil samples were used to determine water and organic matter content and the 10 g soil samples were used for PAH analysis.

3.2.4 Water Samples

Water samples from Guzelyali Port were collected along with the concurrent air samples for both summer and winter seasons. Air samples were collected using a PS-1 sampler. Water samples were collected at the beginning of each air sampling manually from a depth of 30 cm using high density polyethylene containers without leaving a headspace. The average sampling duration was 6.4±1.2 hours and the average sampling volumes were 89±16 m^3 and 49±11 L for air and water samples, respectively.

3.3 Preparation for Sampling

3.3.1 Glassware

All glassware used in the sampling and analysis procedures was washed with hot water and detergent, rinsed a number of times with hot and then distilled water. Subsequently the glassware were rinsed with a series of polar and non-polar solvents (acetone, hexane) and dried in an oven at 110°C for 4 hours. The openings of the glassware were covered with aluminum foil as soon as they were removed from oven. Glassware was rinsed with dichloromethane prior to use.

3.3.2 Glass Fiber Filters, 47 mm Glass Fiber Filters, and Quartz Filters

Quartz filters used in PUF sampler and glass fiber filters used for dry deposition samples and water samples were wrapped loosely with aluminum foil and baked in a muffle furnace at 450°C overnight to remove any organic residues. Then they were allowed to cool to room temperature in a desiccator.

Prior to sampling for TSP, glass fiber filters were wrapped loosely with aluminum foil and they were baked in a muffle furnace at 450°C for 2 hours to remove any organic residues. They were then allowed to cool to room temperature in a desiccator and weighed using a micro balance capable of weighting 0.1 mg.

3.3.3 PUF Cartridges

PUF cartridges (including polyurethane foam and XAD-2 resin) used in PUF samples were cleaned by Soxhlet extraction using (1:1) acetone:hexane mixture for 12 hours. After extraction the cartridges were wrapped loosely with aluminum foil and dried in an oven 70°C. Cleaned cartridges were stored in glass jars capped with Teflon-Lined lids.

3.3.4 XAD-2 Resin for Water Samples

Resin was placed in beakers, rinsed with a series of polar and non-polar solvents (acetone, hexane) and dichloromethane and wrapped loosely with aluminum foil and then dried in an oven 70°C. Then it was allowed to cool to room temperature in a desiccator. Cleaned resin was stored in glass jars capped with Teflon-Lined lids.

3.3.5 Dry Deposition Plates and Cellulose Acetate Strips

Plates and cellulose acetate strips were cleaned with detergent and hot water, rinsed with tap water several times and with DI water. Subsequently they were rinsed with a series of polar and non-polar solvents (acetone, hexane). Then, they were wrapped with aluminum foil. Glass fiber filter sheets (7.5x12 cm) were mounted on dry deposition plates and both sides covered with cellulose acetate strips (1x12 cm).

3.3.6 Sample Handling

Cleaned and prepared glass fiber filters, PS-1 filters, PUF cartridges and dry deposition plates were transported to the field in their containers without allowing any exposure to ambient air prior to sampling in order to protect from any contamination. After sampling PS-1 filters and dry deposition filters were wrapped with foil and transferred into storage bags. PUF cartridges were wrapped with foil and transferred into glass jars. The glass fiber filters for TSP sampling were placed to a storage bags. Then samples were brought back to laboratory and PS-1 filters, dry

deposition filters and PUF cartridges were stored in the dark at –20°C until they were analyzed. After sample collection filters for TSP were kept in a desiccator overnight and they were reweighed.

The soil samples were brought back to laboratory and and stored at 4 °C until they were analyzed. The soil samples were divided into two portions. One of them was analyzed to determine organic matter and water contents and the other was analyzed for PAHs.

After collection, the water samples were brought back to laboratory. The water was passed through glass fiber filter (diameter, 47 mm) and then approximately 10 gram of XAD-2 resin column. The XAD-2 resin was stored in a refrigerator until extraction.

3.4 Preparation for Analysis

3.4.1 Sample Extraction and Concentration

Air filters, sorbent cartridges and dry deposition filters were spiked with PAH surrogate standards prior to extraction in order to determine analytical recovery efficiency. All samples were Soxhlet extracted with a mixture of dichloromethane (DCM): petroleum ether (PE) (20:80, v:v) for 12 h. All extracts were concentrated using a rotary evaporator. The sample extracts were evaporated to approximately 5 ml, and the solvent was exchanged into hexane by addition of 15 ml hexane and evaporating the mixture to ~5 ml, again by addition of 10 ml hexane and evaporating the mixture to ~5 ml. The temperature of water bath was maintained at 30°C during sample concentration and solvent exchange. The sample in 5 ml hexane was transferred into a 40 ml vial. The flask used for evaporation was rinsed with 5 ml hexane and this was also added into the same vial. Then, the sample (~10 ml) was blown down to ~2 ml with a high purity stream of nitrogen (~ 150-200 ml min^{-1}).

Soil samples (10 g), XAD-2 resin and water filters were placed in glass jars capped with Teflon-Lined lids. Samples were spiked with PAH surrogate standards prior to extraction in order to determine analytical recovery efficiency and were soaked in 50 ml of a 1:1 acetone:hexane mixture overnight. Then, they were ultrasonically extracted for 30 min. Extract was dried with anhydrous sodium sulfate. For the concentration step, the same procedures used for the air and dry deposition samples were applied.

3.4.2 Sample Clean-up and Fractionation

Samples (air, dry deposition, soil and water) were cleaned up and fractionated on an alumina-silicic acid column containing 3 g silicic acid and 2 g alumina. Silicic acid was prepared by oven drying at ~100°C for several hours in a flask loosely covered with aluminum foil to remove moisture. It was cooled in a desiccator. Three grams of silicic acid was deactivated by adding 100 µL of deionized water (DI) and shaking the mixture (silicic acid+3% water). The mixture was sat at room temperature for 1 h before use, and used within 12 hours. Alumina was prepared by oven drying at 450°C for several hours. After cooling to room temperature, 2 g of alumina was deactivated by addition of 120 µL DI water (alumina+6% water). Na_2SO_4 placed in beakers and baked in a muffle furnace at 450 °C for several hours, then cooled to room temperature in a desiccator. The column was prewashed with 20 ml DCM fallowed by 20 ml PE. The sample in 2 ml hexane was added into the column with a 2 ml rinse of PE and eluent was collected in a vial at a rate of two drops per second. After letting the sample was pass through column, 20 ml PE was added and eluent was collected in the same vial. This fraction (Fraction 1) contained the PCBs and PCNs. Then the vial used for eluent collection was changed, 20 ml DCM was added into the same rate (Fraction 2). Fraction 2 contained the PAHs and most of the pesticides. For both fractions the solvent was exchanged into hexane and the final sample volume was adjusted to 1 ml by nitrogen blown-down.

3.5 Determination of TSP and Its Organic Matter (OM) Content

After sample collection, glass fiber filters were kept in a desiccator overnight and they were reweighed. TSP was determined by subtracting the initial weight from the final weight. To determine the OM content of the particles, filters were then baked for 1 h at 450 °C in a furnace, then they were allowed to cool to room temperature in a desiccator and re-weighed. Organic matter content was determined by subtracting the final weight (after baking) from the initial weight (before baking). It is possible that the determination of OM content by this method may be interfered by the weight loss of glass fiber filters at high temperatures. The hourly weight loss of filters at 450 °C with time was monitored for 12 hours. It was observed that the maximum weight loss (3 mg) occurs within a 2 h period and the weight loss decreases to 0.3 mg h^{-1} and becomes stable for the remaining period. To minimize the interference from weight loss of filters at high temperatures in OM determination, concurrent blank filters were used for each sample. Determined OM contents were corrected using the weight loss in blank filters during baking. The average weight loss of blank filters (0.38 mg) was significantly lower than the average weight loss of the samples (2.5 mg) indicating that the interference was not significant in OM determination.

3.6 Determination of Water and OM Content of Soil Samples

Soil moisture content was determined by weighing sub-samples of soils before and after drying at 103ºC in an oven for 24 h, and organic matter content was determined by loss on ignition in a muffle furnace at 600ºC for 4 h using Standard Methods of 2540-B and 2540-E, respectively (Eaton, Clesceri, Rice, & Greenberg, 2005). Method 2540-E has been commonly used because it offers an approximation of the amount of organic matter present in the solid fraction (Backe, Cousins, & Larsson, 2004; Nadal, Schuhmaher, & Domingo, 2004).

3.7 Analysis of Field Samples

All the samples were analyzed for PAHs with an Agilent 6890N gas chromatograph (GC) equipped with a mass selective detector (Agilent 5973 inert MSD). A capillary column (HP5-ms, 30m, 0.25 mm, 0.25 μm) was used. The initial oven temperature was held at 50°C for 1 min and raised to 200°C at 25°C min^{-1}, 200 to 300°C at 8°C min^{-1}. The injector, ion source, and quadropole temperatures were 295, 300, and 180°C, respectively. High purity helium was used as the carrier gas at constant flow mode (1.5 ml min^{-1}). The MSD was run in selected ion-monitoring mode. Compounds were identified based on their retention times, target and qualifiers ions. Qualification was based on internal standard calibration procedure.

3.8 Quality Assurance and Quality Control

3.8.1 Sample Collection Efficiency

Sample collection efficiency can be evaluated using the important parameters for the samplers used in this study. These parameters are adsorption on the filters, volatilization and breakthrough for SOC sampling with polyurethane foam (PUF). Polyurethane foam (PUF) has been extensively used for SOC sampling for sample volumes ranging from 300 to 600 m^3. The most volatile compound in a previous study was found in the back plug in an amount less than 11% of the front plug (average for all compounds was 4%). It has been determined by many researchers that with these samplers using PUF breakthrough is not a problem at reasonable flow rates and sample volumes (Cakan, 1999). In this study in addition to PUF, XAD-2 resin which has a higher collection and retention efficiency than PUF for volatile PAHs was used. This combination increases adsorption capacity and minimizes post-collection volatilization problems (Odabasi, 1998). In this study, the sample volume used ~174 m^3 was significantly lower than the volumes used in other studies. Therefore, for the present study breakthrough of PAH vapors from the sorbent cartridge were not likely during sampling. Zhang & McMurry (1991) predicted that for air samplers with pressure drops equal to 10 Pa, evaporative losses from filter

during sampling are small (≤ 10%). Based on this prediction, it can be said that evaporative losses from PS-1 filter were insignificant in this study.

3.8.2 Procedural Recoveries

The recoveries of target compounds were tested externally for PUFs, air filters and dry deposition filters. Hi-vol PUFs (n=6), Hi-vol filters (n=6), and dry deposition filters (n=3) were spiked with a mid-range PAH calibration standard (4.0 μg ml^{-1}) prior to extraction and clean-up to determine the analytical recoveries. Average procedural recoveries of PAHs ranged from 80±19% (dibenz[*a*,*h*]anthracene) to 120±6% (pyrene).

All samples were spiked with PAH internal standards prior to extraction to determine the analytical recovery efficiencies. Average recoveries of PAH internal standards are given in Table 3.5. Each sample was checked for the internal standard recovery efficiencies if they were in the range of 50-120%. Naphthalene, acenaphthylene, and acenaphthene were identified but not quantified since the recovery efficiencies for naphthalene-d_8 and acenapthene-d_{10} were generally low and variable.

Table 3.5 Summary of recovery efficiencies (%) of internal standards (average±std)

PAHs	Ambient Air		Water		Dry Deposition	Soil
	Particle Phase	Gas Phase	Particle Phase	Dissolved Phase		
Phenanthrene-d10	70.6±13.6	69.4±14.8	73.1±14.0	58.8±9.2	68.7±12.6	77.4±4.8
Chrysene-d12	82.5±16.0	81.6±10.0	74.5±12.0	58.4±7.6	70.7±14.1	75.9±5.9
Perylene-d12	80.6±21.4	71.8±14.5	72.8±11.5	54.7±6.7	65.7±17.5	80.6±21.4

3.8.3 Blanks

Field blanks were analyzed to determine the amount of contamination from sample collection and preparation. The amounts found in the blanks are presented in Table 3.6.

Table 3.6 PAH amounts (ng) in blanks (average±std)

PAHs	Ambient Air		Water		Soil	Dry Deposition
	Particle Phase	Gas Phase	Particle Phase	Dissolved Phase		
FLN	15.0±7.2	42.8±18.6	16.8±2.7	56.1±2.4	5.8 ±0.8	14.4±1.9
PHE	57.3±30.4	140.1±44.5	41.8±5.4	136.7±7.6	16.5±2.3	53.4±2.9
ANT	1.1±0.5	4.6±4.4	2.0±0.4	2.8±0.4	0.6± 0.1	0.9±0.1
CRB	0.5±0.4	2.2±1.2	0.3±0.02	3.1±0.2	0.3± 0.03	n.d
FL	9.1±6.0	22.7±10.6	5.8±0.8	43.4±6.3	2.2±0.5	6.9±1.3
PY	9.6±8.1	30.4±24.6	4.0±0.5	22.4±5.4	1.7±0.4	6.5±0.7
BaA	0.4±0.3	1.6±1.5	0.3±0.1	1.1±0.03	0.3± 0.1	n.d.
CHR	2.6±1.3	6.1±3.1	1.6±0.1	7.3±1.2	1.3± 0.4	2.6±0.9
BbF	1.5±1.3	1.1±1.2	0.7±0.1	1.6±0.2	0.8± 0.2	n.d.
BkF	0.7±0.4	0.5±0.6	0.4±0.04	1.8±0.1	0.4±0.2	n.d.
BaP	0.6±0.4	0.5±0.4	0.4±0.1	n.d.	0.4±0.2	n.d.
IcdP	0.6±0.5	0.3±0.4	0.4±0.04	n.d.	0.5±0.1	n.d.
DahA	0.6±0.6	n.d.	0.2±0.1	n.d.	n.d.	n.d.
BghiP	0.6±0.5	0.6±0.5	0.4±0.1	1.7± n.d.	0.4±0.1	n.d.

n.d.: not detected

3.8.4 Detection Limits

The lower limit of quantification is based on the sensivity of the analytical equipment. Instrumental detection limits (IDL) were determined from liner extrapolation from the lowest standard in calibration curve using the area of a peak having a signal/noise ratio of 3. This ratio was used because peaks with smaller ratios can not be reliably integrated. The quantifiable PAH amount was approximately 0.15 pg for 1 µl injection. For the compounds detected in blanks the limit of detection of the method (LOD) was defined as the mean blank mass plus three standard deviations. Instrumental detection limit was used for the compounds that were not detected in blanks. LOD for PAHs are given Table 3.7. In general, PAH amounts in the samples were substantially higher than LODs. Sample quantities exceeding the LOD were quantified and blank-corrected by subtracting the mean blank amount from the sample amount.

Table 3.7 LODs (ng) of PAH compounds for different sample matrices

LOD (ng)	Ambient Air		Water		Dry Deposition	Soil
	Particle Phase	Gas Phase	Particle Phase	Dissolved Phase		
FLN	36.5	98.8	24.9	63.4	20.0	8.2
PHE	148.4	273.7	57.8	159.5	62.1	23.3
ANT	2.5	17.8	3.2	4.0	1.1	1.0
CRB	1.7	5.9	0.3	3.7	n.a.	0.3
FL	27.1	54.5	8.3	62.4	10.6	3.6
PY	33.9	104.4	5.4	38.5	8.7	3.0
BaA	1.4	6.2	0.6	1.2	n.a.	0.6
CHR	6.6	15.5	2.0	10.8	5.2	2.5
BbF	5.3	4.8	1.1	2.2	n.a.	1.4
BkF	2.0	2.3	0.6	2.0	n.a.	1.0
BaP	1.8	1.8	0.5	n.a.	n.a.	0.9
IcdP	2.1	1.4	0.5	n.a.	n.a.	0.9
DahA	2.5	n.a.	0.4	n.a.	n.a.	n.a.
BghiP	2.2	2.2	0.6	n.a.	n.a.	0.8

n.a.: not available

3.8.5 Calibration Standards

The calibration standard solution contained 16 PAHs, carbazole and five deuterated PAHs (naphthalene-d8, acenaphthene-d10, phenanthrene-d10, chrysene-d12, and perylene-d12) that were used to determine the analytical recoveries. Six levels of calibration standards (0.04, 0.4, 1.0, 4.0, 6.0, 10.0 μg ml^{-1} for PAHs, and deuterated PAHs at a fixed concentration of 8 μg ml^{-1}) were used to prepare the calibration curves. In all cases the linear fit was good with $r^2 \geq 0.999$.

3.8.6 GC-MS Performance

The MS was tuned daily using the HP ChemStation Standard AutoTune routine with perfluorotributylamine (PFTBA). If any key ion abundance observed during daily tune differed by more than 10% absolute abundance from that observed during the previous daily tuning, the instrument was retuned until the above condition was met. A midrange calibration standard containing 4.0 μg ml^{-1} of PAHs was analyzed during every twelve hour period to confirm system performance. If the percent difference of a response factor any compound was greater than 20%, the initial calibration was assumed to be invalid, and system was recalibrated. Samples were analyzed occasionally as duplicates. Differences in duplicate samples were less than 5%.

3.8.7 Compound Identification

Agilent ChemStation software was used for the identification of PAHs in the samples. Identification of individual PAHs was based on their retention times (within ±0.05 minutes of the retention time of calibration standard). Identification was confirmed by the abundance of the qualifier ion relative to the target ion (relative intensity of qualifier ion). If the relative intensity in the sample spectrum was within ±20% of the relative intensity in the standard spectrum, identification was confirmed. PAHs identified in the samples were quantified using the internal standard calibration procedure.

3.8.8 Evaluation of Analytical Method

The analytical method used for samples was tested by analyzing four aliquots of standard urban dust reference material (SRM-1649) from the National Institute of Standards and Technology (NIST). Results of this analysis, NIST certified values, and the values reported by Halsall et al. (1994) and Odabasi (1998) from the analysis of the same material are given in Table 3.8 for comparison. As seen in Table 3.8, resulting concentrations of SRM-1649 analysis in this study were in good agreement

with the certificated values by NIST and the values reported by Halsall et al. (1994) and Odabasi (1998).

Table 3.8 Concentrations of PAHs analyzed in SRM-1649 (mg kg^{-1}) (average±std)

PAH	This Study (n=4)	NIST (Certified)[a]	Odabasi, 1998	Halsall et al., 1994
ACN	0.17±0.04	n.a.	n.a.	n.a.
ACT	0.14±0.01	n.a.	0.31±0.18	0.27±0.17
FLN	0.14±0.01	n.a.	0.47±0.10	0.36±0.09
PHE	4.35±0.35	4.14±0.37	5.76±1.85	5.05±0.85
ANT	0.50±0.02	0.43±0.08	0.47±0.01	0.41±0.08
CRB	0.26±0.02	n.a.	n.a.	n.a.
FL	7.32±0.35	6.45±0.18	7.51±0.24	n.a.
PY	6.21±0.27	5.29±0.25	5.95±0.14	6.56±0.32
BaA	2.87±0.69	2.21±0.07	2.50±0.02	2.38±0.29
CHR	7.55±0.45	3.05±0.06	2.89±0.03	3.59±0.21
BbF	6.90±0.51	6.45±0.64	6.04±0.07	5.74±0.45
BkF	3.70±0.18	1.91±0.03	n.a.	n.a.
BaP	2.70±0.10	2.51±0.09	2.56±0.03	3.30±0.23
IcdP	3.48±0.19	3.18±0.72	3.86±0.01	n.a.
DahA	1.08±0.06	0.29±0.02	n.a.	0.56±0.05
BghiP	4.51±0.27	4.01±0.91	4.32±0.10	4.22±0.82

[a] Certificated values by NIST

CHAPTER FOUR
RESULTS AND DISCUSSIONS

This chapter presents the results of ambient concentrations of PAHs, their gas/ particle partitioning, dry deposition fluxes, water concentrations and air-water exchange, soil concentrations and air-soil exchange. Experimental particle-phase dry deposition velocities were also calculated using the measured fluxes and concentrations. Results of these measurements were compared to the values reported in the literature.

4.1 Ambient Air Concentrations

The concentrations of gas and particle phases of PAHs were measured in suburban and urban sites, Izmir, Turkey. Gas and particle-phase concentrations of individual PAHs at all three sites (Suburban, Urban 1, and Urban 2) are presented in Table 4.1. Gas and particle-phase total PAH ($\sum_{14}$PAH) concentrations ranged from 23.5 (Suburban) to 109.7 (Urban 1) and 12.3 (Suburban) to 34.5 (Urban 1) ng m^{-3}, respectively (Table 4.1). Average total PAH (gas+particle) concentrations were 36±39, 144±163 and 92±58 ng m^{-3} for Suburban, Urban 1, and Urban 2 sites, respectively. Concentrations observed in this study were within the range of previously reported values in other urban and industrial sites around the world (Table 2.2). Fang et al. (2004a) have reported the total (gas+particle) atmospheric concentrations of Σ_{13}-PAH as 320, 477, and 679 ng m^{-3} for rural, urban and industrial sites in Taiwan, respectively. Total Σ_{14}PAH concentrations (36±39, 144±163, 92±58 ng m^{-3}) measured at the Suburban, Urban 1, and Urban 2 sites in the present study are considerably lower than those reported for urban sites in Bursa (Tasdemir & Esen, 2007a) and in Chicago (Odabasi et al., 1999a). However, total Σ_{14}PAH concentrations measured at all sites in this study are significantly higher than those reported by Mandalakis et al. (2002) for urban Athens.

Table 4.1 Ambient air concentrations of individual PAH compounds for Suburban, Urban 1 and Urban 2 sites (ng m^{-3}) (average±SD).

PAHs	Suburban		Urban 1		Urban 2	
	Gas	Particle	Gas	Particle	Gas	Particle
FLN	4.1±4.5	0.6±1.0	12.5±10.3	0.1±0.1	11.3±8.0	0.2±0.2
PHE	11.7±12.1	1.9±2.6	40.8±36.2	1.0±0.8	36.5±18.0	2.1±2.6
ANT	0.5±0.7	0.1±0.1	5.6±6.2	0.1±0.1	2.0±2.0	0.2±0.3
CRB	0.4±0.8	0.2±0.3	1.0±2.0	0.1±0.1	0.5±0.8	0.1±0.1
FL	3.7±4.1	1.5±2.5	27.3±43.5	2.8±3.7	11.5±8.8	2.8±3.8
PY	2.4±2.4	1.4±2.2	20.2±27.0	3.1±4.2	8.6±6.1	2.6±3.3
BaA	0.1±0.1	0.5±1.0	0.6±0.5	3.0±4.8	0.2±0.2	1.2±1.5
CHR	0.4±0.3	1.5±2.5	1.6±1.0	6.2±8.6	0.8±0.8	3.1±3.6
BbF	0.05±0.04	0.9±1.3	0.03±0.02	3.4±4.1	0.1±0.1	2.1±2.2
BkF	0.02±0.01	0.8±1.2	0.02±0.01	3.6±4.6	0.04±0.1	1.7±1.9
BaP	0.02±0.02	0.7±1.0	0.008±0.006	3.1±4.7	0.02±0.02	1.3±1.4
IcdP	0.01±0.01	0.9±1.4	0.006±0.004	3.4±4.5	0.02±0.03	1.3±1.3
DahA	0.02±0.03	0.4±0.7	0.003±0.001	1.3±1.9	0.04±0.05	0.4±0.5
BghiP	0.03±0.04	0.9±1.1	0.008±0.005	3.4±3.8	0.03±0.03	1.4±1.3
$\sum_{14}$ PAH	23.5±23.8	12.3±16.2	109.7±111.7	34.5±45.7	71.7±37.3	20.4±23.6

The PAH levels measured at the Suburban site in this study are similar to those reported by Bozlaker, Muezzinoglu, & Odabasi (2007) for an industrial site in Izmir, by Tsapakis & Stephanou (2005) for urban Heraklion, by Ohura et al. (2004) for industrial sites in Fuji and Shimizu, and by Dachs et al. (2002) for urban/industrial Baltimore. The PAH levels at the urban sites determined in this study are comparable to those reported by Possanzini et al. (2004) for downtown Rome and by Halsall et al. (1994) for urban sites in London and Manchester (Table 2.2).

Figure 4.1 shows the average individual PAH concentrations measured in this study. Higher concentrations were observed for low molecular weight PAHs (Figure 4.1). The gas/particle phase distributions of individual PAHs at different sites are illustrated in Figure 4.2. Results indicated that about 69, 81, and 82% of $\sum_{14}$PAHs were in the gas phase for the Suburban, Urban 1, and Urban 2 sites, respectively.

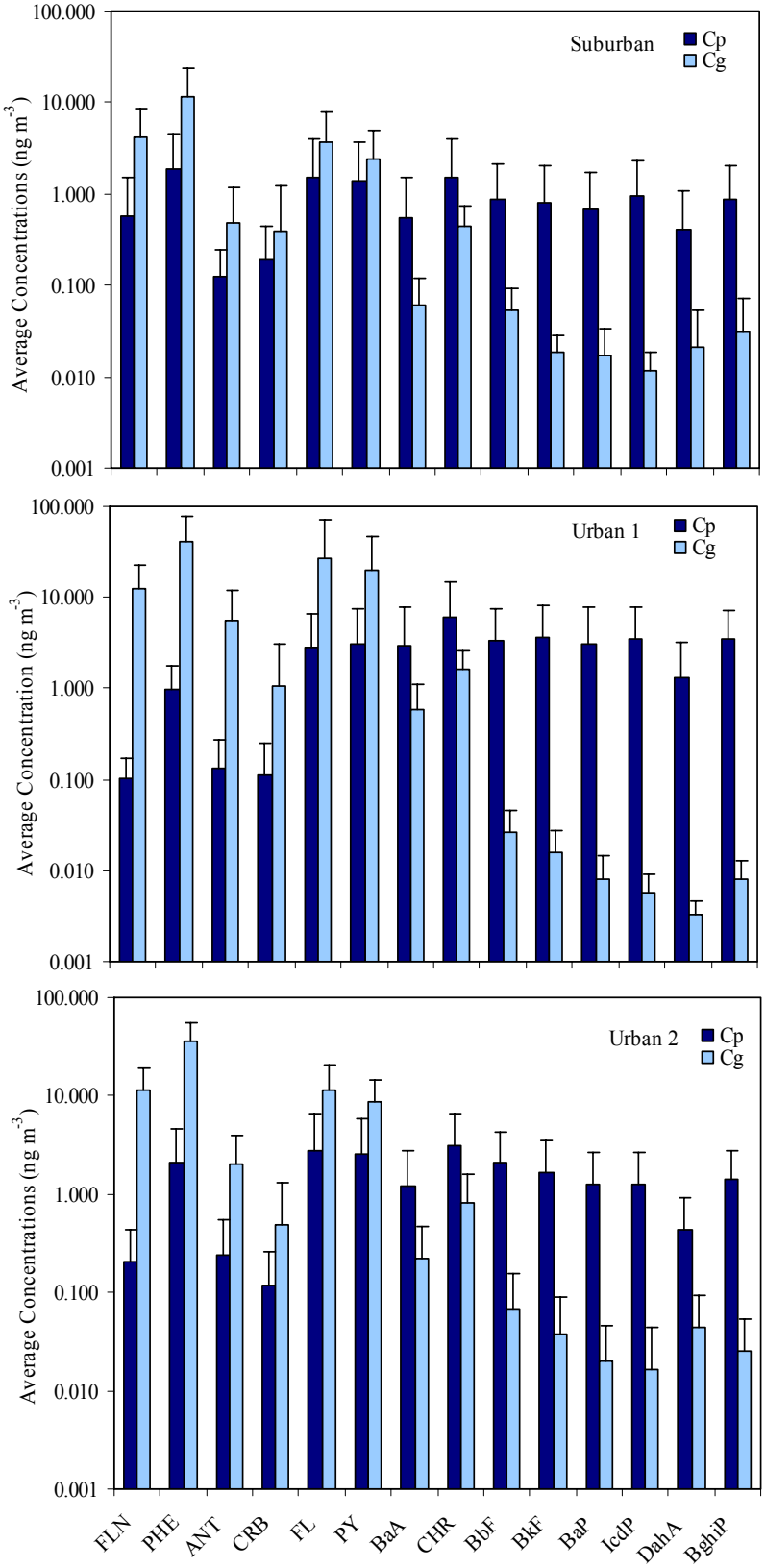

Figure 4.1 Average gas and particle concentrations at Suburban, Urban 1 and Urban 2 sites, Izmir. Error bars are 1 SD.

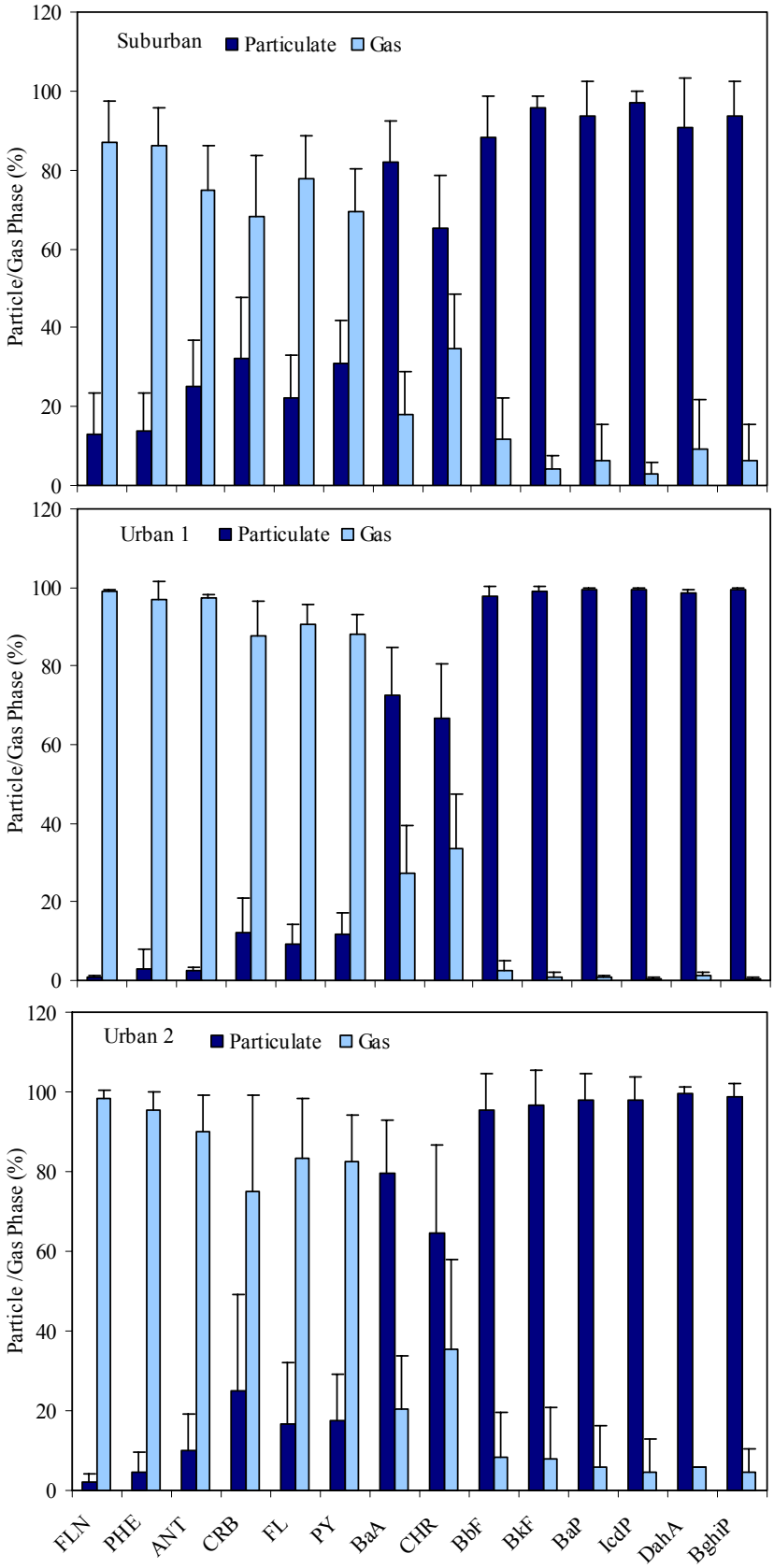

Figure 4.2 Average gas/particle phase distribution of individual PAHs. Error bars are 1 SD.

Because of their higher volatility, low to medium molecular weight PAHs (3-5 rings) were more abundant in the gas-phase in the present study, similar to the previous studies (Fang et al., 2004a; Gevao, Hamilton-Taylor, & Jones, 1998; Ohura et al., 2004; Tasdemir & Esen, 2007a). Higher ambient PAH concentrations were measured in the gas-phase and $\sum_{14}$PAH concentrations were dominated by lower molecular weight PAHs. These results were in good agreement with those reported previously (Dachs et al., 2002; Halsall et al., 1994; Mandalakis et al., 2002; Odabasi et al., 1999a; Ohura et al., 2004; Possanzini et al., 2004; Tasdemir & Esen, 2007a).

In Suburban site, phenanthrene, fluorene, fluoranthene, and pyrene accounted for 42, 14, 12, and 10% of Σ_{14}PAHs in summer period, in Urban 1 site they were 41, 12, 14, and 15% of Σ_{14}PAHs and in Urban 2 site they were 50, 10, 21, and 8% of Σ_{14}PAHs. In winter period, contributions of phenanthrene, fluorene, fluoranthene and pyrene in Suburban, Urban 1, and Urban 2 sites were 35, 12, 16, and 11%, 26, 8, 22, and 16%, and 39, 13, 14, and 13% of Σ_{14}PAHs, respectively. These percentages were similar to the ones reported previously by Bozlaker, Muezzinoglu, & Odabasi (2007), Gevao, Hamilton-Taylor, & Jones (1998), and Odabasi et al. (1999a).

4.1.1 Effect of Meteorological Parameters on Air Concentrations of PAHs

The effect of wind speed and direction on atmospheric concentrations of individual PAHs was investigated using multiple linear regression analysis (Sofuoglu, Cetin, Bozacioglu, Sener, & Odabasi, 2004):

$$C_t = m_1 T + m_2 U + m_3 \cos WD + b \qquad (4.1)$$

where C_t is the total (gas+particle phase) PAH concentration (ng m^{-3}), T is the average atmospheric temperature (°C), U is the wind speed (m s^{-1}), WD is the predominant wind direction (radians) during the sampling period, and m_1, m_2, m_3, and b are the regression parameters.

The results of multiple linear regression analysis are presented in Table 4.2. Temperature, wind speed and wind direction together accounted for 1% (carbazole) to 31% (anthracene), 54% (carbazole) to 82% (anthracene), and 8% (carbazole) to 85% (pyrene) of the variability in the atmospheric PAH concentrations for Suburban, Urban 1, and Urban 2 sites, respectively (Table 4.2). The m_1 values were insignificant for all PAHs for Urban 1 site. The m_1 values were statistically significant for all PAHs ($p<0.05$-0.1) except carbazole for Suburban site, carbazole and fluoranthene for Urban 2 site. Generally negative m_1 values were obtained for PAHs indicated that their concentrations increased with decreasing temperature. This was probably due to increased PAH emissions from combustion sources like residential heating with decreased ambient temperature. For most of the compounds, m_2 had negative values and they were statistically significant for most of the compounds. This indicated that their concentrations decreased as the wind speed increased and advection was also an important parameter controlling the concentrations of atmospheric PAHs. The regression parameter related to wind direction (m_3) varied between negative and positive values and it was statistically significant for the urban sites (Urban 1 and Urban 2) while it was insignificant for the Suburban site. Negative values for m_3 indicate that relatively higher concentrations were observed when the wind was from southerly directions while positive values point northerly directions for high concentrations. The results were consistent with the locations of predominant sources (urban Izmir plume at north of the Suburban, Urban 1, and Urban 2 sites, nearby highways and residential areas at south of Urban 1 and Urban 2 sites). Results of MLR analysis indicated that in the present study meteorological parameters were more effective on the ambient PAH concentrations at urban sites compared to the Suburban site.

Table 4.2 Summary of regression parameters for equation (4.1).

PAHs	Suburban					Urban 1					Urban 2				
	m_1	m_2	m_3	r^2	n	m_1	m_2	m_3	r^2	n	m_1	m_2	m_3	r^2	n
FLN	-0.28[a]	-0.51[a]	0.60	0.26	63	-0.27	-4.70[a]	3.68	0.62	14	-0.53[a]	-2.62[a]	-7.26[a]	0.83	16
PHE	-0.71[a]	-1.53[a]	2.39	0.24	63	-0.14	-20.38[a]	15.68	0.67	14	-1.,01[a]	-2.58	-22.71[a]	0.68	16
ANT	-0.05[a]	-0.04	0.06	0.31	63	-0.41[b]	-2.79[a]	4.48[a]	0.82	14	-0.08[a]	-0.17	-3.54[a]	0.78	16
CRB	0.00	0.03	0.08	0.01	63	-0.05	-0.98[a]	1.57[b]	0.54	14	0.01	0.24	0.14	0.08	16
FL	-0.39[a]	-0.42	0.67	0.25	63	-3.00	-16.70[b]	39.11[a]	0.63	14	-0.29	0.07	-9.27[b]	0.31	16
PY	-0.28[a]	-0.41[b]	0.64	0.28	63	-1.89	-12.03[a]	26.03[a]	0.67	14	-0.64[a]	-2.52[a]	-4.81[a]	0.85	16
BaA	-0.06[a]	-0.08	0.14	0.28	63	-0.25	-2.49[a]	4.34[a]	0.76	14	-0.10[a]	-0.46[b]	-1.41[a]	0.69	16
CHR	-0.16[a]	-0.26[a]	0.40	0.26	63	-0.47	-4.45[a]	7.08[a]	0.78	14	-0.22[a]	-1.61[a]	-3.93[a]	0.77	16
BbF	-0.07[a]	-0.13[a]	0.22	0.25	63	-0.20	-1.91[a]	2.70[a]	0.74	14	-0.12[a]	-1.01[a]	-2.21[a]	0.74	16
BkF	-0.07[a]	-0.12[a]	0.20	0.27	63	-0.24	-2.08[a]	3.27[a]	0.74	14	-0.11[a]	-0.79[a]	-1.52[a]	0.73	16
BaP	-0.05[a]	-0.11[a]	0.20	0.23	63	-0.22	-2.21[a]	3.91[a]	0.75	14	-0.08[a]	-0.59[a]	-1.29[a]	0.70	16
IcdP	-0.06[a]	-0.17[a]	0.32	0.19	63	-0.17	-2.27[a]	3.16[a]	0.75	14	-0.07[a]	-0.69[a]	-1.18[a]	0.72	16
DahA	-0.02[b]	-0.12[a]	0.29[a]	0.24	63	-0.06	-0.94[a]	1.33[a]	0.72	14	-0.02[a]	-0.18[a]	-0.53[a]	0.75	16
BghiP	-0.05[a]	-0.16[a]	0.30	0.22	63	-0.16	-1.80[a]	2.44[a]	0.73	14	-0.06[a]	-0.74[a]	-1.31[a]	0.70	16

[a] $p<0.05$
[b] $p<0.10$

4.1.2 Sources of PAHs

PAHs are almost entirely anthropogenic in origin and are major byproducts of the incomplete combustion of all types of organic matter (e.g., gasoline, diesel and other fuels) (Ravindra, Sokhi, & Van Grieken, 2008; Fang et al., 2004b). PAH emission sources are primarily categorized as follows: heavy oil combustion, natural gas combustion, wood and coal combustion, diesel combustion, and vehicles (Yang & Chen, 2004).

Winter/summer total PAH (gas+particle) concentration ratios ranged between 1.4 (carbazole) - 5.9 (benz[*a*]anthracene), 3.1 (phenanthrene) - 11.0 (benzo[*a*]pyrene) and 0.6 (carbazole) - 13.2 (benz[*a*]anthracene) for Suburban, Urban 1 and Urban 2 sampling sites, respectively. Higher PAH concentrations observed during winter were probably due to the increasing emissions from residential heating (Figure 4.3). Different ratios for individual compounds indicate that residential heating emissions have a different profile than summer-time emissions. Similar increases in winter PAH concentrations were recently reported (Bae, Yi, & Kim, 2002; Bozlaker, Muezzinoglu, & Odabasi, 2007; Gevao, Hamilton-Taylor, & Jones, 1998; Kiss, Varga-Puchony, Rohrbacher, & Hlavay, 1998; Ohura et al., 2004; Park, Kim, & Kang, 2002; Schnelle-Kreis, Sklorz, Peters, Cyrys, & Zimmermann, 2005).

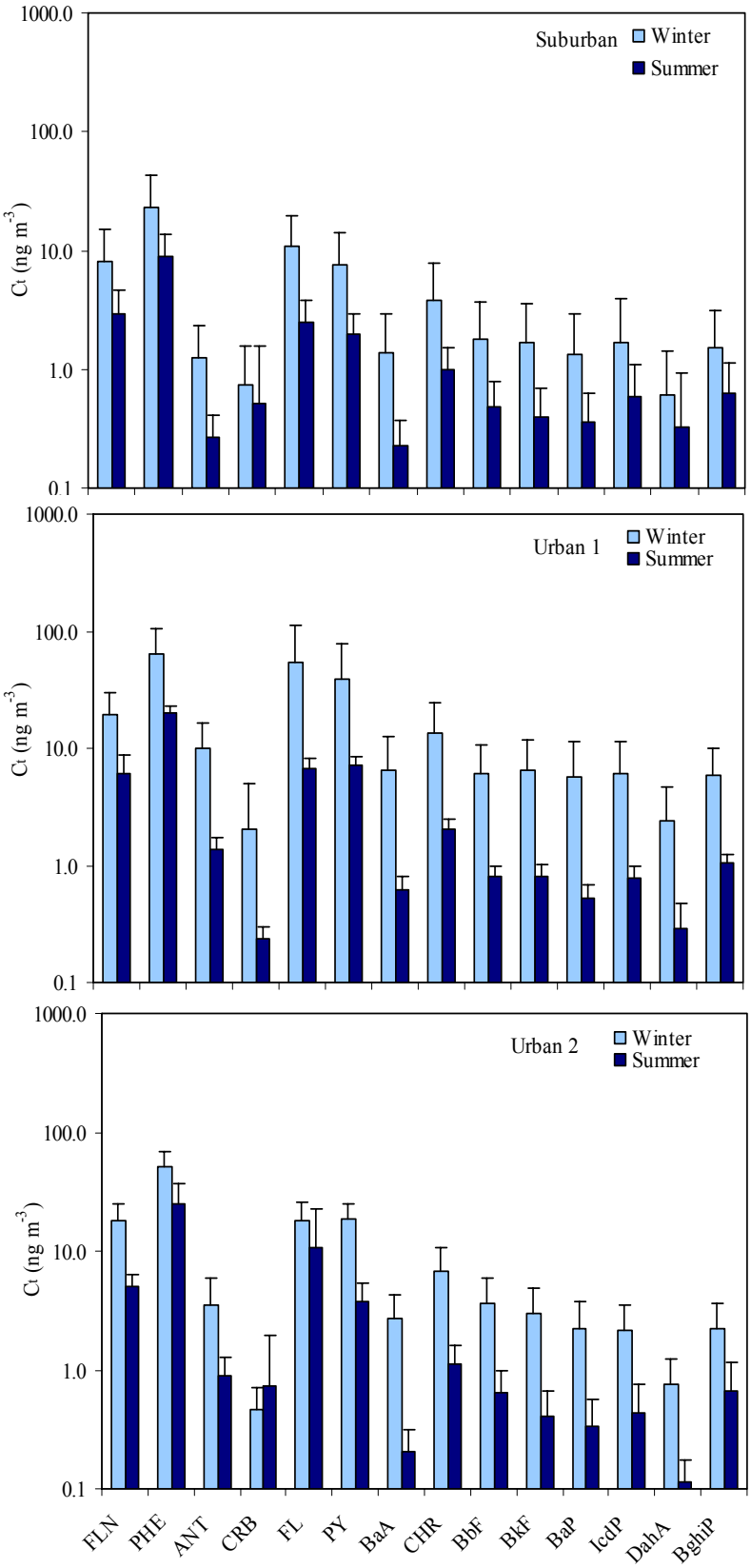

Figure 4.3 Seasonal variation of individual PAH compounds in this study. Error bars are 1 SD.

The concentration ratios of individual PAHs in ambient samples and source emissions are frequently employed as diagnostic tools to identify their origin in ambient air (Manoli, Kouras, & Samara, 2004; Tang et al., 2005). Figure 4.4 illustrates an example of such diagnostics as a plot of FLN/(FLN+PY) against IcdP/(IcdP+BghiP) for particulate PAHs. Both FLN/(FLN+PY) and IcdP/(IcdP+BghiP) are greater than 0.5 in the case of coal/biofuel emissions (Liu et al., 2007).

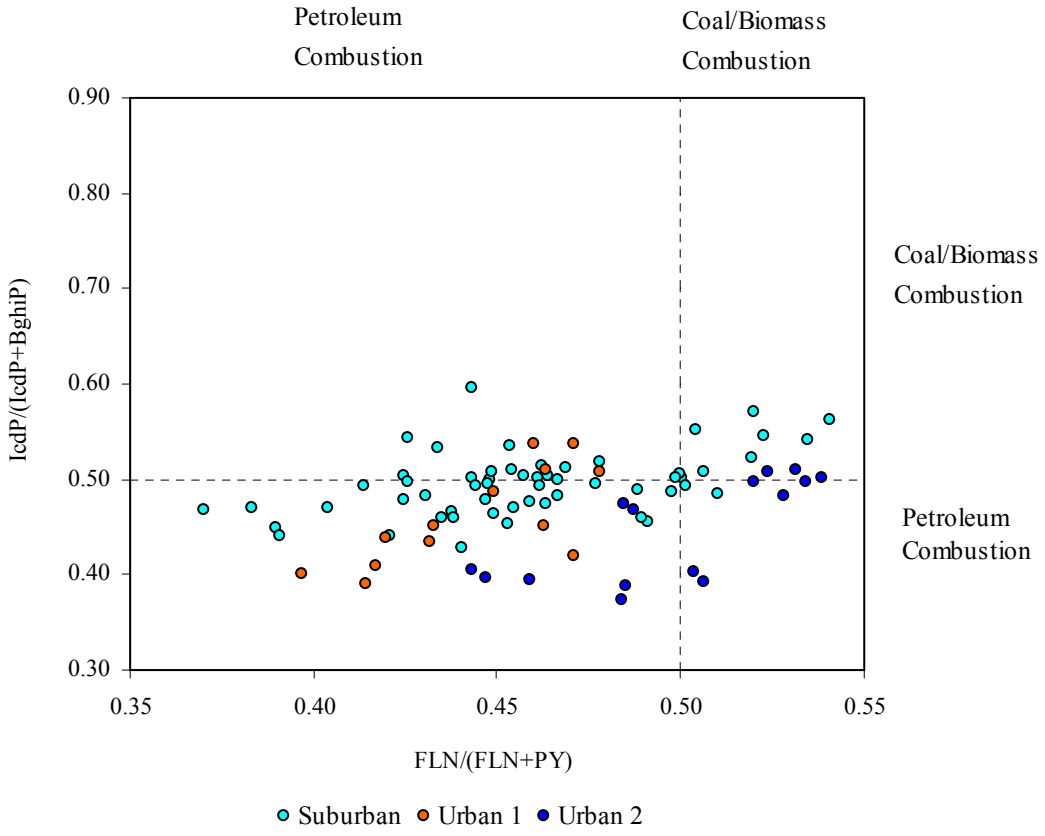

Figure 4.4 Plot of FLN/(FLN+PYR) against IcdP/(IcdP+BghiP) for PAH source diagnostics. Two dashed lines represent the thresholds for petroleum combustion and coal/biomass burning.

In Figure 4.4, most of the Urban 1 and Urban 2 samples fall in the left-bottom quadrant, indicating predominant influence of petroleum combustion. There are differences observed in PAH composition profiles between suburban and urban sites. Suburban samples fall in the left-bottom and top quadrants suggesting that coal/biomass combustion and vehicular emissions are major PAH sources at this site.

In North China emission sources of particle-phase PAHs were also identified using a diagnostic plot of FLN/(FLN+PY) vs. IcdP/(IcdP+BghiP). Samples appeared in top-right quadrant, suggesting coal/biomass combustion emissions. No difference was detected in PAH composition profiles between the urban and rural sites (Liu et al., 2007).

Li & Kamens (1993) observed that the ratio of BaA/BaP was 0.5 for gasoline exhaust, and 1.0 for both diesel exhaust and wood combustion. In the present study the BaA/BaP ratios were significantly higher for winter (1.05 and 1.27) than summer (0.70 and 0.71) at Suburban and Urban 2 sites, respectively. These results indicated that, in addition to traffic emissions, wood and coal combustion are the major PAH sources in winter at Suburban and Urban 2 sites. In summer, traffic emissions were dominated at these sites. At Urban 1 site, BaA/BaP ratio was similar for winter (1.17) and summer (1.21) suggesting traffic, coal and wood combustion are the major sources of PAHs for these seasons. Many other diagnostic ratios for PAHs are used to identify the potential emission sources at different sites. The diagnostic ratios calculated in this study and reported ones by other studies are compared in Table 4.3. In conclusion, the diagnostic plot and diagnostic PAH ratios approaches indicate that traffic emissions (petroleum combustion) were the dominant PAH sources at all sites for both seasons. During winter, residential heating was also a significant PAH source at all sites.

Table 4.3 Concentrations diagnostic ratios for ambient air PAHs for major emission sources in this study.

Diagnostic Ratios	Values (Winter / Summer)			Sources			
	Suburban	Urban 1	Urban 2	Gasoline	Diesel	Coal	Wood
BaA/CHR	0.33 0.24	0.43 0.30	0.39 0.18	0.28-1.2[a] 0.47-0.59[c]	0.17-0.36[a]	1.0-1.2[a] 1.05-1.17[c]	0.66-0.92[c]
BaA/(BaA+CHR)	0.24 0.19	0.30 0.23	0.28 0.15	0.22-0.55[b,d]	0.38-0.64[b,d]	-	0.43[d]
BaP/BgiP	0.84 0.61	0.85 0.48	0.99 0.51	0.3-0.4[a]	0.46-0.81[a]	0.9-6.6	-
IcdP/BghiP	1.02 0.91	0.98 0.74	0.97 0.66	0.27-0.4[c] <0.4[e]	1[c,e]	1.06-1.12[c]	0.23-0.33[c]
IcdP/(IcdP+BghiP)	0.50 0.47	0.49 0.43	0.49 0.40	0.21-0.22[b,d] 0.18[c]	0.35-0.70[b,c,d,e]	0.56[e]	0.62[d,e]
BbF/BkF	1.08 1.37	0.94 0.99	1.21 1.66	1.07-1.45[c]	>0.5[e]	3.53-3.87[c]	0.76-1.08[c]
PHE/ANT	20.50 36.57	7.29 15.01	17.79 29.12	3.4-8[a]	7.6-8.8[a]	3[a]	-
FLN/(FLN+PY)	0.51 0.58	0.38 0.44	0.49 0.58	0.40[c,d] <0.5[e]	0.60-0.70[c,d] >0.5[e]	-	0.74[c]
FL/(FL+PY)	0.59 0.54	0.55 0.49	0.48 0.69	0.40[b]	0.60-0.70[b]	-	-
BghiP/BaP	1.25 1.70	1.33 2.11	1.05 1.98	2.5-3.3[d]	1.2-2.2[d]	-	-
BaP/(BaP+CHR)	0.24 0.25	0.27 0.20	0.23 0.21	0.73[e]	0.5[e]	-	-
PY/BaP	8.65 6.61	8.26 14.74	12.15 18.11	~1[e]	~10[e]	-	-

[a] Simcik, Eisenreich, & Lioy, 1999; [b] Tang et al., 2005; [c] Fang et al., 2004b; [d] Manoli, Kouras, & Samara, 2004; [e] Ravindra, Sokhi, & Van Grieken, 2008

4.1.3 Gas-Particle Partitioning of PAHs

Partitioning of atmospheric organic compounds between the gas and particle phases is parameterized using the gas/particle partition coefficient. The gas/particle partition coefficient (K_P) is expressed using the Equation (2.1). The octanol-air partitioning coefficient (K_{OA}) can be used to predict K_P with the assumption of predominant distribution process is absorption. The relationship between K_P and K_{OA} is expressed using the Equation (2.3). Plots of log K_P vs. log K_{OA} have been used in field and laboratory studies to evaluate the gas-particle partitioning of POPs. A good correlation between log K_P and log K_{OA} and a slope near 1 indicates that octanol is a good surrogate for the partitioning of POPs into aerosol organic matter (Sofuoglu et al., 2004). Figure 4.5 is a plot of log K_P (m^3 ng^{-1}) measured at Suburban and Urban 1 sites vs. log K_{OA}. For the plot containing all data, K_P and K_{OA} were well correlated (r^2= 0.80-0.95). The regression parameters, m and b were 0.48 and 6.36 for Suburban and 0.89 and 10.7 for Urban 1 sites, respectively. For individual samples, K_P and K_{OA} were also well correlated (r^2=0.72-0.97 and 0.94-0.98 for Suburban and Urban 1 sites). The slope values (m) for Suburban and Urban 1 sites ranged between 0.22 to 0.74, and 0.74 to 1.01, respectively. The variation of slope values for Suburban and Urban 1 sites suggests that atmospheric particles for different sites have different sorbing properties. Good correlation between log K_P and log K_{OA} suggests that K_{OA} is a useful predictor for the partitioning of PAHs into aerosol OM. Even though strong correlations were observed between log K_P and log K_{OA}, some of the previously reported slopes were significantly diferent than 1. As a result of plots of log K_P and log K_{OA}, slope values of 0.45-0.99 for OCPs (Sofuoglu et al., 2004), 0.79, 0.99, 0.74, and 0.65 for PAHs, OCPs, PCBs, and PCNs, respectively (Finizio et al., 1997; Shoeib & Harner, 2002; Falconer & Harner, 2000; Harner & Bidleman, 1998). Goss & Schwarzenbach (1998) have suggested that the slope might be deviate from 1 for equilibrium partitioning when log K_P is plotted vs. log K_{OA}. Deviations from a unity slope further indicate that atmospheric particles have sorbing properties different from that of octanol.

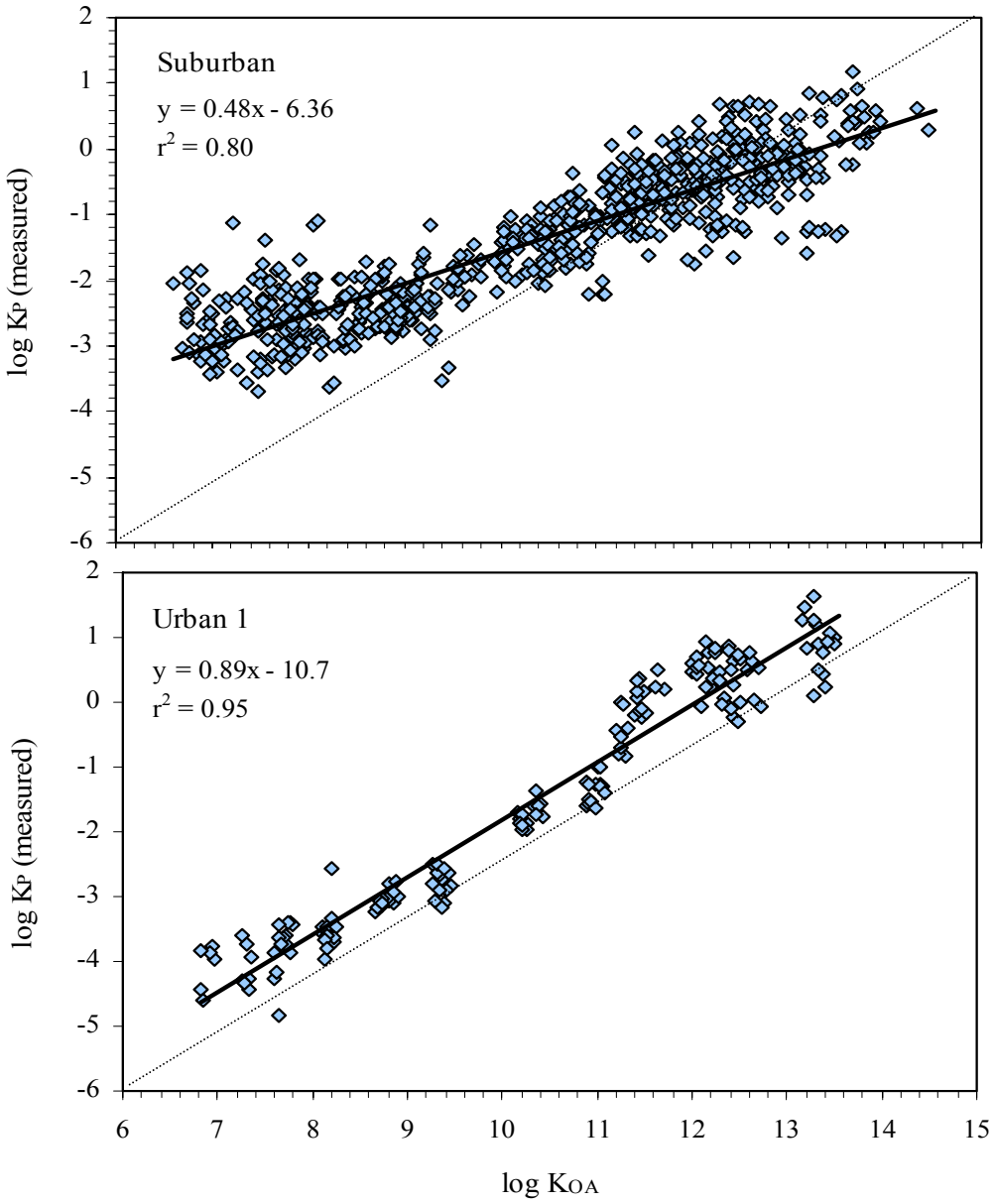

Figure 4.5 Plots of log K_P (m^3 ng^{-1}) measured at Suburban and Urban 1 sampling sites vs. log K_{OA}. The solid diagonal line represents a 1:1 relationship (equilibrium).

The atmospheric PAH concentrations measured in this study were used to investigate the partitioning of PAHs between particle and gas-phase. The experimental gas-particle partition coefficients (K_P) for individual PAHs were calculated using Equation (2.1). The octanol-air partitioning coefficient (K_{OA}) can be used to predict K_P with the assumption of predominant distribution process is absorption. Strong association of PAHs with soot particles in soot-water systems suggests that besides absorption, adsorption partitioning could also be an important

sorption mechanism in the atmosphere. The a_{EC} value (62.7 m^2 g^{-1}) used in Equations (2.4) and (2.6) was taken from a recent study by Jonker, & Koelmans (2002). It was assumed that a_{EC}/a_{AC}= 1, f_{OM}=1.6 f_{OC}, and f_{OC}/f_{EC}= 3 where f_{OC} is the fraction of total organic carbon (Dachs & Eisenreich, 2000; Ribes et al., 2003). Under these assumptions, modeled K_P values were calculated using Equation (2.3) for absorptive partitioning and Equation (2.4) for both absorptive and adsorptive partitioning (Odabasi, M., Cetin, E., & Sofuoglu, A., 2006). The modeled K_P values for absorptive partitioning and for both absorptive and adsorptive partitioning were compared to the measured ones in Figure 4.6. The correlations between experimental and modeled K_P values were significant (r^2=0.79 and 0.94 for Suburban and Urban 1 sites, respectively). Octanol based absorptive partitioning model predicted lower partition coefficients especially for relatively volatile PAHs. However, overall there is a relatively good agreement between the measured K_P and soot-based model predictions. Ratios of measured/modeled partition coefficients ranged between 0.15 (benzo[*g,h,i*]perylene) - 651 (fluorene) (80±394, average±SD) and 1.2 (chrysene) - 15.5 (fluorene) (4.5±6.0, average±SD) for K_{OA} model in Suburban and Urban 1 sites, respectively. Soot model predictions were relatively better and measured to modeled ratios ranged between 0.11 (benzo[*g,h,i*]perylene) - 232 (fluorene) (30±141, average±SD) and 0.6 (chrysene) - 5.6 (fluorene) (2.3±2.7, average±SD) for Suburban and Urban 1 sites, respectively. Recent studies reported that the soot based model showed a good predictability at an urban site (Chicago, IL) but underestimated the values at a rural site (Eagle Harbor) by an order of magnitude (Vardar et al., 2004; Galarneau, Bidleman, & Blanchard, 2006). It was suggested that characterizing atmospheric soot, determining the temperature dependence of soot-air partitioning, and quantifying the exchangeable fraction of each PAH on aerosols will help to explain the differences between predicted and observed partition coefficients (Galarneau, Bidleman, & Blanchard, 2006).

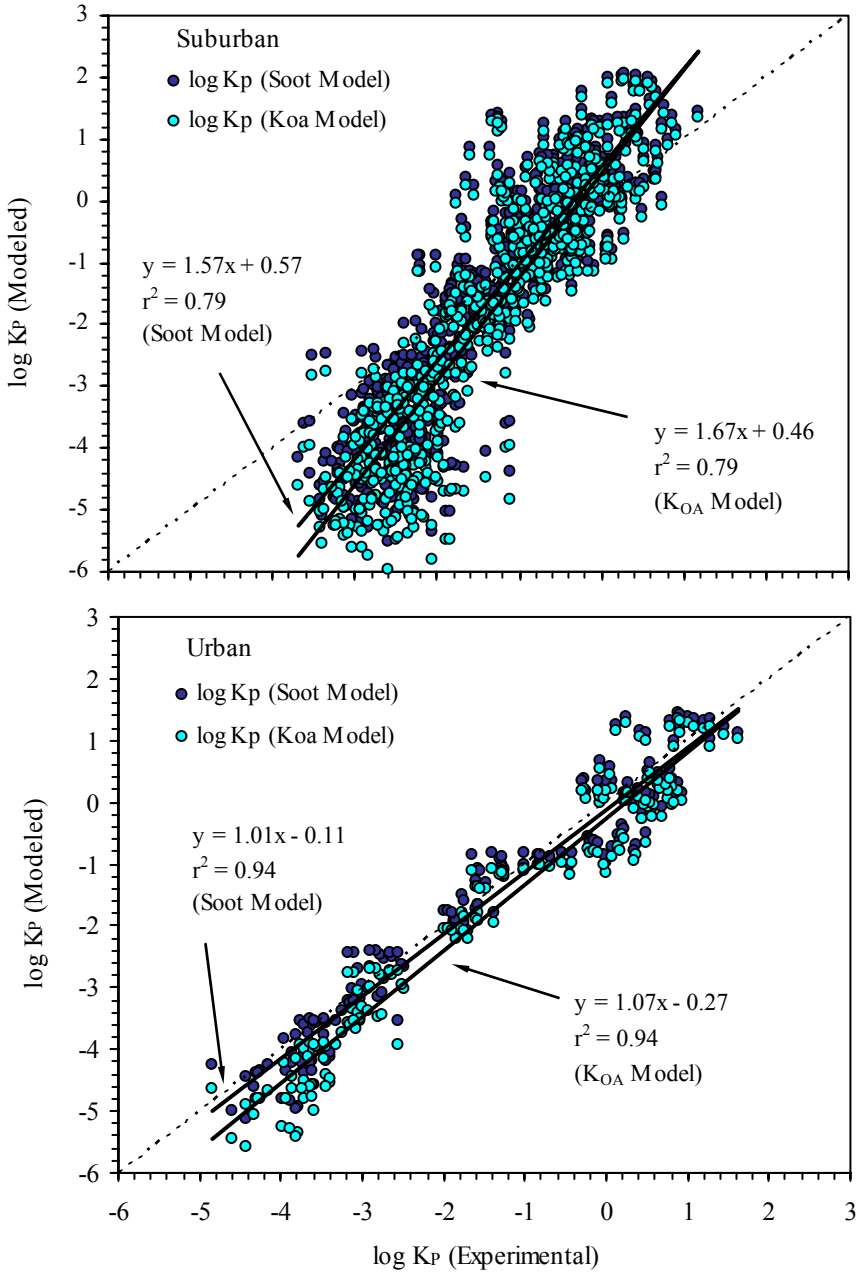

Figure 4.6 Comparison of the measured and predicted K_P values by two partitioning models. The solid diagonal line represents a 1:1 relationship (equilibrium).

It was observed that gas particle partitioning of PAHs was different for Suburban and Urban 1 samples. This was evident by the more shallow slopes obtained from the plots of log K_P vs. log K_{OA} at the Suburban site compared to those for Urban 1 site. Recently, Vardar et al. (2004) have reported steeper slopes for lake samples relative to the land samples in Chicago. It was suggested that the observed differences between the lake and land samples may be due to the different properties of particles (i.e., aged particles as a result of longer residence time for lake samples), non-exchangeability and differences in activity coefficients of PAHs. Similarly, in the present study Urban 1 samples had steeper slopes than the Suburban samples. However, unlike the Chicago samples that had different levels of TSP concentrations (i.e., low for lake and higher for land samples) Suburban and Urban 1 samples of the present study had similar average TSP concentrations (~70-80 μg m^{-3}, respectively). Previous experimental studies have shown that a greater fraction of the higher molecular weight PAHs are associated with fine particles relative to the lower molecular weight compounds (Kiss et al., 1998; Tasdemir & Esen, 2007b; Odabasi et al., 1999b). Recent studies indicated that the contribution of wind-entrained soil particles to atmospheric coarse PM is significant at the Suburban site (Yatkin & Bayram, 2007; Yatkin & Bayram, 2008). The contribution of local soil to the coarse PM increases especially the particle-phase concentrations of low molecular weight PAHs. This increase in particle-phase concentration will result in larger K_P values especially for low molecular weight PAHs (Equation 2.1) and consequently more shallow slopes for log K_P vs. log K_{OA} plots (Figure 4.5).

4.2 Particle Phase Dry Deposition Fluxes and Velocities

The range for particle-phase fluxes of individual PAHs measured with dry deposition plates ranged between 132 (benz[*a*]anthracene) to 3144 (phenanthrene) ng m^{-2} day^{-1} at the Suburban site and between 34 (dibenz[*a*,*h*]anthracene) to 1492 (phenanthrene) ng m^{-2} day^{-1} at Urban 1 site (Table 4.4). Average fluxes of $\sum_{14}$PAH for both sites were 8160±5024 and 4286±2782 ng m^{-2} day^{-1}, respectively.

Table 4.4 Average particle phase dry deposition fluxes and velocities of individual PAHs (average±SD).

PAHs	Dry deposition flux (ng m^{-2} day^{-1})		Dry deposition velocity (cm s^{-1})	
	Suburban	Urban 1	Suburban	Urban 1
FLN	1338±825	622±518	4.5±4.0	6.4±4.6
PHE	3144±2308	1492±1301	3.2±3.7	1.9±1.5
ANT	172±100	63±40	2.3±1.8	1.4±1.6
CRB	170±88	90±51	2.9±3.5	3.1±3.4
FL	615±574	732±618	0.9±0.9	0.6±0.5
PY	815±759	428±293	1.1±1.3	0.4±0.4
BaA	132±128	78±54	0.6±0.5	0.1±0.1
CHR	237±224	350±281	0.3±0.2	0.1±0.1
BbF	441±295	162±56	1.2±1.3	0.1±0.1
BkF	170±178	94±62	0.4±0.4	0.06±0.04
BaP	154±206	66±39	0.5±0.5	0.07±0.05
IcdP	313±531	90±52	0.6±0.7	0.06±0.04
DahA	393±946	34±20	2.0±3.1	0.08±0.08
BghiP	242±327	113±75	0.5±0.6	0.06±0.03
	$\sum_{14}$ PAH Dry deposition flux		Overall dry deposition velocity	
	8160±5024	4286±2782	1.5±2.4	1.0±2.3

Phenanthrene and fluorene accounted for 35 and 17% of Σ_{14}-PAH fluxes at Suburban site while they accounted for 32 and 15% of Σ_{14}PAH fluxes in Urban 1 site (Figure 4.7). Low molecular weight PAHs were at higher levels in flux samples compared to air samples and the opposite was the case for high molecular weight PAHs (Figure 4.7).

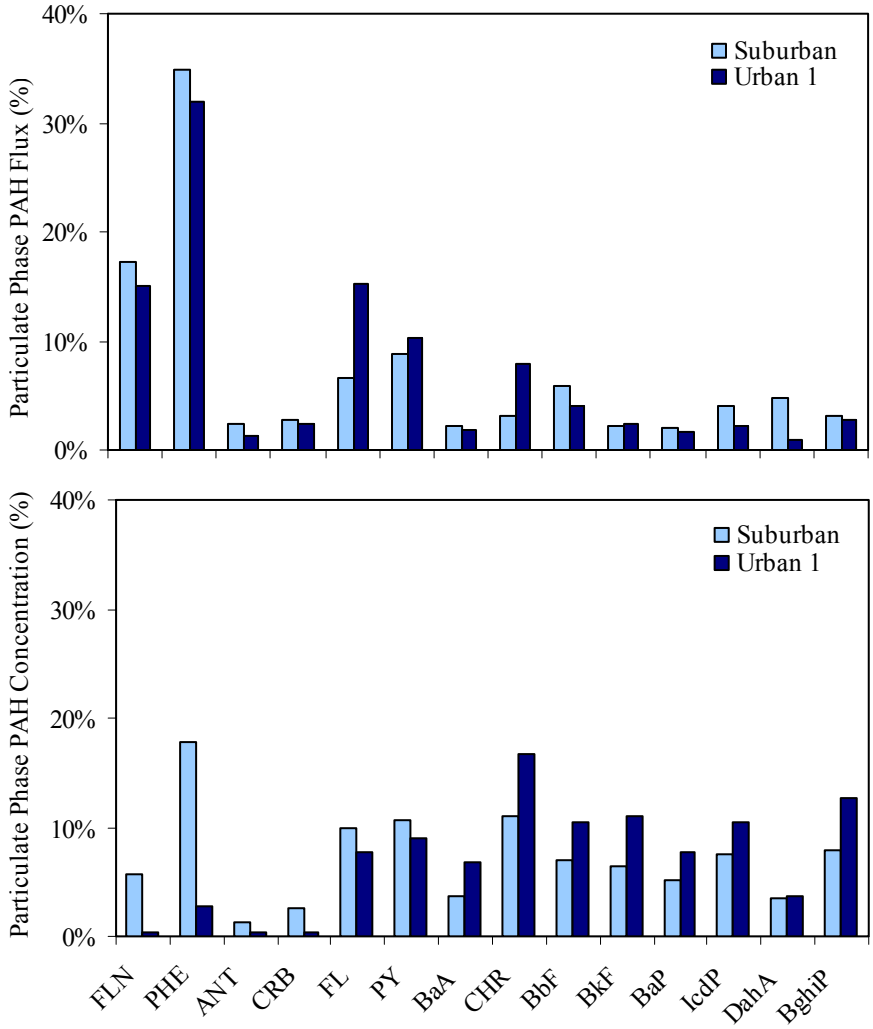

Figure 4.7 Percentages of particle phase dry deposition fluxes and particle concentrations of PAH compounds.

No previous measurement of PAH dry deposition in this area was available for comparison. Deposition fluxes measured in this study were within the range of values reported previously elsewhere. The particle-phase PAH dry deposition fluxes measured by Franz, Eisenreich, & Holsen (1998) for rural Lake Michigan and reported by Tasdemir & Esen (2007b) for Bursa were considerably lower. However, fluxes measured in this study were lower than those reported for urban Chicago (Franz, Eisenreich, & Holsen, 1998; Odabasi et al., 1999b), and for the industrial, urban and rural areas in Taiwan (Fang et al., 2004a) (Table 2.3).

Particle-phase dry deposition velocities (V_d, cm s^{-1}) of PAHs were calculated using the dry deposition fluxes measured with dry deposition plates and atmospheric particle phase concentrations. V_d ranged between 0.3±0.2 cm s^{-1} (chrysene) and 4.5±4.0 cm s^{-1} (fluorene) in Suburban, and between 0.06±0.03 cm s^{-1} (benzo[*g,h,i*]perylene) and 6.4±4.6 cm s^{-1} (fluorene) in Urban 1 sites (Table 4.4). The overall average deposition velocities for PAHs were 1.5±2.4 and 1.0±2.3 cm s^{-1} for Suburban and Urban 1 sites, respectively. The difference in deposition velocities may be due to different size distributions of urban and suburban particles. Since large particles dominate the atmospheric dry deposition, higher deposition velocities can be attributed to larger particles from re-suspension of polluted soil and dust particles from unpaved roads and non-vegetated areas in Suburban site. Using greased dry deposition plates Franz, Eisenreich, & Holsen (1998) have reported that deposition velocities for the individual PAHs were between 0.4-2.1 and 1.0-3.7 cm s^{-1} in summer and winter in Chicago, respectively. Odabasi et al. (1999b) have reported V_d values between 4.3-9.8 cm s^{-1} with an average of 6.7 cm s^{-1} in urban Chicago for a summer/fall period. Similarly, Vardar, Odabasi, & Holsen (2002) determined the mean overall dry deposition velocity of PAHs as 4.5 cm s^{-1} for winter period in Chicago.

The variation in the dry deposition velocities is a function of particle size distribution and the meteorological conditions (i.e., wind speed and temperature) (Tasdemir & Esen, 2007b; Tasdemir et al., 2004). There was a decrease in dry deposition velocity with increasing molecular weight in this study (Table 4.4 and Figure 4.8). The decrease in deposition velocity with increasing molecular weight is supported by other experimental studies which have shown that a greater fraction of the higher molecular weight PAHs are associated with fine particles relative to the lower molecular weight compounds (Kiss et al., 1998; Tasdemir & Esen, 2007b; Odabasi et al., 1999b). A similar decrease in deposition velocity with increasing molecular weight was previously reported for PAHs (Bozlaker, Muezzinoglu, & Odabasi, 2007; Franz, Eisenreich, & Holsen, 1998; Odabasi et al., 1999b; Shannigrahi, Fukushima, & Ozaki, 2005; Tasdemir & Esen, 2007b; Vardar, Odabasi, & Holsen, 2002).

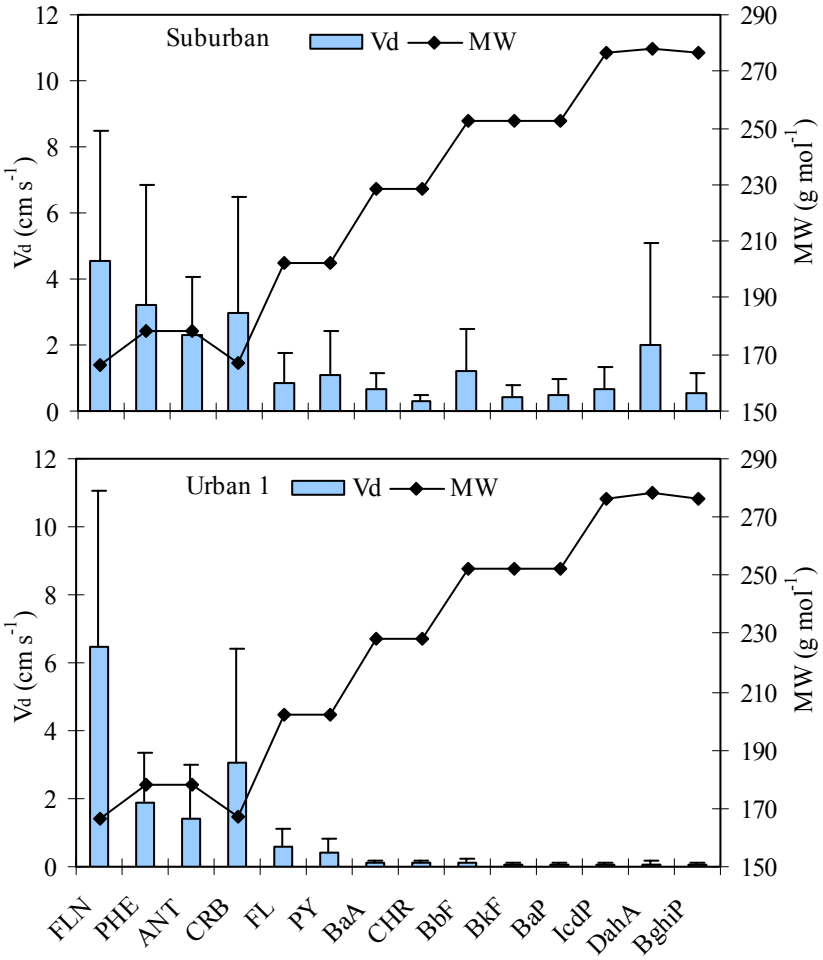

Figure 4.8 Average dry deposition velocities of PAH compounds associated with particles. Error bars are 1 SD.

4.3 PAH Concentrations in Soil

Soil samples were collected at the Suburban site. Water and organic matter content and measured Σ_{14}PAH concentrations are presented in Table 4.5.

Table 4.5 Soil properties and PAH concentrations (ng g^{-1} dry wt).

Date	Water Content (%)	Organic Matter (Dry Sample) (%)	Soil conc. of $\sum_{14}$PAH (ng g^{-1} dry wt)
23.05.2003	4.8	10.0	47.5
26.05.2003	5.1	9.7	47.2
25.06.2003	1.6	11.3	79.9
29.07.2003	3.5	11.1	68.0
28.08.2003	4.2	10.5	36.7
04.11.2003	4.2	11.3	75.2
05.12.2003	5.7	11.2	61.4
14.01.2004	7.3	10.6	47.0
11.02.2004	5.7	9.6	45.9
01.04.2004	5.7	10.1	49.9
Average±SD	4.8±1.5	10.5±0.7	55.9±14.4

The average soil PAH concentrations measured in this study ranged between 0.4±0.3 (benzo[*a*]pyrene) and 19.7±9.4 (phenanthrene) ng g^{-1} dry weight and they were within the range of previously reported values (Table 2.4). Σ_{14}PAH concentrations in soil reported by Zhang et al. (2006) for the urban area in Hong Kong, by Nadal, Schuhmacher & Domingo (2004) for the industrial and unpolluted areas in Spain, by Motelay-Massei et al. (2004) for industrial, urban and remote areas in France, and by Cousins & Jones (1998) for a rural area in UK were higher than the values measured in this study while the concentrations reported by Zhang et al. (2006) for a rural area in Hong Kong were lower.

Recently measured Σ_{14}PAH soil concentrations at Aliaga industrial region were generally significantly higher than those measured in the present study (Bozlaker, Muezzinoglu, & Odabasi, 2007).

Similar to the air samples the PAH profile in soil was dominated by lower molecular weight compounds (Figure 4.9). Phenanthrene, fluoranthene, pyrene and chrysene accounted for 34, 14, 11, and 11% of the Σ_{14}PAH, respectively. Since the sampling point is relatively far from the local sources, this can be explained by the higher molecular weight compounds being deposited more easily than the lower molecular weight ones which are mainly in gaseous form and capable of long-range transport. Bozlaker, Muezzinoglu, & Odabasi (2007) have recently reported that the PAH profile at an industrial site was dominated by high molecular weight compounds and this was attributed to the nearby sources (steel plants with electric arc furnaces) emitting significant amounts of particle-phase PAHs.

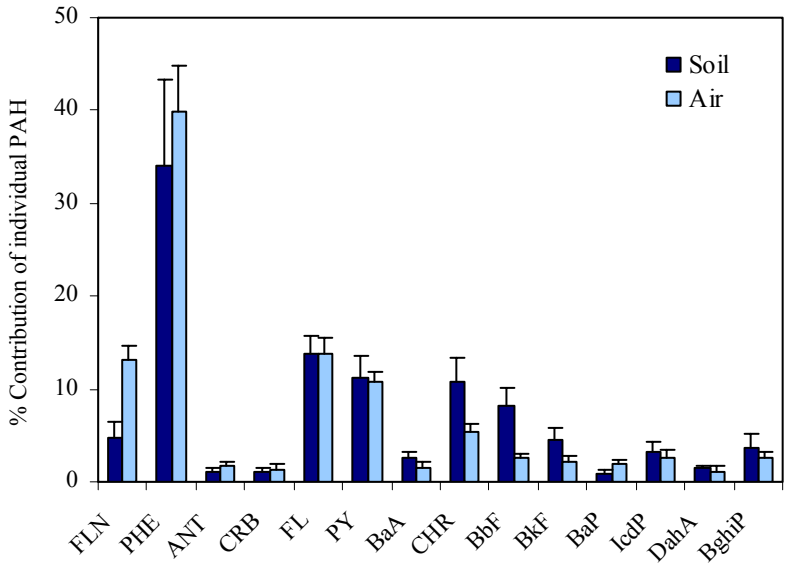

Figure 4.9 PAH profiles in ambient air and soil. Error bars are 1 SD.

4.3.1 Air-Soil Exchange of PAHs

Concurrent air and soil concentrations are ideally used to assess the fugacity gradients of individual PAHs between the soil-air interfaces. The soil to air fugacity ratios $[(f_S/f_A)=(C_S\rho_S/K_{SA})/C_A)]$ >1 indicate that the soil is a source with net volatilization of compounds from soil, values <1 indicate that the soil is a sink and net gas-phase deposition occurs from air to soil. The uncertainty of the calculated

fugacity ratios and fluxes was assessed using a propagated error analysis. For each compound, measurement errors in C_A and C_S, K_{SA} and MTC values were taken into account. The uncertainties of C_A, C_S, and K_{OA} (used to calculate K_{SA}) were assumed to be 15% (Harner & Shoeib, 2002; Meijer et al., 2003; Odabasi, M., Cetin, B., & Sofuoglu, A., 2006; Odabasi, M., Cetin, E., & Sofuoglu, A., 2006) and uncertainty in the overall MTC was 40%. The average water and organic matter contents of soil samples were found as 4.8 and 10.5% (in dry sample), respectively (Table 4.5). OM contents were used in fugacity calculations. Organic matter fraction was assumed to be 1.5 times of the organic carbon fraction. The measured average density of soil solids (2.0±0.1 g cm^{-3}, n=6) was used for all calculations.

Temperature dependent K_{OA} values of the PAHs used in Equation (2.10) were calculated as a function of temperature using the regression parameters (A and B) recently reported by Odabasi, M., Cetin, B., & Sofuoglu, A. (2006); Odabasi, M., Cetin, E., & Sofuoglu, A. (2006) using Equation (2.5). A statistically significant correlation was found between log Q_{SA} and log K_{OA} (r^2=0.91, p<0.01) indicating that the octanol is a good surrogate for soil organic matter (Figure 4.10).

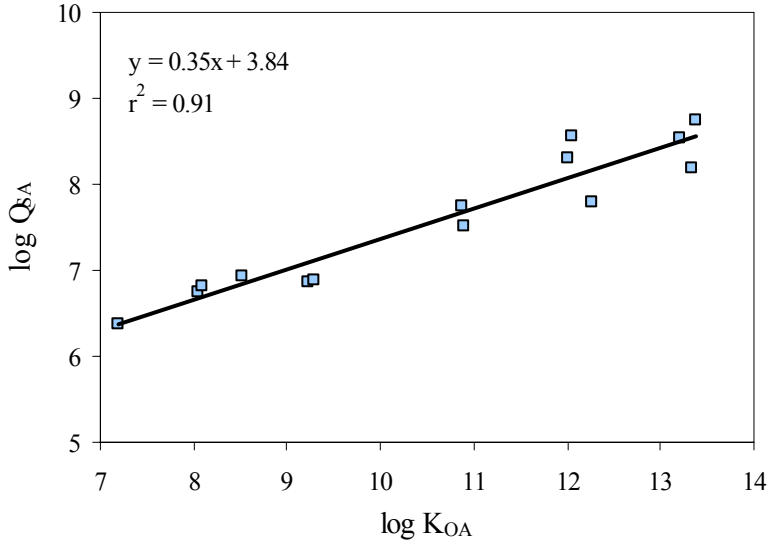

Figure 4.10 log Q_{SA} vs log K_{OA}.

For a system in equilibrium, f_S/f_A value is approximately equal to 1 (Cousins & Jones, 1998; Harner, Green, & Jones, 2000). A propagation of the errors that are associated with the calculation indicated that the equilibrium is represented by an f_S/f_A of 1.0±0.26 (i.e., a range of 0.74-1.26). Generally, the fugacity ratios of all compounds fell outside this uncertainty range and it can be concluded that for these compounds the soil and ambient air are not in equilibrium. For some samples (overall, 5% of the data set) the fugacity ratios for phenanthrene, anthracene, carbazole, fluoranthene, and pyrene were in the equilibrium range. Figure 4.11 shows the relationship between fugacities in soil and air. Heavier molecular weights PAHs (fluoranthene-benzo[*g,h,i*]perylene) with fugacity ratios <1 were mainly deposited. Once deposited, these compounds with high K_{SA} values tend to accumulate in soil for long periods. Thus, the soil acted as a sink for these compounds. The contaminated soil acts as a secondary source to the atmosphere for low molecular weight, 3-ring PAHs (fluorene, phenanthrene, anthracene, carbazole) for some samples (Figure 4.11). Similarly, Cousins & Jones (1998) have reported fugacity ratios greater than 1 for the low molecular weight PAHs.

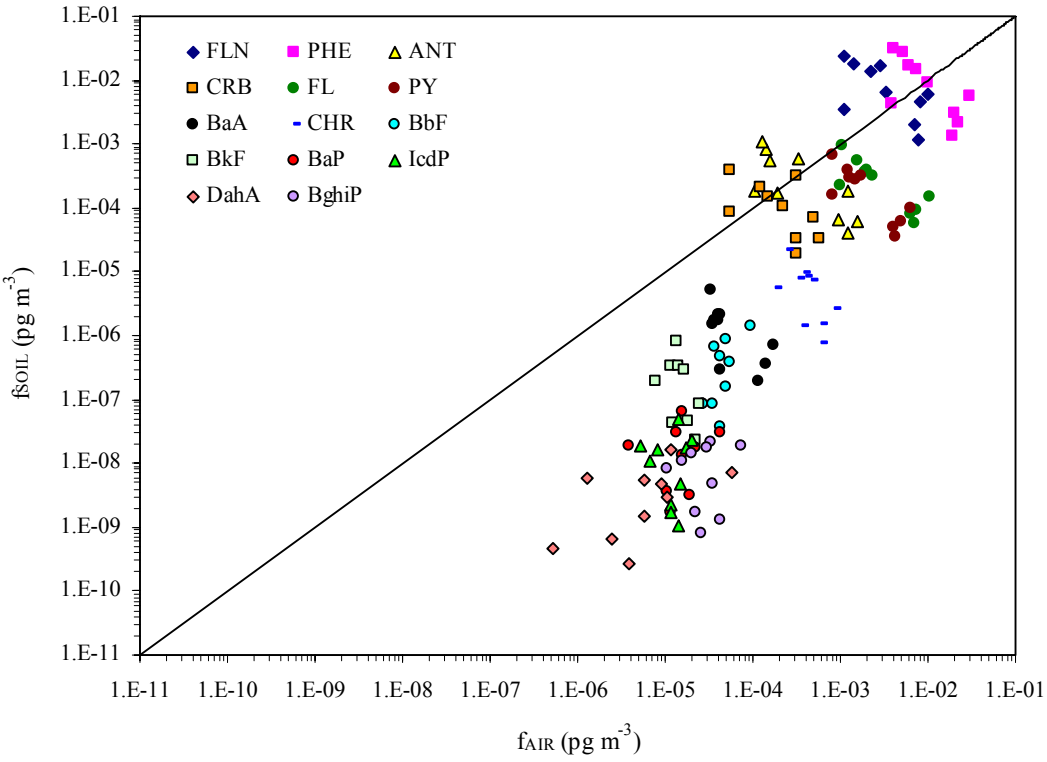

Figure 4.11 Relationship between the PAH fugacities in soil and air. The solid diagonal line represents a 1:1 relationship (equilibrium).

The calculated instantaneous air-soil gas exchange fluxes of PAHs using equations 2.10, 2.11, and 2.12 are presented in Table 4.6. The average net $\sum_{14}$PAH flux ranged from 17 to 31456 ng m^{-2} day^{-1} in summer, while in winter it ranged from 5 to 36295 ng m^{-2} day^{-1}. Fluorene, phenanthrene, anthracene and carbazole were deposited in winter while they were volatilized in summer. Other compounds (fluoranthene- benzo[*g,h,i*]perylene) were deposited in both periods (Figure 4.12). Generally, winter fluxes were higher than summer fluxes. Since the ambient gas-phase PAH concentrations were higher in winter, higher depositional fluxes were observed during this period (Figure 4.13).

Table 4.6 Air/soil gas exchange fluxes of PAHs for summer and winter periods.

PAHs	Net gas flux (ng m^{-2} day^{-1})					
	Summer			Winter		
	AVG±SD	Min	Max	AVG±SD	Min	Max
FLN	-21248±16531[a]	-2360[a]	-44801[a]	9025±3149	6969	13716
PHE	-31456±17701[a]	-11342[a]	-50755[a]	36295±4289	31215	41527
ANT	-873±715[a]	-78[a]	-1866[a]	2117±357	1804	2491
CRB	-118±323[a]	12	-639[a]	750±347	469	1138
FL	1981±885	709	3150	13584±2540	10999	16945
PY	1479±558	603	2041	8623±1259	7656	10430
BaA	51±16	30	68	196±85	79	279
CHR	469±207	156	747	1028±311	687	1394
BbF	83±46	46	160	65±19	38	80
BkF	19±7	7	25	32±10	22	43
BaP	25±13	7	38	24±9	15	36
IcdP	17±12	6	36	21±4	16	26
DahA	25±39	2	105	5±3	1	9
BghiP	43±34	13	101	52±19	31	77

[a] Negative values indicate volatilization of PAHs from soil

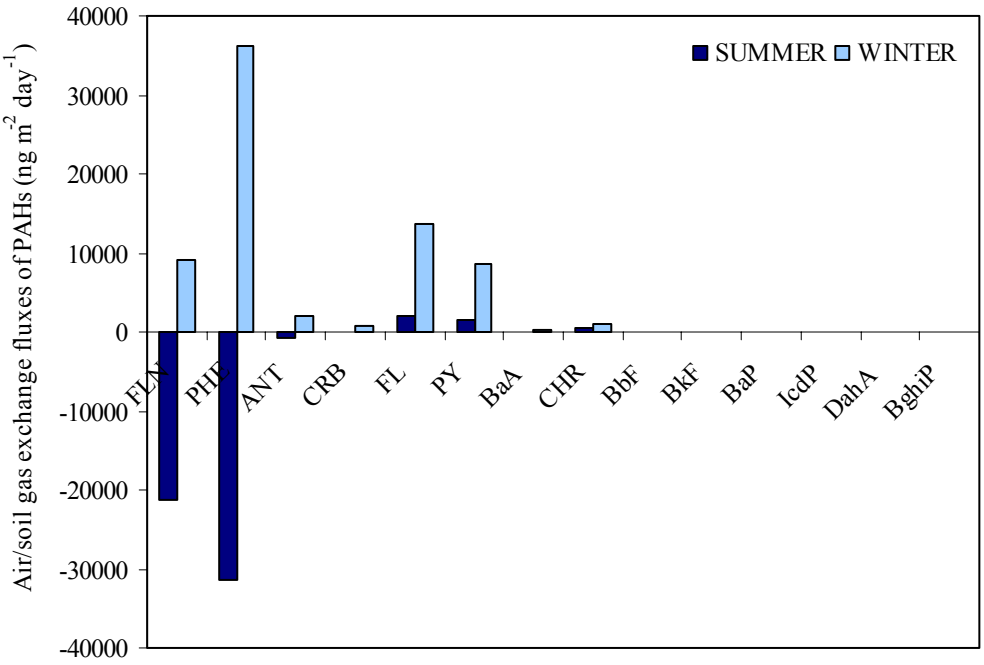

Figure 4.12 Air/soil gas exchange fluxes of individual PAHs.

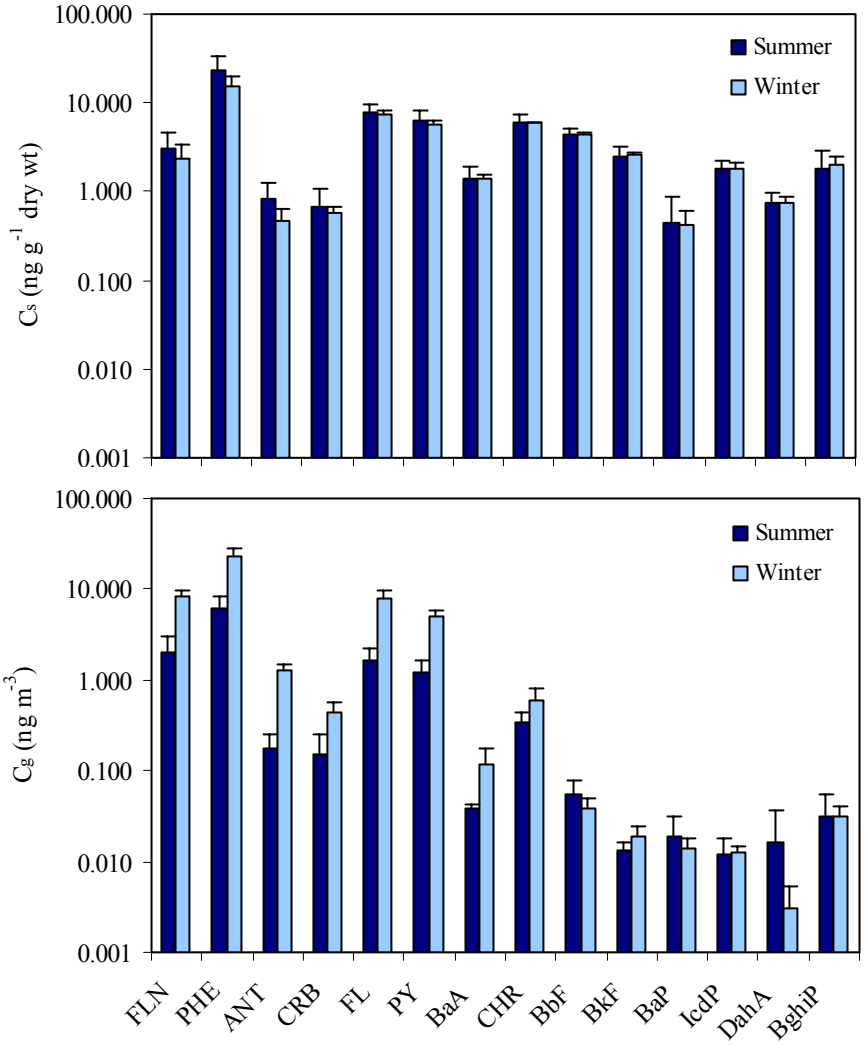

Figure 4.13 Seasonal variation of individual PAH compounds in soil and air. Error bars are 1 SD.

Annual gaseous absorption and volatilization fluxes were used along with the dry deposition fluxes and wet deposition fluxes measured recently at the Suburban (Odabasi, 2007) to determine the relative contributions of different mechanisms to the soil PAH inventory (Table 4.7). All mechanisms were comparable for ΣPAHs however their input was dominated by gas absorption. Gas absorption was dominated for lower molecular weights PAHs, however dry deposition was dominated for higher molecular weights PAHs. The contribution of volatilization was only significant for fluorene (67%), phenanthrene (44%), anthracene (27%), and carbazole (29%). Wet deposition was <8% for all compounds. These results suggested a net PAH accumulation in the soil (Table 4.7).

Table 4.7 Annual fluxes of PAHs at Suburban site (ng m^{-2} $year^{-1}$).

PAHs	Dry deposition	Wet deposition	Gas absorption	Volatilization
FLN	488,408	49,649	3,294,254	7,755,647
PHE	1,147,664	202,318	13,247,676	11,481,305
ANT	62,960	13,082	772,616	318,786
CRB	62,198	6,826	181,743	101,235
FL	224,366	41,968	2,605,403	n.a.
PY	297,573	34,954	1,698,905	n.a.
BaA	48,328	4,928	39,780	n.a.
CHR	86,399	11,125	252,710	n.a.
BbF	161,036	11,861	27,393	n.a.
BkF	62,078	5,937	9,032	n.a.
BaP	56,125	3,539	9,086	n.a.
IcdP	114,192	5,969	6,871	n.a.
DahA	143,505	2,673	6,174	n.a.
BghiP	88,212	5,247	17,081	n.a.
Σ_{14}PAHs	3,043,045	400,077	22,168,725	19,656,974

n.a.: not available

4.4 Water Concentrations in Guzelyali Port

Concentrations and phase-distributions of PAHs in water are presented in Table 4.8. Total dissolved-phase PAH concentrations ($\sum_{14}$PAHs) were 10.32±2.82 and 4.90±2.21 ng L^{-1} (average±SD) for winter and summer seasons, respectively and they were 5.41±2.77 and 3.50±1.57 ng L^{-1} for particle-phase. Dissolved-phase PAH concentrations were significantly higher than particulate phase PAH concentrations and dominated by more volatile compounds such as fluorene, phenanthrene, fluoranthene, and pyrene (Table 4.8, Figure 4.14).

Table 4.8 Concentrations of PAHs in water (ng L^{-1}) (average±SD).

PAHs	Dissolved phase		Particle phase	
	Winter	Summer	Winter	Summer
FLN	1.49±0.62	0.44±0.23	0.42±0.39	0.30±0.25
PHE	3.40±1.43	2.66±1.44	1.28±0.80	1.46±0.88
ANT	0.40±0.10	0.14±0.05	0.07±0.05	0.03±0.02
CRB	0.41±0.07	0.14±0.03	0.03±0.01	0.05±0.04
FL	2.76±0.72	0.55±0.29	0.86±0.39	0.32±0.13
PY	1.19±0.37	0.69±0.24	0.64±0.31	0.34±0.12
BaA	0.09±0.06	0.03±0.01	0.20±0.16	0.06±0.03
CHR	0.27±0.07	0.15±0.06	0.59±0.40	0.24±0.10
BbF	0.08±0.05	0.05±0.05	0.34±0.24	0.20±0.10
BkF	0.06±0.04	0.01±0.01	0.26±0.16	0.10±0.04
BaP	0.13±0.08	0.02±0.01	0.17±0.09	0.09±0.03
IcdP	0.11± n.a.	0.02±0.01	0.23±0.16	0.10±0.03
DahA	n.d.	n.d.	0.07±0.05	0.04±0.02
BghiP	0.02±0.02	0.01±0.004	0.25±0.16	0.17±0.05
$\sum_{14}$PAHs	10.32±2.82	4.90±2.21	5.41±2.77	3.50±1.57

n.d.: not detected

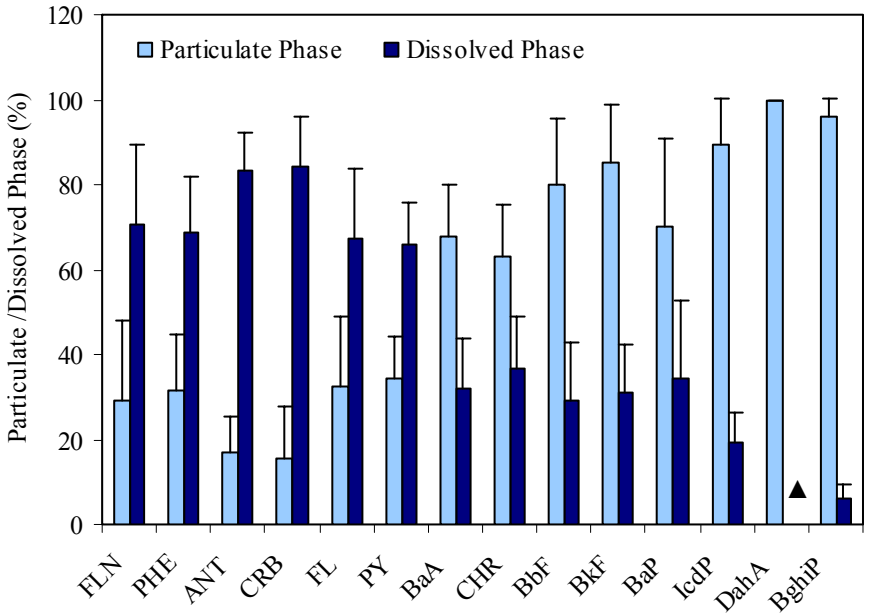

Figure 4.14 Phase distribution of individual PAHs in water. Error bars represent one standard deviation. (▲) not detected.

Figure 4.15 shows the average variations of individual PAH concentration measured in water and air samples. Phenanthrene was the most abundant compound measured in water and air samples. Higher concentrations were observed for lighter PAH species.

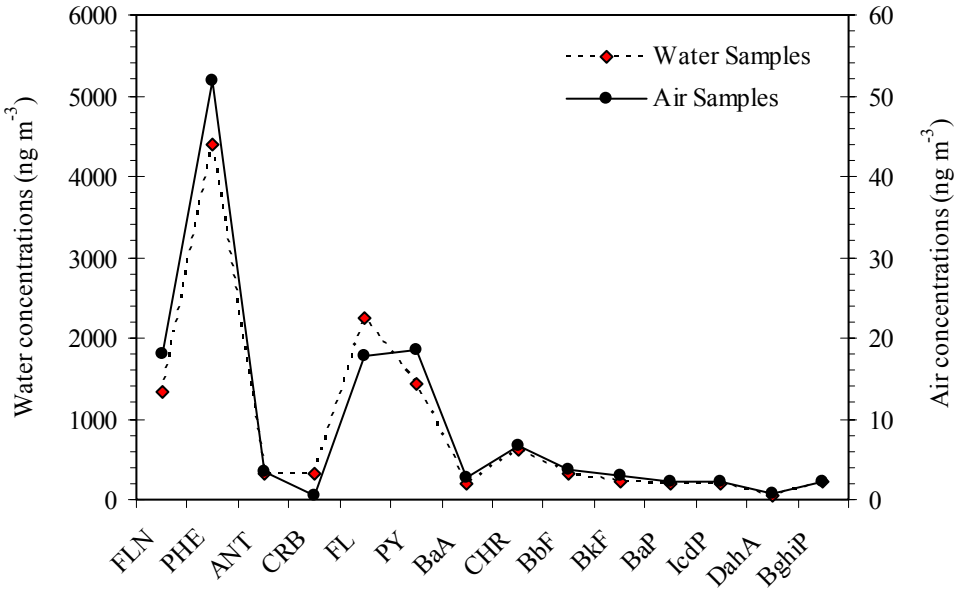

Figure 4.15 Average total concentrations of indvidual PAHs in water and air.

Average winter concentrations were higher than summer concentrations for both water and air samples (Table 4.8, Figure 4.16). The increase in PAH emissions as a result of residential heating during winter might be the main reason for this observation.

In this study average total (dissolved + particle) Σ_{14}PAH concentration was 12.07 ng L^{-1}. The concentrations observed in this study were within the ranges previously measured at different sites. Σ_{14}PAH concentration measured in this study is considerably lower than those reported by Zhou & Maskaoui (2003) for Daya Bay in China, by Zhang et al. (2004a); Zhang et al. (2004b) for Minjiang and Tonghui Rivers in China. In Qiantang River, China, Σ_{12}PAH concentration was 119.2 ng L^{-1} (Chen, Zhu, & Zhou, 2007) and in Thermaikos Gulf, Macedonia, Σ_{12}PAH concentrations were between 61.3 and 133 ng L^{-1} (Manoli et al., 2000). In Chesapeake Bay, Σ_{11}PAH (p+d) concentration was 39.9 ng L^{-1} (Ko & Baker, 2004),

and in Pearl River, China Σ_{12}PAH (p+d) concentrations were between 196.3 and 247 ng L^{-1} (Luo et al., 2004). The PAH levels measured in this study were higher than to those reported by Telli-Karakoc et al. (2002) for Izmit Bay in Turkey. Σ_{13}PAH (p+d) concentrations for Raritan Bay in New York reported by Gigliotti et al. (2002) were similar to those reported in the present study.

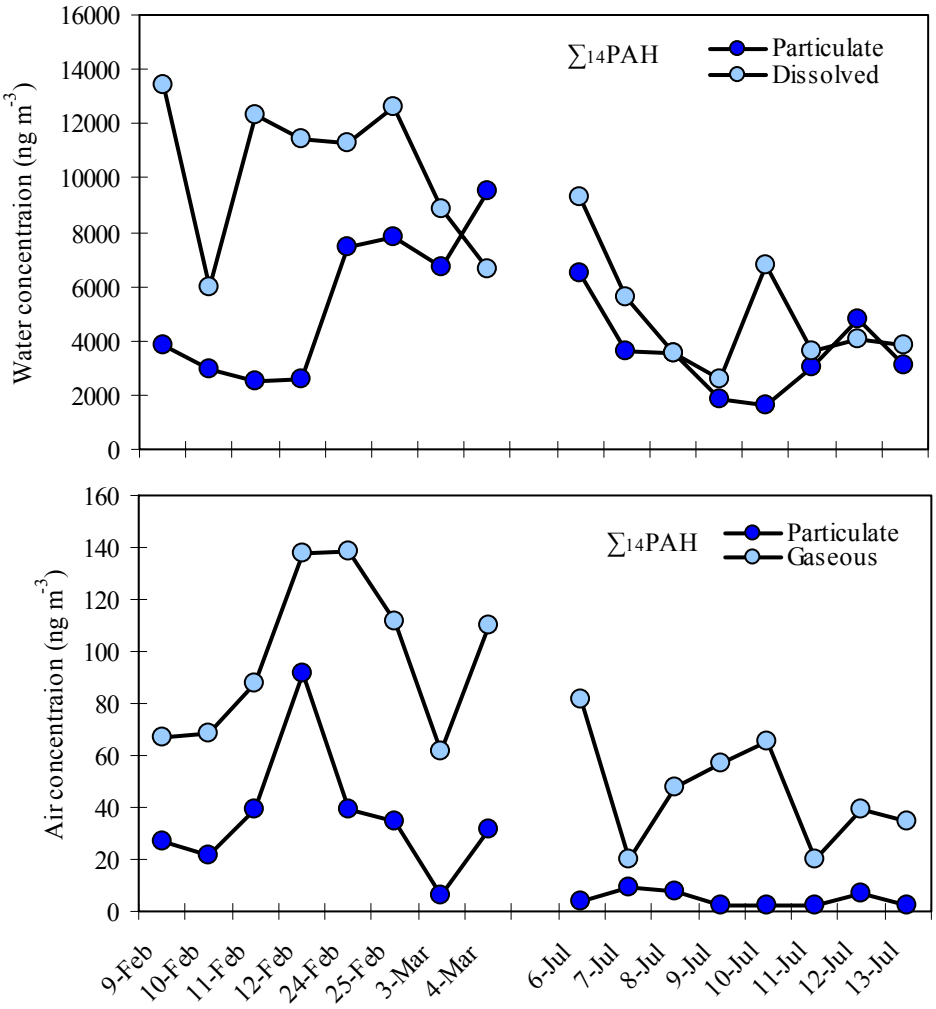

Figure 4.16 Variation of PAHs in water and ambient air.

4.4.1 Air-Water Exchanges of PAHs

Concurrent air and water concentrations are ideally used to assess the state of equilibrium for individual POPs between the air-water interfaces. The water-air fugacity ratio ($f_W/f_A=H'C_w/C_g$) >1.0 indicates net volatilization of compounds from water, values <1.0 indicate net gas-phase deposition from air. For a system in equilibrium, f_W/f_A value is ~1.0.

The uncertainty of the calculated fugacity ratios and fluxes was assessed using a propagated error analysis. For each compound, measurement errors in C_a and C_w, H and K_a values are taken into account. The uncertainties of C_a and C_w were determined as 10% from the relative standard deviations of sample surrogate recoveries (Bamford, Ko, & Baker, 2002; Cetin & Odabasi, 2007). Uncertainty in saline water H values for PAHs was <13%. Salting-out constants (K_s, L mol^{-1}) for PAHs were calculated with the method by Ni & Yalkowski (2003) using their octanol-water partition coefficients ranged between 0.263 (carbazole) and 0.390 (benzo[*g,h,i*]perylene). H^*, the Henry's law constant in saline water was calculated using [log (H^*/H)= K_s C_s] where C_s is the molar concentration of salt solution (measured as 0.51 and 0.62 M for winter and summer samples, respectively). Propagating the additional uncertainty for salting-out correction increases the uncertainty for H <16%. Unlike k_a, k_w is not linearly related to wind speed. Averaging wind speeds for long periods may underestimate k_w and K_a. The relationship of Henry's law constant (H) with temperature is also non-linear. To determine the nonlinear influences of meteorological parameters on K_a, a sensitivity analysis was conducted using data averaged over 1 min intervals. The change in K_a ranged from 0.01% (dibenz[*a,h*]anthracene) to 3% (fluorene) relative to the estimates on the basis of long-term averages of wind speed and temperarue. The overall uncertainty of K_a value was assumed to be 40%, based on the results of sensitivity analysis, previous evaluations, and the uncertainties in the air and water-side mass transfer coefficients (k_a and k_w) (Bamford, Ko, & Baker, 2002; Hoff et al., 1996; Nelson, McConnell, & Baker, 1998; Nightingale, Liss, & Schlosser, 2000).

A propagation of the errors that are associated with the calculation indicated that the equilibrium is represented by an f_W/f_A of 1.0±0.21 (i.e., a range of 0.79-1.21). The fugacity ratios of all compounds (except the ratios for fluorene, phenanthrene, anthracene, benzo[*a*]pyrene, and indeno[*1,2,3-cd*]pyrene for some samples) fall outside this uncertainty range and we can be confident that for these compounds the water and ambient air are not in equilibrium (Figure 4.17). Fugacity ratios for some compounds (anthracene, benzo[*a*]anthracene, benzo[*a*]pyrene, and indeno[*1,2,3-cd*]pyrene) were >1.0 for some samples (overall, 7% of the data set) indicating net volatilization from surface water while the ratios for other compounds (<1.0) indicated deposition to the surface water (Figure 4.17).

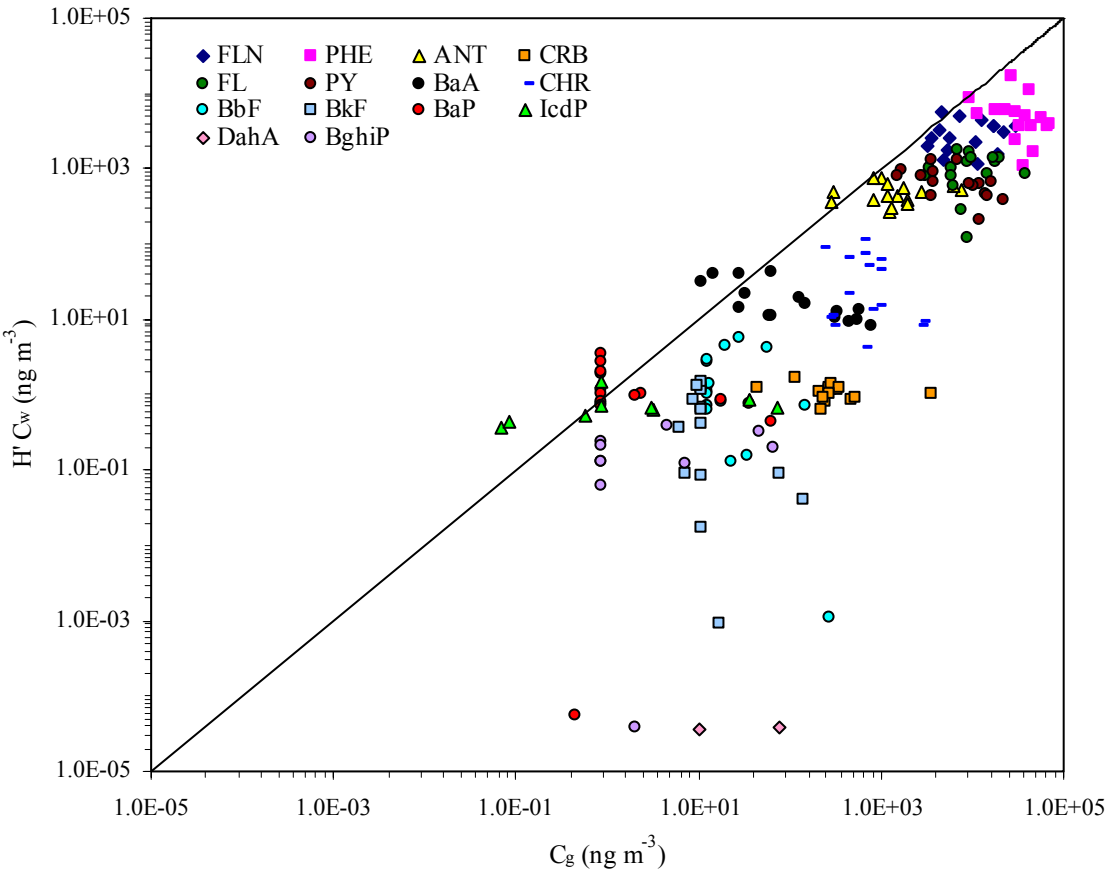

Figure 4.17 Relationship between the PAH fugacities in water and air. The solid diagonal line represents a 1:1 relationship (equilibrium).

Censoring can be used to decrease the weight of below detection values in the data set. Recent studies (Brankov, Rao, & Porter, 1999; Singh & Nocerino, 2001) have indicated that for small size censored samples (n≤10), the simple substitution of LOD/2 for censored data may be used and sometimes outperformed more complicated methods. In the present study, values below the detection limit were replaced by the half of the LOD. This was done only if there was a corresponding measured gas or dissolved-phase concentration. Censored below detection PAH values were 3 and 16% for dissolved and gas-phases, respectively. Net fluxes of PAHs were calculated using Equations (2.15)-(2.20), and 16 paired atmospheric gas and dissolved-phase water samples collected at the sampling site (Table 4.9).

Table 4.9 Air/water gas exchange fluxes of PAHs for winter and summer periods.

PAHs	Net gas flux (ng m^{-2} day^{-1})					
	Winter			Summer		
	AVG±SD	Min	Max	AVG±SD	Min	Max
FLN	2162±735	1319	3666	156±118	34	357
PHE	9847±3672	5659	16686	2626±2097	524	5974
ANT	581±598	176	1701	52±58	-7[a]	161
CRB	89±51	18	184	294±537	70	1621
FL	2829±1465	1416	5473	2260±3332	267	10293
PY	3470±790	2460	4855	531±459	88	1505
BaA	126±89	4	257	4±10	2	23
CHR	351±384	83	988	127±50	46	193
BbF	9±17	2	52	17±28	4	85
BkF	6±8	2	27	8±15	2	44
BaP	2±5	-0.07[a]	13	5±9	0.1	20
IcdP	n.d.	n.d.	n.d.	5±9	-0.08[a]	23
DahA	n.d.	n.d.	n.d.	13±16	2.4	24
BghiP	0.24±0.04	0.2	0.3	5±8	0.2	21

[a] Negative values indicate volatilization of PAHs from water
n.d.: not detected

The net gas-exchange PAH flux ranged from 3.0 (deposition, benzo[*a*]pyrene) to 6477 (deposition, phenanthrene) ng m^{-2} day^{-1}. Net PAH fluxes were mainly deposition from air to water during the sampling periods. All PAH compounds except benzo[*a*]pyrene and indeno[*1,2,3-cd*]pyrene were generally deposited during the each periods (Table 4.9, Figure 4.18). Thus, the water acted as a sink for these compounds for both seasons.

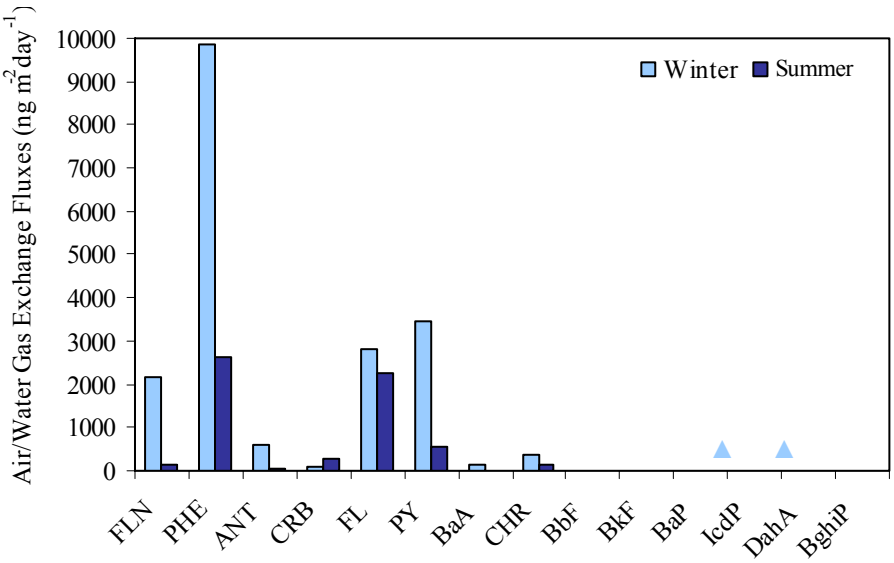

Figure 4.18 Air/water gas exchange fluxes of individual PAHs. (▲) not detected.

Air-water gas exchange fluxes for PAHs obtained in this study within the ranges of previously reported values. Gigliotti et al. (2002) have reported that PAH fluxes ranged between -198 (fluorene) and 290 (phenanthrene) ng m^{-2} day^{-1} in Raritan Bay and -3464 (pyrene) and 2009 (phenanthrene) ng m^{-2} day^{-1} in New York Harbor. In another study conducted in Mumbai Harbor, India PAH fluxes ranged between -5380 (pyrene) and 910 (benzo[*k*]fluoranthene) ng m^{-2} day^{-1} (Pandit et al., 2006).

The importance of deposition as an input or volatilization as a removal process relative to advection of PAHs out of the water column of Izmir Bay was further assessed by comparing the residence times of dissolved-phase PAHs in the water column reflecting only air-water fluxes versus the residence time of water in the inner Bay. The hydraulic residence time for the inner Bay water is 85 days (Sayin,

2003). The residence time of PAHs in the water column (τ_{AW}), considering only dissolved-phase PAH concentrations that are subject to air-water exchange, is given by (Gigliotti et al., 2002):

$$\tau_{AW} = Inventory / Net\ Flux = (C_{dissolved}\ h_w) / F_g \qquad (4.2)$$

The residence times of PAHs were calculated using the estimated net fluxes (F_g, ng m^{-2} day^{-1}), measured dissolved-phase concentrations ($C_{dissolved}$, ng m^{-3}), and the average water depth for the inner Bay (h_w, 10 m). τ_{AW} values of PAHs ranged from 9 to 3386 days and the hydraulic to gas-exchange residence time ratios were between 1.5 and 36.1 (Table 4.10). These results suggest that PAH gas-exchange in the Bay is at least as or a more important mechanism than advection.

Table 4.10 PAH residence times due to gas-exchange and their comparison to hydraulic residence time of Bay water.

PAHs	Residence time of PAHs (days)			Ratio: Hydraulic res. time/PAH res. time		
	AVG±SD	Summer	Winter	AVG±SD	Summer	Winter
FLN	27±37	49	7	9.65±7.54	4.58	14.08
PHE	9±10	16	4	19.81±15.55	10.12	28.30
ANT	32±42	55	11	8.08±8.47	4.49	11.21
CRB	44±60	13	76	9.44±21.53	16.86	2.02
FL	10±8	8	12	31.66±55.97	54.26	9.05
PY	16±24	28	4	17.58±15.01	7.07	28.09
BaA	70±137	65	76	10.11±12.20	3.19	17.03
CHR	17±14	16	18	10.75±10.40	9.47	12.02
BbF	160±199	64	256	4.32±7.74	7.39	1.62
BkF	118±138	31	204	36.09±105.67	71.41	5.18
BaP	3386±4440	252	5625	1.51±3.86	3.65	0.29
IcdP	652±791	652	n.a.	1.77±3.05	1.77	n.a.
DahA	n.a.	n.a.	n.a.	n.a.	n.a.	n.a.
BghiP	237±302	126	498	4.01±7.16	5.88	0.25

n.a.: not available

In addition to gas-exchange, other atmospheric inputs into the Bay (i.e., dry particle and wet deposition) contribute to the water column total PAH inventory. Dry deposition fluxes were calculated and used along with the recently measured wet deposition fluxes (Odabasi, 2007) to estimate relative importance of different mechanisms (i.e., dry deposition, wet deposition, gas absorption, and volatilization). The dry deposition fluxes of POPs associated with particles can be estimated using Equation (2.8). Reported overall particle dry deposition velocities (V_p) for various POPs range between 0.4 and 6.7 cm s^{-1} (Tasdemir et al., 2004; Odabasi et al., 1999b). Dry deposition velocities of PAHs were determined using particle dry deposition and ambient air samples collected at two sites (Urban 1 and Suburban) within a few kilometers of the sampling site of the present study. V_p values ranged between 0.3 (chrysene) - 4.5 cm s^{-1} (fluorene) for PAHs. Dry deposition fluxes (F_p) for PAHs in Guzelyali Port were estimated using these deposition velocities and measured particle-phase air concentrations.

Annual gaseous absorption and volatilization fluxes were calculated using equations (2.16) and (2.17) and were used along with the estimated dry deposition fluxes and wet deposition fluxes measured recently at a suburban site in Izmir (Odabasi, 2007) to determine the relative contributions of different mechanisms to the pollutant inventory of the Bay water column (Table 4.11). This assessment is based on the mechanisms included in the present study (particle dry deposition, wet deposition, gas absorption, and volatilization). Additional mechanisms (river/stream outflows, terrestrial run-off, domestic and industrial wastewater discharges) could also significantly contribute to the Bay water column pollutant inventory. However, it is not possible to estimate their magnitude and relative importance. All studied mechanisms were comparable for ΣPAHs however their input was dominated by dry deposition. Generally, wet deposition, gas absorption and dry deposition contributed to the water column PAH inventory. However, gas absorption for fluorene to chrysene and and dry deposition for higher molecular weight PAHs were dominating. Wet deposition was <6% for all compounds. The contributions of volatilization were %1 for anthracene and benzo[*a*]pyrene (Table 4.11).

Table 4.11 Annual fluxes of PAHs at Urban 2 site (ng m^{-2} $year^{-1}$).

PAHs	Dry deposition	Wet deposition	Gas absorption	Volatilization
FLN	296,990	49,649	447,378	n.a.
PHE	2,098,908	202,318	2,364,274	n.a.
ANT	174,151	13,082	141,359	3,220
CRB	109,880	6,826	69,958	n.a.
FL	748,699	41,968	928,883	n.a.
PY	908,037	34,954	730,247	n.a.
BaA	247,430	4,928	29,447	1,736
CHR	274,220	11,125	87,179	n.a.
BbF	792,554	11,861	4,820	n.a.
BkF	215,751	5,937	2,587	n.a.
BaP	199,448	3,539	2,318	144
IcdP	257,492	5,969	3,016	32
DahA	268,284	2,673	4,900	n.a.
BghiP	238,573	5,247	1,378	n.a.
Σ_{14}PAHs	6,830,417	400,077	4,817,743	5,132

n.a.: not available

CHAPTER FIVE
CONCLUSIONS AND SUGGESTIONS

5.1 Conclusions

Fourteen PAH compounds including fluorene, phenanthrene, anthracene, fluoranthene, pyrene, benz[*a*]anthracene, chrysene, benzo[*b*]fluoranthene, benzo[*k*]fluoranthene, benzo[*a*]pyrene, indeno[*1,2,3-cd*]pyrene, dibenzo[*a,h*]anthracene, benzo[*g,h,i*]perylene were investigated in ambient air, soil and water samples in Izmir, and generally all of the target compounds were found in all samples.

Ambient air studies were carried out at three sampling sites including Suburban, Urban 1 and Urban 2 sites and their spatial and seasonal variations were investigated. Highest Σ_{14}PAH concentrations were obtained from Urban 1 site with average winter concentrations of 144.2±163.2 ng m^{-3}, indicating that domestic heating and traffic emission are very likely to be the PAH sources. PAH concentrations obtained in this study were within the range of previously measured values around the world. Phenanthrene was the most abundant compound at all sites, followed by fluoranthene, fluorene and pyrene. Gas-phase concentrations were higher than the particle phase concentrations at all sites. The gas/particle phase distribution varied widely for PAHs. The gas-phase percentage generally decreased with increasing molecular weight.

Many diagnostic ratios between PAHs, are used to characterize potential emission sources at different sites. In conclusion the diagnostic plot and diagnostic PAH ratios approaches indicate that traffic emissions (petroleum combustion) were the dominant source of PAHs at all sites for both seasons. For winter, in addition to traffic emissions, residential heating was also a significant source of PAHs at all sites.

Gas-particle partitioning of PAHs were also examined using octanol-based and soot-based models. Octanol based absorptive partitioning model predicted lower partition coefficients especially for relatively volatile PAHs. However, overall there was a relatively better agreement between the measured K_P and soot-based model predictions.

Dry deposition plates were used to measure the particulate dry deposition of PAHs. The particulate dry deposition velocities for PAHs in the ambient air were also determined using concurrent flux and ambient concentration measurements. Dry deposition samples were collected in Suburban and Urban 1 sampling sites concurrently with ambient air samples. Average particle phase Σ_{14}PAH fluxes measured with dry deposition plates were 8160 and 4286 ng m^{-2} day^{-1}, for Suburban and Urban 1 sites, respectively. Particulate fluxes were dominated by phenanthrene and the average flux of phenanthrene was ~2.1 times higher at Suburban site than the one measured at Urban 1 site. Particle dry deposition velocities ranged from 4.5 (fluorene) to 0.3 cm s^{-1} (chrysene) for Suburban site and 4.6 (fluorene) to 0.03 cm s^{-1} (benzo[*g,h,i*]perylene) for Urban 1 site with an overall average velocity of 1.4±2.4 cm s^{-1} for both sites. The particle dry deposition velocities of PAHs were within the range of previously reported values around the world.

The air-soil exchange of PAHs was investigated using paired air-soil samples collected from Suburban site. The average soil concentrations of PAHs measured in this study ranged between 0.4±0.3 (benzo[*a*]pyrene) and 19.7±9.4 (phenanthrene) ng g^{-1} dry weight and they were within the range of previously reported values. Like the air samples the PAH profile in soil was dominated by lower molecular weight compounds. Phenanthrene was the most abundant compound in soil samples, followed by fluoranthene, pyrene and chrysene. The average net $\sum_{14}$PAH air-soil exchange flux ranged from 17 to 31456 ng m^{-2} day^{-1} in summer, while in winter it ranged from 5 to 36295 ng m^{-2} day^{-1}. Fluorene, phenanthrene, anthracene and carbazole were deposited in winter while they were volatilized in summer seasons. Other compounds (flouranthene - benzo[*g,h,i*]perylene) were deposited in both periods. Generally, winter fluxes were higher than summer fluxes. Since the ambient

gas-phase PAH concentrations were higher in winter, higher depositional fluxes were observed during this period. Gas absorption was dominated for lower molecular weight PAHs, however dry deposition was dominated for higher molecular weight PAHs. The contribution of volatilization was only significant for fluorene, phenanthrene, anthracene and carbazole. Wet deposition was <8% for all compounds. Results indicated a net accumulation of PAHs in the Suburban soil.

The air-water exchange of PAHs was also investigated using paired air-water samples (n=16) collected from Guzelyali Port in Izmir Bay. Average dissolved-phase Σ_{14}PAH concentrations were 10.3±2.8 and 4.9±2.2 ng L^{-1} in winter and summer, respectively. Phenanthrene was the most abundant compound in all samples, followed by fluoranthene, fluorene and pyrene. Average ambient gas-phase Σ_{14}PAH concentrations were between 97.7±31.1 (winter) and 45.8±21.5 ng m^{-3} (summer). Net air-water exchange fluxes ranged from 3.0 (benzo[*a*]pyrene) (deposition) to 6477 (phenanthrene) ng m^{-2} day^{-1} (deposition). Net PAH fluxes were mainly deposition from air to water during the sampling periods. All PAH compounds except benzo[*a*]pyrene and indeno[*1,2,3-cd*]pyrene were generally deposited during the each periods. Thus, the water acted as a sink for these compounds for both seasons. Estimated particulate dry deposition fluxes ranged between 301±372 (carbazole) - 5750±7140 ng m^{-2} day^{-1} (phenanthrene) indicating that dry deposition is also a significant input to surface waters in the study area.

5.2 Suggestions

In order to identify the origin of PAHs in ambient air, the PAH profiles of individual source emissions or the ratios of certain PAH species (diagnostic ratios) are frequently employed. There are several publications concerning the emissions of PAHs from different sources. In recent studies, PAHs have been used in chemical mass balance (CMB) or positive matrix factorization (PMF) for source apportionment of the ambient mass. No previous studies on PAH source profiles in this area was available for PMF or CMB. For this reason, in this study diagnostic plot and ratios are used to characterize potential emission sources. PAH profiles should

be obtained for a number of local sources, including traffic emission, domestic heating, and various industrial processes. Different sampling sites such as industrial areas should be included in the study.

Air-water exchange studies should be expanded to be representative for whole Izmir Bay. The observed impact of seasonal (summer-winter) variations on the fluxes suggests that additional studies should be carried out in spring and fall.

REFERENCES

Bae, S. Y., Yi, S. M., & Kim, Y. P. (2002). Temporal and spatial variations of the particle size distribution of PAHs and their dry deposition fluxes in Korea. *Atmospheric Environment, 36*, 5491-5500.

Backe, C., Cousins, I. T., & Larsson, P. (2004). PCB in soils and estimated soil-air exchange fluxes of selected PCB congeners in the south of Sweden. *Environmental Pollution, 128*, 59-72.

Bamford, H. A., Ko, F. C., & Baker, J. E. (2002). Seasonal and annual air-water exchange of polychlorinated biphenyls across Baltimore Harbor and the Northern Chesapeake Bay. *Environmental Science and Technology, 36*, 4245-4252.

Bamford, H. A., Poster, D. L., & Baker, J. E. (1999). Temperature dependence of Henry's law constants of thirteen polycyclic aromatic hydrocarbons between 4 degrees C and 31 degrees C. *Environmental Toxicology and Chemistry, 18*, 1905-1912.

Berko, H. N. (October, 1999). *Technical Report No. 2: Polycyclic aromatic hydrocarbons (PAHs) in Australia*. Retrieved May, 2002, from http://www.environment.gov.au/atmosphere/airquality/publications/report2/index.html

Bidleman, T. F., & Leone, A. D. (2004). Soil-air exchange of organochlorine pesticides in the Southern United States. *Environmental Pollution, 128*, 49-57.

Bozlaker, A., Muezzinoglu, A., & Odabasi, M. (2007). Atmospheric concentrations, dry deposition and air-soil exchange of polycyclic aromatic hydrocarbons (PAHs) in an industrial region in Turkey. *Journal of Hazardous Material* (in press).

Brankov, E., Rao, S. T., & Porter, P. S. (1999). Identifying pollution source regions using multiply censured data. *Environmental Science and Technology, 33*, 2273-2277.

Cakan, A. (1999). The direct measurement of the dry deposition of organochlorine pesticides and polychlorinated naphthalenes. PhD Thesis. Illinois Institute of Technology, Chicago.

Caricchia, A. M., Chiavarini, S., & Pezza, M. (1999). Polycyclic aromatic hydrocarbons in the urban atmospheric particulate matter in the city of Naples (Italy). *Atmospheric Environment, 33*, 3731-3738.

Cetin, B. (2007). The distribution and cycling of polybrominated diphenyl ethers (PBDEs) in environmental compartments at Izmir area. PhD Thesis. Dokuz Eylul University, Izmir.

Cetin, B., & Odabasi, M. (2007). Air-water exchange and dry deposition of polybrominated diphenyl ethers at a coastal site in Izmir Bay, Turkey. *Environmental Science and Technology, 41*, 785-791.

Chen, Y., Zhu, L., & Zhou, R. (2007). Characterization and distribution of polycyclic aromatic hydrocarbon in surface water and sediment from Qiantang River, China. *Journal of Hazardous Materials, 141*, 148-155.

Cousins, I. T., McLachlan, M. S., & Jones, K. C. (1998). Lack of an aging effect on the soil-air partitioning of polychlorinated biphenyls. *Environmental Science and Technology, 32*, 2734-2740.

Cousins, I. T., & Jones, K. C. (1998). Air-soil exchange of semi-volatile organic compounds (SOCs) in the U.K. *Environmental Pollution, 102*, 105-118.

Dabestani, R., & Ivanov, I. N. (1999). A complication of physical, spectroscopic and photophysical properties of polycyclic aromatic hydrocarbons. *Photochemistry and Photobiology, 70*, (1), 10-34.

Dachs, J., & Eisenreich, S. J. (2000). Adsorption onto aerosol soot carbon dominates gas-particle partitioning of polycyclic aromatic hydrocarbons. *Environmental Science and Technology, 34*, 3690-3697.

Dachs, J., Glenn IV, T. R., Gigliotti, C. L., Brunciak, P., Totten, L. A., Nelson, E. D., et al. (2002). Processes driving the short-term variability of polycyclic aromatic hydrocarbons in the Baltimore and northern Chesapeake Bay atmosphere, USA. *Atmospheric Environment, 36*, 2281-2295.

Dachs, J., Ribes, S., Drooge, B. V., & Grimalt, J. (2004). Response to the comment on "Influence of soot carbon on the soil-air partitioning of polycyclic aromatic hydrocarbons". *Environmental Science and Technology, 38*, 1624-1625.

Eaton, A. D., Clesceri, L. S., Rice, E. W., & Greenberg, A. E. (2005). *Standard methods for the examination of water and wastewater* (21st ed.). Centennial Edition, American Public Health Association (APHA), American Water Works Association (AWWA), Water Environment Federation (WEF).

European Commission DG Environment (2001). *Economic evaluation of air quality targets for PAHs.* Retrieved May, 2002, from http://ec.europa.eu/environment/enveco/air/index.htm#pahs

European Communities (July 27, 2001). *Ambient Air Pollution by Polycyclic Aromatic Hydrocarbons (PAH) Position Paper.*

Environment Canada (2002). *Toxic Chemicals in Atlantic Canada-Polynuclear Aromatic Hydrocarbons (PAHs).* Retrieved January, 2003, from http://www.atl.ec.gc.ca/epb/envfacts/pah.html

Environmental Protection Division (1993). *Ambient water quality criteria for polycyclic aromatic hydrocarbons (PAH)*. Overview report. Retrieved June, 2002, from http://www.env.gov.bc.ca/wat/wq/BCguidelines/pahs/pahs_over.html

EPI Suite Estimation Software, V3.20; U.S. Environmental Protection Agency: Washington, D.C., 2007; Retrieved September, 2007, from http://www.epa.gov/opptintr/exposure/pubs/episuitedl.htm.

Esen, F., Tasdemir, Y., & Vardar, N. (2007). Atmospheric concentrations of PAHs, their possible sources and gas-to-particle partitioning at a residential site of Bursa, Turkey. *Atmospheric Research* (in press).

Falconer, R. L., & Harner, T. (2000). Comparison of the octanol air partition coefficient and liquid phase vapor pressure as descriptors for particle/gas partitioning using laboratory and field data for PCBs and PCNs. *Atmospheric Environment, 34*, 4043-4046.

Fang, G. C., Chang, K. F, Lu, C., & Bai, H. (2004a). Estimation of PAHs dry deposition and BaP toxic equivalency factors (TEFs) study at urban, industry park and rural sampling sites in central Taiwan, Taichung. *Chemosphere, 55*, 787-796.

Fang, G. C., Chang, C. N., Wu, Y. S., Fu, P. P. C., Yang, I. L., & Chen, M. H. (2004b). Characterization, identification of ambient air and road dust polycyclic aromatic hydrocarbons in central Taiwan, Taichung. *Science of the Total Environment, 327*, 135-146.

Finizio, A., Mackay, D., Bidleman, T. F., & Haner, T. (1997). Octanol-air partition coefficient as a predictor of partitioning of semivolatile organic chemicals. *Atmospheric Environment, 31*, 2289-2296.

Franz, T. P., Eisenreich, S. J., & Holsen, T. M. (1998). Dry deposition of particulate polychlorinated biphenyls and polycyclic aromatic hydrocarbons to Lake Michigan. *Environmental Science and Technology, 32*, 3681-3688.

Galarneau, E., Bidleman, T. F., & Blanchard, P. (2006). Seasonality and interspecies differences in particle/gas partitioning of PAHs observed by the Integrated Atmospheric Deposition Network (IADN). *Atmospheric Environment, 40*, 182-197.

Gevao, B., Hamilton-Taylor, J., & Jones K. C. (1998). Polychlorinated biphenyl and polycyclic aromatic hydrocarbon deposition to and exchange at the air-water interface of Esthwaite Water, a small lake in Cumbria, UK. *Environmental Pollution, 102*, 63-75.

Gigliotti, C. L., Brunciak, P. A., Dachs, J., Glenn IV, T. R., Nelson, E. D., Totten, L. A., et al. (2002). Air-water exchange of polycyclic aromatic hydrocarbons in the New York- New Jersey, USA, Harbor Estuary. *Environmental Toxicology and Chemistry, 21*, 235-244.

Goss, K., Schwarzenbach, R. P. (1998). Gas/solid and gas/liquid partitioning of organic compounds: critical evaluation of the interpretation of equilibrium constants. *Environmental Science and Technology, 32*, 2205-2032.

Halsall, C. J., Coleman, P. J., Davis, B. J., Burnett, V., Waterhouse, K. S., Harding-Jones, P., et al. (1994). Polycyclic aromatic hydrocarbons in U.K. urban air. *Environmental Science and Technology, 28*, 2380-2386.

Harner, T., & Bidleman, T. F. (1998). Octanol-air partition coefficient for describing particle/gas partitioning of aromatic compounds in urban air. *Environmental Science and Technology, 32*, 1494-1502.

Harner, T., Green, N. J. L., & Jones, K. C. (2000). Measurements of octanol-air partition coefficients for PCDD/Fs: a tool in assessing air-soil equilibrium status. *Environmental Science and Technology, 34*, 3109-3114.

Harner, T., & Shoeib, M. (2002). Measurements of octanol-air partition coefficients (K_{OA}) for polybrominated diphenyl ethers (PBDEs): Predicting partitioning in the environment. *Journal of Chemical Engineering Data, 45*, 1069-1074.

Hicks, B. B., Baldocchi, D. D., Meyers, T. P., Hosker Jr., R. P., & Matt, D. R. (1987). A preliminary multiple resistance routine for deriving dry deposition velocities from measured quantities. *Water, Air and Soil Pollution, 36*, 311-330.

Hippelein, M., & Mclachlan, M. S. (1998). Soil/air partitioning of semivolatile organic compounds. 1. Method development and influence of physical-chemical properties. *Environmental Science and Technology, 32*, 310-316.

Hoff, R. M., Strachan, W. M. J., Sweet, C. W., Chan, C. H., Shackleton, M., Bidleman, T. F., et al. (1996). Atmospheric deposition of toxic chemicals to the Great Lakes: A review of data through 1994. *Atmospheric Environment, 30*, 3505-3527.

Jonker, M. T. O., & Koelmans, A. A. (2002). Sorption of polycyclic aromatic hydrocarbons and polychlorinated biphenyls to soot and soot-like materials in the aqueous environment: mechanistic considerations. *Environmental Science and Technology, 36*, 3725-3734.

Kiss, G., Varga-Puchony, Z., Rohrbacher, G., & Hlavay, J. (1998). Distribution of polycyclic aromatic hydrocarbons on atmospheric aerosol particles of different sizes. *Atmospheric Research, 46*, 253-261.

Ko, F. C., & Baker, J. E. (2004). Seasonal and annual loads of hydrophobic organic contaminants from the Susquehanna River basin to the Chesapeake Bay. *Marine Pollution Bulletin, 48*, 840-851.

Li, C., & Kamens, R. (1993). The use of polycyclic aromatic hydrocarbons as source signatures in receptor modeling. *AtmosphericEnvironment, 27A*, 523-532.

Liu, S., Tao, S., Liu, W., Liu, Y., Dou, H., Zhao, J., et al. (2007). Atmospheric polycyclic aromatic hydrocarbons in North China: A winter-time study. *Environmental Science and Technology, 41*, 8256-8261.

Lohmann, R., & Lammel, G. (2004). Adsorptive and absorptive contributions to the gas-particle partitioning of polycyclic aromatic hydrocarbons: State of knowledge and recommended parametrization for modeling. *Environmental Science and Technology, 38*, 3793-3803.

Luo, X., Mai, B., Yang, Q., Fu, J., Sheng, G., & Wang, Z. (2004). Polycyclic aromatic hydrocarbons (PAHs) and organochlorine pesticides in water columns from the Pearl River and the Macao harbor in the Pearl River Delta in South China. *Marine Pollution Bulletin, 48*, 1102-1115.

Mandalakis, M., Tsapakis, M., Tsoga, A., & Stephanou, E. G. (2002). Gas-particle concentrations and distribution of aliphatic hydrocarbons, PAHs, PCBs and PCDD/Fs in the atmosphere of Athens (Greece). *Atmospheric Environment, 36*, 4023-4035.

Manoli, E., Kouras, A., & Samara, C. (2004). Profile analysis of ambient and source emitted particle-bound polycyclic aromatic hydrocarbons from three sites in northern Greece. *Chemosphere, 56*, 867-878.

Manoli, E., Samara, C., Konstantinou, I., & Albanis, T. (2000). Polycyclic aromatic hydrocarbons in the bulk precipitation and surface waters of Northern Greece. *Chemosphere, 41*, 1845-1855.

Meijer, S. N., Harner, T., Helm, P. A., Halsall, C. J., Johnston, A. E., & Jones, K. C. (2001). Polychlorinated naphthalenes in U.K. soils: Time trends, markers of source, and equilibrium status. *Environmental Science and Technology, 35*, 4205-4213.

Meijer, S. N., Shoeib, M., Jantunen, L. M. M., Jones, K. C., & Harner, T. (2003). Air-soil exchange of organochlorine pesticides in agricultural soils. 1. Field measurements using a novel in situ sampling device. *Environmental Science and Technology, 37*, 1292-1299.

Motelay-Massei, A., Ollivon, D., Garban, B., Teil, M. J., Blanchard, M., & Chevreuil, M. (2004). Distribution and spatial trends of PAHs and PCBs in soils in the Seine River basin, France. *Chemosphere, 55*, 555-565.

Nadal, M., Schuhmacher, M., & Domingo, J. L. (2004). Levels of PAHs in soil and vegetation samples from Tarragona County, Spain. *Environmental Pollution, 132*, 1-11.

National Library of Medicine, Specialized Information Services, Toxnet. Retrieved March, 2006, from http://toxnet.nlm.nih.gov/.

Nelson, E. D., McConnell, L. L., & Baker, J. E. (1998). Diffusive exchange of gaseous polycyclic aromatic hydrocarbons and polychlorinated biphenyls across the air-water interface of the Chesapeake Bay. *Environmental Science and Technology, 32*, 912-919.

Ni, N., & Yalkowsky, H. (2003). Prediction of Setschenow constants. *International Journal of Pharmacy, 254*, 167-172

Nightingale, P. D., Liss, P., & Schlosser, P. (2000). Measurements of air-sea transfer during an open ocean algal bloom. *Geophysical Research Letters, 27*, 2117-2120.

Odabasi, M. (2007). Dokuz Eylul Universtiy, Environmental Engineering Department, Unpublished results.

Odabasi, M. (1998). The measurement of PAH dry deposition and air-water exchange with the water surface sampler. PhD Thesis. Illinois Institute of Technology, Chicago.

Odabasi, M., Vardar N., Sofuoglu A., Tasdemir Y., & Holsen T. M. (1999a). Polycyclic aromatic hydrocarbons (PAHs) in Chicago air. *The Science of the Total Environment, 227*, 57-67.

Odabasi, M., Sofuoglu A., Vardar N., Tasdemir Y., & Holsen T. M. (1999b). Measurement of dry deposition and air-water exchange of polycyclic aromatic hydrocarbons with the water surface sampler. *Environmental Science and Technology, 33*, 426-434.

Odabasi, M., Cetin, B., & Sofuoglu, A. (2006). Henry's law constant, octanol-air partition coefficient and supercooled liquid vapor pressure of carbazole as a function of temperature: Application to gas/particle partitioning in the atmosphere. *Chemosphere, 62*, 1087-1096.

Odabasi, M., Cetin E., & Sofuoglu A. (2006). Determination of octanol-air partition coefficients and supercooled liquid vapor pressures of PAHs as a function of temperature: Application to gas/particle partitioning in an urban atmosphere. *Atmospheric Environment, 40*, 6615-6625.

Ohura, T., Amagai, T., Fusaya, M., & Matsushita, H. (2004). Spatial distributions and profiles of atmospheric polycyclic aromatic hydrocarbons in two industrial cities in Japan. *Environmental Science and Technology, 38*, 49-55.

Pandit, G. G., Sahu, S. K., Puranik, V. D., & Raj, V. V. (2006). Exchange of polycyclic aromatic hydrocarbons across the air-water interface at the creek adjoining Mumbai harbor, India. *Environmental International, 32*, 259-264.

Park, S. S., Kim, Y. J., & Kang, C. H. (2002). Atmospheric polycyclic aromatic hydrocarbons in Seoul, Korea. *Atmospheric Environment, 36*, 2917-2924.

Possanzini, M., Di Palo, V., Gigliucci, P., Sciano, M. C. T., & Cecinato, A. (2004). Determination of phase-distributed PAH in Rome ambient air by denuder/GC-MS method. *Atmospheric Environment, 38*, 1727-1734.

Ravindra, K., Sokhi, R., & Van Grieken, R. (2008). Atmospheric polycyclic aromatic hydrocarbons: Source attribution emission factors and regulation. *Atmospheric Environment* (in press).

Ribes, S., Van Drooge, B., Dachs, J., Gustafsson, Ø., & Grimalt, J. O. (2003). Influence of soot carbon on the soil-air partitioning of polycyclic aromatic hydrocarbons. *Environmental Science and Technology, 37*, 2675-2680.

Roger, A. (2000). Atmospheric Oxidation. Handbook *of Property Estimation Methods for Chemicals: Environmental and Health Sciences* (31-34). CRC Press LLC.

Sayın, E. (2003). Physical features of the Izmir Bay. *Continental Shelf Research, 23*, 957-970.

Schnelle-Kreis, J, Sklorz, M., Peters, A., Cyrys, J., & Zimmermann, R. (2005). Analysis of particle associated semi-volatile aromatic and aliphatic hydrocarbons in urban particulate matter on a daily basis. *Atmospheric Environment, 39*, 7702-7714.

Schwarzenbach, R. P., Gschwend, P. M., & Imboden, D. M. (2003). *Environmental Organic Chemistry* (Second Edition), New York: Wiley-Interscience.

Seyfioglu, R. (2004). Measurement of formaldehyde dry deposition and air-water exchange with surrogate surfaces. PhD Thesis. Dokuz Eylul University, Izmir.

Shannigrahi, A. S., Fukushima, T., & Ozaki, N. (2005). Comparison of different methods for measuring dry deposition fluxes of particulate matter and polycyclic aromatic hydrocarbons (PAHs) in the ambient air. *Atmospheric Environment, 39*, 653-662.

Shoeib, M., & Harner, T. (2002). Using measured ocatanol-air partition coefficients to explain environmental partitioning of organochlorine pesticides. *Environmental Toxicology and Chemistry, 21*, 984-990.

Simcik, M. F., Eisenreich, S. J., & Lioy, P. J. (1999). Source apportionment and source/sink relationships of PAHs in coastal atmosphere of Chicago and Lake Michigan. *Atmospheric Environment, 33*, 5071-5079.

Singh, A., & Nocerino, J. (2001). *Robust estimation of mean and variance using environemental data sets with below detection limit observations*. Retrieved December 10, 2007, from http://www.epa.gov/nerlesd1/tsc/images/robust_estim.pdf

Slaski, J. J., Archambault, D. J., & Li, X. (2000). *Evaluation of polycyclic aromatic hydrocarbon (PAH) accumulation in plants. The potential use of PAH accumulation as a marker of exposure to air emissions from oil and gas flares.* Retrieved May, 2002, from http://environment.gov.ab.ca/info/library/6697.pdf

Sofuoglu, A., Cetin, E., Bozacioglu, S. S., Sener, G. D., & Odabasi, M. (2004). Short-term variation in ambient concentrations and gas/particle partitioning of organochlorine pesticides in Izmir, Turkey. *Atmospheric Environment, 38*, 4483-4493.

Tang, N., Hattori, T., Taga, R., Igarashi, K., Yang, X., Tamura, K., et al. (2005). Polycyclic aromatic hydrocarbons and nitropolycyclic aromatic hydrocarbons in urban air particulates and their relationship to emission sources in the Pan-Japan Sea countries. *Atmospheric Environment, 39*, 5817-5826.

Tasdemir, Y., & Esen, F. (2007a). Urban air PAHs: Concentrations, temporal changes and gas/particle partitioning at a traffic site in Turkey. *Atmospheric Research, 84*, 1-12.

Tasdemir, Y., & Esen, F. (2007b). Dry deposition fluxes and deposition velocities of PAHs at an urban site in Turkey. *Atmospheric Environment, 41*, 1288-1301.

Tasdemir Y., Odabasi, M., Vardar, N., Sofuoglu, A., Murphy, T. J., & Holsen, T. M. (2004). Dry deposition fluxes and velocities of polychlorinated biphenyls (PCBs) associated with particles. *Atmospheric Environment, 38*, 2447-2456.

Telli-Karakoc, F., Tolun, L., Henkelmann, B., Klimm, C., Okay, O., & Schramm, K. W. (2002). Polycyclic aromatic hydrocarbons (PAHs) and polychlorinated biphenyls (PCBs) distributions in the Bay of Marmara sea: Izmit Bay. *Environmental Pollution, 119*, 383-397.

Ten Hulscher, T. E. M., Van Der Velde, L. E., & Bruggeman, W. A. (1992). Temperature dependence of Henry's law constant for selected chlorobenzenes, polychlorinated biphenyls and polycyclic aromatic hydrocarbons. *Environmental Toxicology and Chemistry, 22*, 1179-1188.

Tsapakis, M., & Stephanou, E. G. (2005). Occurrence of gaseous and particulate polycyclic aromatic hydrocarbons in the urban atmosphere: study of sources and ambient temperature effect on the gas/particle concentration and distribution. *Environmental Pollution, 133*, 147-156.

U.S. Department of Health and Human Services, Public Health Services. Agency for Toxic Substances and Disease Registry (1995). *Toxicological profile for polycyclic aromatic hydrocarbons*. Retrieved June, 2002, from http://www.atsdr.cdc.gov/toxprofiles/tp69.html

van Jaarsveld, J. A., Van Pul, W. A. J., & De Leeuw, F. A. A. M. (1997). Modeling transport and deposition of persistent organic pollutants in the European Region. *Atmospheric Environment, 31*, 1011-1024.

van Noort, P. C. M. (2003). A thermodynamics-based estimation model for adsorption of organic compounds by carbonaceous materials in environmental sorbents. *Environmental Toxicology and Chemistry, 22*, 1179-1188

Vardar, N., Tasdemir, Y., Odabasi, M., & Noll, K. E. (2004). Characterization of atmospheric concentrations and partitioning of PAHs in the Chicago atmosphere. *Science of the Total Environment, 327*, 163-174.

Vardar, N., Odabasi, M., & Holsen, T. M. (2002). Particulate dry deposition and overall deposition velocities of polycyclic aromatic hydrocarbons. *Journal of Environmental Engineering, 128*, 269-274.

Virtual Computational Chemistry Laboratory (2004). Retrieved March, 2006, from http://146.107.217.178/lab/alogps/start.html

Wesely, M. L., & Hicks, B. B. (1977). Some factors that affect the deposition rates of sulfur dioxide and similar gases on vegetation. *APCA Journal, 27*, 1110-1116.

World Health Organization (1998). Environmental Health Criteria 202. Selected non-heterocyclic polycyclic aromatic hydrocarbons. Retrieved May, 2005, from http://www.inchem.org/documents/ehc/ehc/ehc202.htm

Yang, H. H., & Chen, C. M. (2004). Emission inventory and sources of polycyclic aromatic hydrocarbons in the atmosphere at a suburban area in Taiwan. *Chemosphere, 56*, 879-887.

Yatkin, S., & Bayram, A. (2008). Source apportionment of PM10 and PM2.5 using positive matrix factorization and chemical mass balance in Izmir, Turkey. *Science of the Total Environment, 390*, 109-123.

Yatkin, S., & Bayram, A. (2007). Elemental composition and sources of particulate matter in the ambient air of a Metropolitan City. *Atmospheric Research, 85*, 126-129.

Zhang, H. B., Luo, Y. M., Wong, M. H., Zhao, Q. G., & Zhang G. L. (2006). Distributions and concentrations of PAHs in Hong Kong soils. *Environmental Pollution, 141*, 107-114.

Zhang, Z., Huang, J., Yu, G., & Hong, H. (2004a). Occurrence of PAHs, PCBs, and organochlorine pesticides in the Tonghui River of Beijing, China. *Environmental Pollution, 130*, 249-261.

Zhang, Z. L., Hong, H. S., Zhou, J. L., & Yu, G. (2004b). Phase association of polycyclic aromatic hydrocarbons in the Minjiang River Estuary, China. *The Science of the Total Environment, 323*, 71-86.

Zhang, X., & McMurry, P. H. (1991). Theoretical analysis of evaporative losses of adsorbed or absorbed species during atmospheric aerosol sampling. *Environmental Science and Technology, 25*, 456-459.

Zhou, J. L., & Maskaoui, K. (2003). Distribution of polycyclic aromatic hydrocarbons in water and surface sediments from Daya Bay, China. *Environmental Pollution, 121*, 269-281.